Stony Brook University

Sphingolipids in Breast Cancer Progression and Inflammatory Responses

A Dissertation Presented

by

Benjamin J. Newcomb

to

The Graduate School

in Partial Fulfillment of the

Requirements

for the Degree of

Doctor of Philosophy

in

Molecular and Cellular Biology

(Biochemistry and Molecular Biology)

Stony Brook University

May 2016

Stony Brook University
The Graduate School

Benjamin J. Newcomb

We, the dissertation committee for the above candidate for the
Doctor of Philosophy degree, hereby recommend
acceptance of this dissertation.

Dr. Yusuf A Hannun, MD
Director, Stony Brook Cancer Center
Vice Dean for Cancer Medicine

Jian Cao, M.D.
Professor of Medicine

Lina M. Obeid, MD
Dean of Research, School of Medicine
Professor of Medicine

Chiara Luberto, PhD.
Research Associate Professor

This dissertation is accepted by the Graduate School

Charles Taber
Dean of the Graduate School

Abstract of the Dissertation

Sphingolipids in Breast Cancer Progression and Inflammatory Responses

by

Benjamin J. Newcomb

Doctor of Philosophy

in

Molecular and Cellular Biology

(Biochemistry and Molecular Biology)

Stony Brook University

2016

Acid Sphingomyelianse (ASM) is a key regulatory enzyme that produces the bioactive lipid ceramide, which is converted into other sphingolipids by enzymes such as Ceramide Kinase (CERK). Previous literature has implicated ASM and CERK in inflammatory signaling, but the specific role of ASM and CERK as mediators of inflammatory signaling in breast cancer has remained elusive. In this work, we delineated the role of ASM in p38 activation and

subsequent IL-6 production, as well as the role of CERK as a downstream effector of activated ASM. Since previous literature has shown that TNF-α induced dramatic alterations in the sphingolipid profile of cells, sphingolipidomic analysis was carried out on TNF-α treated MCF7 cells. The data revealed that TNF-α induced robust production of ceramide-1-phosphate (C-1-P) that accompanied an increase in CCL5. Given that previous literature showed CCL5 production is dependent on ASM, this data suggested that CERK may be acting downstream of ASM to produce C-1-P and induce CCL5. Indeed, siRNA ablation of CERK decreased CCL5 production. Furthermore, previous literature implicated C-1-P in Golgi localization of cPLA2. To define a role for ASM as an upstream modulator of CERK activity, the requirement for ASM in cPLA2 localization was tested. Ablation of ASM blocked cPLA2 localization to the Golgi network, suggesting ASM is acting upstream of CERK. Since ASM appeared to have Golgi specific functions, ASM mutants that accumulate in the Golgi network were tested for the ability to induce CCL5. We found that Golgi targeted ASM can induce CCL5 production. Taken together, these results demonstrate a role for CERK and C-1-P in CCL5 production and a role for ASM in modulation of CERK function. These results highlight the previously unappreciated role of C-1-P in CCL5 production and present new opportunities for targeting sphingolipid metabolism in treatment of breast cancers.

DEDICATION

I dedicate this work to my family whose love and support have been constant and unwavering.

“For an occurrence to become an adventure, it is necessary and sufficient for one to recount it.”

~Sartre

TABLE OF CONTENTS

LIST OF FIGURES

LIST OF ILLUSTRATIONS

LIST OF TABLES

LIST OF ABBREVIATIONS

ASM	Acid Sphingomyelinase
C-1-P	Ceramide-1-Phosphate
CCL5	Chemokine (C-C motif) ligand 5
IL-6	Interleukin 6
CERK	Ceramide Kinase
S-SMase	Secretory Acid Sphingomyelinase
L-SMase	Lysosomal Acid Sphingomyelinase
NPD	Nieman-Pick Disease
LN	Lesch Nyhan Disease
PMA	Phorbol 12-Myristate 13-Acetate
TNF-α	Tumor Necrosis Factor Alpha
Bis	Bisindoleilamide
Gö	Gö6976
cPLA$_2$	Cytosolic Phospholipase A
BIRB	BIRB796
GBA	Acid β-Glucosidase
aCDase	Acid Ceramidase

ACKNOWLEDGMENTS

First I would like to thank my family. Nothing would have been possible without my mother and father and their unending love and support. They have always believed in me, and never wanted anything more than to see me happy. My grandmother Aldean has been a constant champion of my desire to attain as much as possible, and she has continually encouraged me to reach higher. I would also like to acknowledge my grandmother Onzie who, through her understanding of the hard work and sacrifice required of a PhD, has continually reaffirmed my goals.

I would especially like to thank Dr. Yusuf Hannun for his unwavering patience and support over the last 5 years. Dr. Hannun's knowledge, insight, and thoughtful guidance were invaluable to the completion of this work.

I would like to express my gratitude to Dr. Lina Obeid for her feedback and encouragement. Her perceptiveness, scientific acumen, and considerate suggestions were instrumental in the completion of this research.

I would like to acknowledge Dr. Chiara Luberto for her thorough instruction in lipid chemistry and lipid signaling. From my early days at MUSC, Chiara was always willing to help and provide advice and assistance.

I thank Dr. Jian Cao for his rigorous scrutiny of my data and assistance in designing experiments. In addition, his prior graduate student, Dr. Nikki Calabrese, was extremely helpful in the design, completion, and analysis of the *in vitro* invasion experiments.

I would like to express my gratitude to Dr. David Perry for his mentorship in the early days of my PhD. His careful instructions helped form the basis of my work.

I would like to thank Janet Allopenna for her patience and help with the myriad crises I engineered during the preparation of this work. Janet is a highly skilled molecular biologist, and was instrumental in the preparation of many of the materials used in this work.

On a more personal note, I would like to thank my girlfriend Nadia for her love and support over the years. Her encouragement and critical insight have helped me through. I would also like to thank Dr. Chris Clarke and Dr. Russ Jenkins. Both have been invaluable mentors, collaborators, and at times, life coaches. Additionally, they have been supportive friends throughout, and I consider their friendship as instrumental to my continued success.

Finally, I would like to thank my friends. In particular, I'd like to thank Achraf for his understanding and help when I was incapacitated following my bike crash. I'd also like to thank Adada, Mikey, Mike PG, Nabil, Bill, Montefusco and all the past and present lab members that have contributed to my success.

Curriculum Vitae

BENJAMIN NEWCOMB
75 Mud Rd
Setauket, NY 11733
1 (206) 265-1600
benjamin.newcomb@stonybrookmedicine.edu

EDUCATION

State University of New York Stony Brook **(2012-continuing)**
Medical Scientist Training Program

Medical University of South Carolina, Charleston, SC **(2009-2012)**
Medical Scientist Training Program

Seattle University, Seattle, WA **(2005)**
B.S. Biology; Minor in Chemistry

SCHOLARSHIPS

Medical University of South Carolina MSTP Training Grant (2010-2012)
Hollings Cancer Center Abney Foundation Scholarship (2011, $23,000)
Zymogenetics Undergraduate Research Award (2004, $3000)
Seattle University Campion Scholarship (2001-2005, $4000/yr)

PUBLICATIONS

Newcomb B, Hannun YA (2015). Sphingolipids as mediators of breast cancer progression, metastasis, response and resistance to chemotherapy. In Hannun YA, Luberto C, Mao C, Obeid LM (Eds), *Bioactive Sphingolipids in Cancer Biology and Therapy* (pp 81-106). Cham, Switzerland: Springer International Publishing.

Hannun YA, **Newcomb B**. A new twist to the emerging functions of ceramides in cancer: novel role for platelet acid sphingomyelinase in cancer metastasis. EMBO Mol Med. 2015 Apr 9;7(6):692-4. doi: 10.15252/emmm.201505161.

Bai A, Szulc ZM, Bielawski J, Pierce JS, Rembiesa B, Terzieva S, Mao C, Xu R, Wu B, Clarke CJ, **Newcomb B**, Liu X, Norris J, Hannun YA, Bielawska A. Targeting (cellular) lysosomal acid ceramidase by B13: design, synthesis and evaluation of novel DMG-B13 ester prodrugs. Bioorg Med Chem. 2014 Dec 15;22(24):6933-44. doi: 10.1016/j.bmc.2014.10.025. Epub 2014 Oct 22

David M. Perry, **Benjamin Newcomb**, Mohamad Adada, Bill Wu, Patrick Roddy, Leah Siskind, Lina Obeid, Yusuf A. Hannun. Essential Role of Acid Sphingomyelinase in Regulating Interleukin-6 Production. J Biol Chem. 2014 Aug 8;289(32):22401-12. doi: 10.1074/jbc.M114.589648. Epub 2014 Jun 20..

David J. Montefusco, Lujia Chen, Songjian Lu, Gregory F. Cooper, **Benjamin Newcomb**, Yusuf A. Hannun, and Xinghua Lu. Distinct Signaling Roles of Ceramide Species in Yeast Revealed Through Systematic Perturbation and Integromics Analyses. Science Signaling resubmission.

David J. Montefusco, **Benjamin Newcomb**, Jason L. Gandy, Sarah E. Brice, Nabil Matmati, L. Ashley Cowart, Yusuf A. Hannun. Sphingoid bases and the serine catabolic enzyme CHA1 define a novel Feedforward/Feedback mechanism in the response to serine availability. J Biol Chem. 2012;287(12):9280-9. Epub 2012 Jan 25. PMCID: PMC3308826

PRESENTATIONS

Benjamin Newcomb, Yusuf A. Hannun. Regulation of CCL5 Production by the Sphingomyelin Degradation Pathway. Poster Presentation, 28th Annual National MD/PhD Student Conference (Keystone, CO. Jul 2013).

Benjamin Newcomb, Yusuf Hannun. Regulation of CCL5 is a Compartment Specific Function of Acid Sphingomyelinase. Poster presentation, 7th Annual MSTP Research Day / Poster Session (Stony Brook, NY. Dec 2012).

Benjamin Newcomb, Jacqueline F. McGinty. Glt1 Regulation in the Nucleus Accumbens of Cocaine Dependent Rats Following Cortical BDNF Administration. Poster presentation, Perry V. Halushka Student Research Day (Charleston, SC. November 2010).

RESEARCH EXPERIENCE

Lab Technician **(2005-2009)**
Fred Hutchinson Cancer Research Center, Seattle, WA
In the lab of Dr. Antonio Bedalov

Competitive Internship, Protein Biochemistry Dept. **(2004)**
Zymogenetics, Seattle, WA
In the lab of Dr. Patsy Lewis

PROFESSIONAL AFFILIATIONS

American Medical Association **(2009- continuing)**
MUSC Oncology in Medicine Group **(2011-2012)**
MUSC Pathology Interest Group **(2009-2012)**

Chapter 1

SPHINGOLIPIDS AS MEDIATORS OF BREAST CANCER PROGRESSION, METASTASIS, RESPONSE AND RESISTANCE TO CHEMOTHERAPY

1.1. Introduction

Breast cancer results from abnormal growth of the breast tissue. The most common form is ductal carcinoma resulting from hyperplasia and neoplastic change in epithelial cells lining the lactiferous ducts. Breast tumors are a heterogeneous mix of tumor, immune, and mesenchymal cells, and vary widely in their histopathologic make up, aggressiveness, and response to therapy. Annually in the US, roughly 250,000 people are diagnosed with breast cancer, and 40,000 die yearly [1].

Breast cancer is one of the oldest know malignancies to be identified, and has caused significant morbidity and mortality throughout history. The earliest written accounts of cancer originate in an ancient Egyptian medical treatise known as the Edwin Smith Papyrus. In the text, dated around 2500 BC, the authors describe treatment of 48 medical cases using a scientific rather than mythological approach [2]. Included therein is a description of a palpable breast tumor and the conclusion that it is incurable. Early attempts at treatment were made using a number of remedies such as arsenic paste and cautery [3]. Other civilizations of the same era used various concoctions and salves made from heavy metals or sulfur to treat breast cancer. For the most part, these early treatments were used, with only minimal modification, for several thousand years.

In the 18th and 19th centuries, the clinicopathalogic signature of breast cancer was becoming clearer. Theodor Schwann (1810-1882) demonstrated that tissues were made up of living cells instead of vacant cell structures as Hook had

proposed 175 years earlier. Schwann, together with Johannes Muller (1801-1858), described cancers as new cells aberrantly growing in tissues and causing dysfunction of the organs [4]. Their work was one of the first clinicopathologic correlations of cancer, and subsequent studies by Walter Walshe (1812-1880) suggested that cancer was caused by chronic inflammation, trauma, and smoking [5]. As the study of breast cancer entered the 20th century, research greatly accelerated as a result of accumulated pathologic knowledge as well as new techniques such as transcutaneous fine needle aspiration [6]. In 1904, Hugo Ribbert (1855-1920) established the theory that breast cancer resulted in the abnormal growth of epithelial cells as a result of chronic inflammation, and scientist began probing the root causes of breast cancer [7].

Despite the growing body of knowledge of the origins and progression of breast cancer, the standard of care had not changed appreciably since the 16th century. William Halsted (1852-1922) attempted to standardize mastectomy techniques, and he demonstrated that his technique of deep excision of the breast and pectoral muscle was highly efficacious at preventing local recurrence of breast cancer [7, 8]. In the late 19th and early 20th centuries, aggressive surgical techniques and early diagnosis significantly reduced the number of deaths from breast cancer, and the 3 year survival rate was over 50% [9].
In the early 20th century, focus began to shift to finding cures for inoperable breast cancers. In the late 1800's, George Beatson (1848-1933) observed that oophorectomy reduced the growth and spread of breast tumors in laboratory animals. He attempted oophorectomy combined with treatment with thyroid

extracts, and saw reduction in tumor growth in some patients [10]. Oophorectomy came into regular clinical practice, but when Stanley Boyd conducted a national survey of cases of breast cancer with oophorectomy, he found that oophorectomy had limited efficacy in a small number of patients [11]. Nevertheless, this hinted at hormonal regulation of breast tumors. Then, in 1910, one of the most important events in cancer biology occurred. Peyton Rous (1879-1970) published his work demonstrating that sarcomas in hens could be retrovirally induced [12]. Rous' work further revolutionized cancer research when it was recognized that his virus could immortalize cells and allow them to be grown ex vivo. Tissue culture techniques progressed rapidly, and new models of breast cancer developed rapidly. Explanted tumors were grown in rodents, and the modern era of chemotherapeutic testing began.

These efforts consolidated much of the knowledge of breast cancer, and breast cancer researchers began taking a multidisciplinary approach to understanding the disease. The work of James Ewing (1866-1943) and Albert Broders (1885-1964) produced a histologic grading system for tumors that is still in use today [9]. Their systems were based on cellular atypia, tumor vascularity, and necrosis, as well as size and level of invasion. Based on these parameters, tumor outcome and response to treatment could be reasonably predicted.

Today, treatment of breast cancer is highly complex, multimodal, and interdisciplinary. By utilizing knowledge gained from decades of research, current breast cancer therapies include targeted therapies, radiation treatment, systemic administration of drugs, and surgery to ablate primary early stage tumors. Our

current understanding of and approach to breast cancer has increased the overall 10 year survival of breast cancer to 83% [1]. However, locally advanced or metastatic tumors have poor outcomes. For example, patients presenting with stage III disease, have a roughly 50% 5-year survival [1]. Therefore, it is easy to understand the value of early detection, as well as the need to improve therapy for aggressive tumors.

Indeed, breast cancer therapy matured throughout the 20th century, and several classes of chemotherapeutics were discovered, beginning with the nitrogen mustards and antimetabolites [13]. In the early 1950's Heidelberger and colleagues found that rat hepatomas had increased uptake of uracil. Therefore, they developed drugs targeting uracil metabolism and achieved a durable reduction in tumor size with 5-florouracil. 5-Florouracil was one of the first antimetabolites, followed by its pro-drug capecitabine in the early 2000's [14, 15]. Antimetabolites interfere with metabolic process, often causing defects in the production of nucleic acids and replication of DNA, leading to replication stress and apoptosis in rapidly dividing or checkpoint deficient cells.

Following the introduction of antimetabolites were the antitumor antibiotics. This class of chemotherapeutics functions primarily through cytotoxic mechanisms including disruption of DNA structure. The earliest antitumor antibiotic was bleomycin, discovered in the mid 1960's [16]. Shortly after the discovery of bleomycin, adriamycin was introduced [17]. Although the antitumor antibiotics were highly effective, their low therapeutic index limited their use. The

need for targeted therapy and dose limiting combinational therapy was quickly realized [18].

Drugs targeting estrogen synthesis were developed soon after the discovery of the antimetabolites. Building upon Beatson's work, estrogen ablative therapy was pursued for many patients throughout the 50's and 60's with varied success. In the early 1970's, Elwood Jensen and colleagues demonstrated that only certain breast cancers expressed estrogen receptors, and that these receptors contributed to tumor growth and predicted response to antiendocrine therapy [19]. Jensen and colleagues went on to develop robust antibodies to the estrogen receptor, and demonstrated a clinically relevant link between ER expression in small tumors and eventual response to antiendocrine therapy [20]. ICI Pharmaceuticals developed Tamoxifen in the 1960's, but it was not used for breast cancer until the 1970's [21].

In the 1990's and early 2000's, naturally derived taxane based chemotherapeutics were developed. Taxanes hinder cytoskeletal remodeling in dividing cells, and interfere with mitotic spindle formation [22, 23]. The production and distribution of taxanes was a highly politicized and controversial issue in the early 1990's, but the effectiveness of taxanes in the treatment of metastatic disease led to their rapid adoption and widespread use [24, 25].

The discovery that tumors are driven by specific and predictable growth and development pathways led to the development of targeted therapies. One of the first rationally developed and targeted therapies to come to market, imatinib mesyate (Gleevec), was developed by Ciba-Geigy (Novartis) using *in silico*

computational methods to design inhibitors of bcr-abl, the aberrant tyrosine kinase in chronic myelogenous leukemia [26]. The success of imatinib validated the use of pathway analysis and bioinformatics as a guide for research and development of novel therapeutics, and heralded in a new era in chemotherapy. In a subset of breast tumors the membrane bound receptor tyrosine kinase Her2 (ERBB2) is overexpressed, and efforts to develop therapies targeting the Her2 receptor were also met with rapid success [27, 28]. One of the best characterized targeted therapies for breast cancer is trastuzumab, a monoclonal antibody that results in blockage of Her2 signaling as well as opsonization of the tumor cells [29]. Opsonization of the tumor cells results in immune mediated clearance of the tumor cells, and future therapeutics may rely more heavily on targeted manipulation of adaptive immunity [30].

1.2. Molecular Genetic Portraits of Breast Cancer

Traditionally, the choice of treatment protocol has been based on anatomic and histopathologic characteristics of the tumor. The American Joint Committee on Cancer has set forth staging criteria for anatomical classification of tumors based on tumor size, node status, and presence or absence of distant metastasis [31]. These TNM criteria are used to establish the stage of the tumor, and by extension, the likely outcomes of the disease can be predicted. T refers to the size of the primary tumor, N refers to whether lymph nodes are affected, and M refers to whether metastasis has occurred. Generally speaking, early stage tumors include tumors up to T2N1M0. Locally advanced tumors include tumors

up to T4N3M0, and metastatic tumors are any T or N status with identifiable metastasis to other organs.

However, it is difficult to predict the biomolecular make up of a tumor vis a vis receptor status from the clinical designation (e.g., TNM or grade). Thus, histopathologic characterization of tumors is also used to establish receptor status for the purposes of choosing targeted therapies and predicting response to endocrine therapy. Tumors generally fall into 1 of 3 therapeutically relevant categories: ER+, Her2+, or triple negative. Based on the stage and receptor status, surgical recommendations are made, and chemotherapeutic regimens are chosen. Thus, the presence or absence of progesterone receptors (PR), estrogen receptors (ER), and the human epidermal growth factor receptor (HER2) determines the type and duration of targeted treatment [32].

The last decade or so has witnessed increasing intensity in molecular profiling and sub-typing of breast cancer based on gene expression profiles and presence of specific mutations in the hope of developing more accurate diagnosis of breast cancer sub-types. Perou et. al. performed hierarchical clustering of gene expression data from a large microarray database and established several gene expression patterns [33]. These expression patterns are known as Luminal type/ER+, Basal type (triple negative), and Her2 like. Thus, these and other results have validated the use of receptor status to stratify tumors into molecular subtypes [34]. Subsequent analysis has demonstrated two distinct subsets of Luminal-like tumors, referred to as Luminal A and Luminal B, both ER positive but relying on different growth pathways for survival and proliferation [35].

Outcome analysis further established functional significance of these molecular subtypes with respect to response to treatment and over all survival of patients [36].

In 2012, the Cancer Genome Atlas (TCGA) published a thorough and multiplatform proteomic and genetic characterization of breast carcinomas and described the main signaling pathways that are up- and down-regulated in each tumor subtype. Luminal type tumors were found to have frequent mutations in GATA3, PIK3CA and MAP3K1 genes. Luminal B tumors, in contrast to Luminal A tumors, have increased incidence of mutations in DNA damage pathway genes. Basal type tumors were found to have high expression of proliferation associated genes as well as HIF1-α/ARNT. Her2 like tumors had high expression of Her2 amplicon genes, as well as active PIK3CA signaling and over expression of Cyclin D1 [37]. These signaling pathways, as they relate to sphingolipids, will be discussed thoroughly in the following sections. Their general characteristics, most common histopathologic findings, and outcomes are summarized in Table 1.

1.3. Bioactive Properties of Sphingolipids

Sphingolipids have diverse functions in cell growth, apoptosis, and inflammation. Ceramide, a bioactive sphingolipid, is at the center of sphingolipid metabolism, and the generation and metabolism of ceramide is tightly controlled. Ceramide is generated through *de novo* synthesis or through the salvage pathway. The *de novo* pathway takes place in the endoplasmic reticulum (ER)

and begins with the condensation of serine and palmatoyl-CoA by the enzyme serine palmitoyl transferase (SPT) to form 3-ketosphinganine. 3-ketosphinganine is then reduced, and acylated by the ceramide synthases to generate the bioactive lipid ceramide.

Ceramide produced by the action of the ceramide synthases has highly divergent activities dependent on the acyl chain length [38]. In normal cellular physiology, short and long chain ceramides are in equilibrium. When these ceramides fall out of equilibrium, cells proliferate aberrantly, or growth arrest. For example, several groups have observed that increases in very long chain ceramides are associated with tumor survival [38-40]. However, generation of short chain ceramides by the CerS is linked to apoptosis through mitochondrial and plasma membrane instability, and Ca^{2+} dependent mechanisms [41-43].

In addition to the *de novo* pathway of ceramide generation, bioactive ceramide can also be generated through the salvage pathway. The salvage pathway involves hydrolysis of complex ceramides, such as sphingomyelin, by the sphingomyelinases. Sphingomyelin serves as a critical structural component of cell membranes, as well as a reservoir for ceramide, and participates indirectly in receptor activation by way of microdomain modulation at the plasma membrane [44, 45]. Ceramide generated from hydrolysis of complex sphingolipids accounts for over half of the cellular ceramide, and is known to activate PKCs, protein phosphatase 1/2A/2C, cathepsin D, and induce pro- and anti-inflammatory proteins [46-50]. With respect to modulating inflammation, ceramide is known to induce IL-1β, VEGF, CCL5, and IL-6 in response to IL-1β

or TNF-α stimulation of cells [51-57]. In contrast to its function as a pro-inflammatory lipid, ceramide has also been found to inhibit production of several cytokines such as IL-5, IL-6, IL-10, and potentially TNF-α and IL-1β [58-61]. This dichotomy in function suggests specific subcellular pools of ceramide have precise signaling functions within the cell. Taken together, ceramide from the salvage pathway has pleiotropic effects on inflammatory signaling and plays a prominent role in the pathogenesis of inflammatory diseases such as cancer, diabetes, pulmonary fibrosis, and infectious processes [62-68]. Additionally, it is now appreciated that many of the functions of ceramide are due to its rapid conversion to other lipids such as sphingosine and C-1-P.

The soluble sphingolipid C-1-P is generated in response to activation of cytokine receptors and increases in cellular Ca^{2+}. The best-characterized functions of C-1-P are as a regulator of $cPLA_2$ function, activator of PI3K signaling, and inflammatory modulator [69-73]. C-1-P acts both intracellularly, and through stimulation of GPCR's on the cell surface. Exogenous C-1-P treatments of cells have demonstrated that GPCR activation by C-1-P induces activation of PI3K and ERK1/2 resulting in migration of macrophages [73, 74]. Intracellular production of C-1-P is stimulated by IL-1β, M-CSF, and Ca^{2+}, and results activation of mitogenic signaling pathways mediated by PI3K, ERK1/2, and NF-κB [73, 75]. Intracellular accumulation of C-1-P leads to production of a variety of cytokines including IL-10, TNF-α, and β-defensins [76-79]. C-1-P also functions as an inhibitor of ceramide production both through direct inhibition of acid sphingomyelinase, and inhibition of SPT [78, 80]. However, the mechanisms

of these inhibitory functions remain unclear. In summary, C-1-P functions as a promoter of cell survival and induces inflammatory signaling through a variety of pathways.

In contrast to C-1-P, sphingosine, another ceramide metabolite, is a powerful inhibitor of cell growth. Apoptotic stimuli frequently result in conversion of ceramide to sphingosine by one of the ceramidases. Subsequent increases in cellular sphingosine inhibits PKCs, in both mammalian and yeast model systems, modulates cell cycle protein function, and induces of apoptosis [81-86]. Functionally, sphingosine acts as an inhibitor of cell growth and proliferation, through inhibition of protein kinases. Activation of apoptosis by sphingosine relies on lysosomal permeabilization and Ca^{2+} release from the enoplasmic reticulum dysfunction [84].

An important metabolite of sphingosine is the soluble lipid S-1-P. Activators of acute S-1-P production include IL-1β, epidermal growth factor, TNF-α, and other cytokines [87-90]. Similar to C-1-P, S-1-P can function both intracellularly, and through specific receptor activation. The best characterized functions of S-1-P relate to angiogensis, migration, and production of inflammatory mediators such as prostaglandins [91]. For example, treatment of cells with TNF-α or EGF results in a rapid accumulation of S-1-P that leads to phosphorylation of ezrin-radixin-moesin (ERM) and subsequent tumor cell invasion through Matrigel® [90, 92]. TNF-α also induces S-1-P dependent production of prostaglandins [56]. Given the defined roles for S-1-P in cell migration, angiogenesis, and inflammation, it is

therefore not surprising to find that S-1-P is strongly associated with tumor progression [93, 94].

1.4. Sphingolipids in Breast Cancer

It is now recognized that many convergent and divergent pathways drive breast tumor growth and spread. Modulation of these pathways by intracellular signaling is an extremely complex topic. In the 1980's it was discovered that lipids behave as potent signaling molecules in addition to structural components of the cell. Bioactive lipids include the phosphoinositides, diacylglycerols, eicosinoids, fatty acids, and sphingolipids. Lipids represent a unique class of signaling molecules because they mostly belong in biological membranes and, as a class of biologic molecules, lipids have an extremely wide range of physicochemical properties.

The sphingolipids are a diverse set of signaling and homeostatic molecules. Head group composition, acyl chain length, and saturation all have significant effects on the lipid properties. Additionally, spatiotemporal distribution of sphingolipid synthesis is highly regulated, and subcellular compartmentalization has drastic effects on the function of individual sphingolipids (thoroughly reviewed in [95]). Sphingolipids were shown to be powerful signaling molecules capable of modulating many of the mitogenic pathways that tumors rely on for growth. Glycosphingolipid studies in the 1970's and earlier focused heavily on the gangliosides and their antigenic function in different cancers [96-98]. Work by Hakomori and others demonstrated that the

gangliosides were important membrane components that affected cell growth, differentiation, and transformation and also served as tumor antigens [99-101]. Work in the mid 1980's demonstrated a powerful bioactive role for sphingolipids in subcellular signaling cascades. The finding that sphingosine is a competitive inhibitor of PKC thrust sphingolipids into the center of cancer research [82]. PKC is a known regulator of several oncogenes, and activated PKC induces a durable and consistent signaling cascade in a variety of cancer cells [102, 103]. Subsequent work in the 1990's identified Protein Phosphatases 1 and 2A as direct targets of ceramide [104]. Ceramide forms the metabolic hub of sphingolipid metabolism and it has been the subject of significant research.

The main sources of bioactive ceramide are through *de novo* synthesis or from catabolism of sphingomyelin and complex sphingolipids. The *de novo* biosynthetic pathway resides in the ER/Golgi and requires the Serine Palmitoyltransferase complex (SPTLC1-3) and the Ceramide Synthases (CerS1-6), Ceramide derived from the *de novo* pathway is then shuttled to the Golgi either by vesicular transport or by non-vesicular transport through the action of Ceramide Transfer Protein (CERT) [105]. The action of CERT on non-vesicular transport of ceramide accounts for the majority of ceramide delivered to the Golgi [105, 106], which appears to be more specifically targeted for the synthesis of sphingomyelin through the action of Sphingomyelin Synthases (SMS1 and 2) [107, 108]. Once ceramide has been delivered to the Golgi, it is also acted upon by several other enzymes, including CERK, and Ceramide Glucosyltransferase

(UCGC). Thus, ceramide-1-phosphate, sphingomyelin, and glycosphingolipids are the major lipid species exported from the Golgi.

In contrast to the *de novo* pathway, the hydrolytic (catabolic) pathways occur at the plasma membrane, in the lysosome/endolysosomal compartments, in mitochondria, and in the Golgi, resulting in the formation of ceramide. These pathways involve one or more of the Sphingomyelinases (SMPD1-5), the Ceramidases (ASAH1-2, and ACER1-3), the Glucocerebrosidases (GBA1-3), Sphingosine and Ceramide kinase (SPHK1-2 and CERK) (reviewed in [109]). Catabolism of sphingosine-1-phosphate and ceramide 1-phosphate is carried out by an S1P lyase and the lipid phosphatases. The salvage or recycling pathway involves hydrolysis of complex sphingolipids in the endolysosomal system, resulting in the formation of sphingosine that can then be salvaged for the re-synthesis of ceramide and other sphingolipids.

It is now increasingly appreciated that any perturbations in the strictly regulated sphingolipid metabolic pathway have significant effects on signaling and growth of breast tumors. The following sections will address the changes seen in sphingolipid metabolism, and the functional consequences thereof, in Luminal, Basal, and Her2-like breast cancer subtypes.

1.5. Sphingolipids in Luminal Type Breast Cancers

Luminal A Type breast tumors have favorable outcomes and are the most heterogeneous group of breast tumors in terms of signaling characteristics [36]. Luminal Type A tumors represent about 50% of breast tumors, and are

responsive to endocrine therapy [110] as they have high expression of hormone receptors, and downstream estrogen receptor (ESR1) signaling partners such as FOXA1 and RUNX1 [111]. Interestingly, Luminal A type tumors frequently have phosphatidylinositol-3-kinase (PI3K) mutations, especially in the PIK3 catalytic subunit (PIK3CA), but these mutations are not associated with up-regulation of PI3K pathway activation as evidenced by phospho-AKT status, a key downstream target of this pathway [112]. This may be due to high expression of S6K and resultant feedback inhibition. Inactivating mutations of mitogen activated protein kinases are known to be exclusive to luminal type tumors. For example, loss of function mutations in MAP3K1 and MAP2K4 were found in high frequency in Luminal Type tumors, suggesting loss of function in the p38-JNK1 signaling cascade [111, 113]. One of the defining characteristics of Luminal Type A tumors is intact p53 and RB1 signaling [37].

Compared to Luminal A breast cancer, Luminal B breast cancer has significantly higher risk of rapid relapse following endocrine therapy [114]. Luminal B tumors are classified as ER+, but have lower expression or ER related genes than Luminal A tumors and higher expression of proliferative genes [35, 115]. Luminal B tumors often have increased HER2 expression, but since HER2 status is used to distinguish a very specific clinical subset of tumors, HER2 status is not relevant to classification of Luminal type tumors. Nevertheless, Luminal B tumors have increased growth factor signaling as compared to Luminal A tumors [116]. In contrast to Luminal A tumors, the proliferative gene signatures of Luminal B tumors seem to stem from increased genomic signaling events

secondary to genetic duplication of proliferative genes [37, 117]. This finding is in accordance with a high frequency of inactivating p53 mutations, loss of ATM, and MDM2 deregulation in Luminal B tumors [37, 118]. Therefore, the defining characteristics of Luminal B tumors are loss of function of the TP53 signaling pathway and amplification of proliferative genes such as cyclin D1. For the most part, Luminal type breast cancers can be considered ER+, HER2-, and the distinction between Luminal A and Luminal B is mainly a molecular genetic definition that is not regularly made in a clinical setting [119]. Luminal tumors rely heavily on cyclin D1 and on growth factor signaling for growth. Therefore, the following section will focus on the interplay between sphingolipids and growth factor receptors, and sphingolipids and cell cycle progression.

A number of interesting correlations between estrogen receptor signaling and sphingolipid metabolic enzymes have been published recently. Many of the studies on sphingolipids in breast cancer have been conducted using breast cancer cell lines, which limits their impact, but several studies with patient samples have been carried out. Among the studies focusing on ER+ cell lines and tumors, UGCG, the CerS, the sphingomyelinases, ASAH1, and Sphingosine Kinase 1 and 2 (SK1 and SK2) play prominent roles [81, 120-124].

1.5.1. Ceramide Glucosyltransferase

Ceramide Glucosyltransferase produces glucocerebrosides from ceramide and glucose. Subsequent action by glucosyltransferases produces a wide variety of glycolipids. In a study of 200 human breast cancer samples, the authors found

high UGCG expression in Luminal A type tumors, and high UGCG expression was also associated with poor outcomes in ER+ tumors [120]. Since ceramide is known to induce apoptosis and to act as a stress signal, conversion to other lipids, such as the glycosphingolipids, can reduce cell stress. In fact, Liu et. al. have reported that breast tissue generally has low expression of UGCG, as compared to other organs, and that high GCS expression is associated with multi-drug resistance and metastatic disease in ER+, HER2+ tumors [125]. In agreement with this study, several groups have reported on the ability of UGCG inhibitors to reverse drug resistance in breast cancer cell lines with high UGCG expression [126, 127]. A recent report has even suggested that UGCG activity is directly inhibited by tamoxifen, and that high UGCG activity can decrease sensitivity to the drug [128]. Besides a potential role in receptor function and endocytosis, several groups have implicated UGCG in the clearance of ceramide following chemotherapy [129, 130].

1.5.2. The Ceramide Synthases

The Ceramide Synthase enzymes produce dihydroceramide from dihydrosphingosine, and the rapid desaturation of dihydroceramide produces ceramide. In a large-scale lipidomics study of breast cancers, Schiffmann et. al. demonstrated a statistically significant increase in C18:0 and C20:0 ceramide in ER+ tumor samples [39]. The authors also demonstrated increased expression of CerS2, CerS4, and CerS6 in malignant tumor samples. Erez-Roman et. al. have also reported elevations in CerS2 and CerS6 in malignant breast tissue samples

as compared to normal solid tissue [131]. However, neither group could conclude whether the elevation in ceramide content or CerS expression was a consequence of or a driver of malignancy in breast carcinomas. Continuation of the CerS studies demonstrated oppositional roles for the long chain and very long chain ceramides. The authors found that CerS2, and by extension the very long chain C-24 and C26 ceramides, increased colony formation in MCF7 breast cancer cells whereas CerS4 and CerS6, which produce long chain ceramides (mostly C14 and C16 ceramides) decreased colony formation [38]. Data mining has revealed robust up-regulation of CerS2, CerS4, and CerS6 in Luminal type tumors (Fig. 1).

The long chain ceramides and the enzymes responsible for their production CerS6 and CerS1 have tumor suppressive properties [132, 133]. CerS6 has been implicated in the response to folate stress, suggesting CerS6 may also play a role in response to antimetabolites [134]. Antimetabolites are employed in the treatment of some early stage breast cancers, and cell culture studies suggest that combined therapy with the antimetabolite pemetrexed and the kinase inhibitor sorafenib can induce increases in the dihydroceramides. The authors showed that the production of dihydroceramide was dependent on the activity of CerS6 and led to apoptosis of luminal type breast cancer cell lines [135]. Other researchers have reported repression of hTERT activity by CerS1 in various cancer cell lines [136, 137], suggesting an inhibitory role for the long chain ceramides in tumor growth.

1.5.3. The Sphingomyelinases

The Sphingomyelinases hydrolyze sphingomyelin to ceramide and phosphocholine. There are several isoforms of sphingomyelinase (SMPD1-5), and both SMPD1 (Acid Sphingomyelinase) and SMPD3 (Neutral Sphingomyelinase 2) have been implicated in breast cancer progression. As seen in Figure 1, SMPD3 is down regulated in all 4 subtypes of breast carcinomas. Loss of heterozygosity and epigenetic regulation of this region has been described, and may account for the down regulation of SMPD3. A comparative epigenetics study reported that there is aberrant CpG methylation around the SMPD3 locus in human breast cancer cell lines as well as several primary tumor samples [138]. Additionally, another group reported that there are frequent loss of heterozygosity events at 16q22.1, that includes the SMPD3 locus [139]. These results suggest SMPD3 may play an anti-tumor role, however this hypothesis has never been directly tested in breast cancer.

The role of Neutral Sphingomyelinase 2 in drug response has been characterized in breast cancer. Expression and activity was significantly up regulated in Adriamycin resistant MCF7 (MCF7-ADR) cells following treatment with a demethylating agent that decreases methylation dependent silencing of genes [140]. Demethylation of DNA was correlated with the subsequent decrease in plasma membrane sphingomyelin, and increased membrane fluidity, attributable to increased activity of Neutral Sphingomyelinase 2. Up-regulated Neutral Sphingomyelinase 2 activity resulted in increased doxorubicin uptake and apoptosis in MCF7-ADR cells, suggesting that silencing of the SMPD3 locus may

be one mechanism by which MCF7 cells acquire resistance to Adriamycin [140]. In line with the work by Vijayaraghavalu et. al. is the finding by Ito and colleagues that apoptosis of Adriamycin sensitive MCF7 cells is mediated by SMPD3 following daunorubicin treatment [141]. Taken together, re-activation of SMPD3 expression may be a powerful tool for restoration of sensitivity to anthracyclines in resistant tumors.

Similar to SMPD3, SMPD1 plays a role in resistance to chemotherapeutics. The receptor tyrosine kinase inhibitor Sunitinib inhibits Acid Sphingomyelinase leading to lysosomal instability and apoptosis in MCF7-Bcl-2 cells [142]. In addition to being an attractive drug target in breast cancer, Acid Sphingomyelinase plays a role in breast tumor progression. Acid Sphingomyelinase was shown to mitigate some of the cytotoxic effects of cisplatin on cytoskeletal remodeling in MCF7 cells [143]. Cytoskeletal dynamics were also shown to rely on sphingomyelinase derived S1P generation at the plasma membrane and subsequent phosphorylation of the ezrin, radixin, and moesin family of proteins [144]. Subsequent studies on SMPD1 in MCF7 cells showed Acid Sphingomyelinase to be necessary for expression of IL-6 following PKC activation by the cell permeable phorbol ester phorbol 12-myristate 13-acetate (PMA) [53]. The authors also show dependence on SMPD1 for matrigel transwell migration of the basal type breast cancer cell line MDA-MB-231 and the HeLa cell line. In accordance with a requirement for SMPD1 expression for tumor progression, aggressive tumor subtypes have increases in SMPD1 expression (Fig. 1).

1.5.4. The Ceramidases

Catabolism of ceramide to other sphingolipids is another potential route by which Luminal Type breast cancers are able to escape the pro-apoptotic effects of ceramide. The ceramidases rapidly convert ceramide to sphingosine, and the chain length specificity and subcellular localization of ceramide metabolizing enzymes may contribute to the relative mitogenic capacity of different ceramides with distinct chain lengths. Down stream products of the ceramidases, especially sphingosine and S1P, have been shown to be potent signaling molecules. Therefore, conversion of a small amount of ceramide is likely to have profound effects on the cell. Acid Ceramidase converts ceramide to sphingosine that is quickly converted to sphingosine-1-phosphate. Several studies have linked acid ceramidase with growth of ER+ cell lines. In support of these data, ASAH1 expression is increased in Luminal tumor samples (Fig. 1) as compared to matched normal tissue, suggesting a pro-tumor role for ASAH1. Indeed, inhibition of Acid Ceramidase causes lysosomal disruption that results in rapid cell death in ER+ cell lines [84, 145]. Furthermore, the inhibition of tumor cell growth is not limited to lysosomal permeabilization. Inhibition of Acid Ceramidase with non-lysomatrophic compounds still results in cell death, suggesting the functional consequence of inhibition extends beyond lysosomal homeostasis [122]. The downstream signaling function of ASAH1/Sphingosine was recently delineated by Lucki et. al. The authors found that induction of ASAH1 by phytoestrogens in MCF7 cells relied on c-SRC and ERK activation and subsequent ERα

recruitment to the ASAH1 promoter. The induction of ASAH1 resulted in cyclin B2 activation and increased cell proliferation [81].

Interestingly, high ASAH1 expression has also been correlated with better outcomes in ER+ breast tumors [123]. The discrepancy between cell culture and *in* vivo studies may be a result of the complexities of the tumor microenvironment. Acid ceramidase has been shown to modulate the tumor microenvironment through regulation of inflammatory cytokines and prostanoid signaling [52, 53].

Stress induced cytokines, such as Tumor Necrosis Factor (TNF-α) and Interleukin-1 (IL-1β), induce enzymatic activity of members of the sphingolipid catabolic pathways [146-148], and these have been shown to regulate inflammatory mediators, such as prostaglandin E2 (PGE2), Chemokine Ligand 5 (CCL5), and Interleukin-6 (IL-6) [52, 53, 149]. Each of these inflammatory mediators has varied effects on breast tumors. Tumor derived PGE2 induces p38/JNK activation in adjacent fibroblasts. The activated p38/JNK signaling cascade resulted in transcription of aromatase and consequent production of estrogen [150]. CCL5 promotes growth and metastasis of ER+ tumors by recruiting macrophages, inducing angiogenesis, and stimulating proliferation of CD44+/CD24- cancer stem like cells [151-153]. The role of IL-6 in breast cancer is multifaceted. In clinical studies on the relationship between IL-6 and breast cancer, high IL-6 is associated with early locally advanced tumors, and good prognosis [154]. Conversely, in late stage tumors IL-6 was associated with worse prognosis [155]. Cell line studies have demonstrated that ER+ cell lines become

growth suppressed by IL-6 and undergo EMT when exposed to IL6 for extended periods of time. Conversely, ER- cell lines are not responsive to exogenous IL-6 (reviewed in [156]). A possible reason for ER- tumors being unresponsive to IL-6 is the finding that ER- tumor cell lines have a very high level of endogenous IL-6 production as compared to ER+ cell lines [157].

1.5.5. The Sphingosine Kinases

Sphingosine kinase phosphorylates sphingosine to produce sphingosine-1-phosphate (S1P). S1P acts as an intracellular signaling molecule as well as an extracellular signaling molecule that interacts with S1P receptors on the cell surface. In a thorough study of SK1 in human breast cancer samples, Watson et. al. found that SK1/S1P participate in non-genomic signaling by ER and cross talk between ER and ERK-1/2. Patients with ER+ tumors displaying high ERK-1/2 and SK1 relapsed nearly 10 years earlier than patients with low SK1 and ERK-1/2. Additionally, the patients with high SK1 and ERK-1/2 were found to be tamoxifen resistant [158]. In accordance with the work by Watson et. al., Zhang et. al. carried out a large scale, pan-cancer meta-study demonstrating a significant correlation between SK1 expression and worse outcomes in a number of solid tumors. The authors reviewed immunohistochemical staining for SK1 in a range of breast tumor samples and calculated a hazard ratio of 1.86 for tumors with high SK1 expression [159]. Mining of microarray data has revealed Luminal Type tumors have high SPHK1 and SPHK2 expression (Fig. 1).

Sphingosine Kinase 1 expression in ER+ tumors is modulated by ER signaling. In a study examining expression of micro RNA miR-515-5p, it was noted that in MCF7 cells this miRNA is correlated with SK1 expression. The authors reported that when the ERα receptor is activated by estradiol (E2), the ERα/E2 complex directly interacts with the promoter sequence that regulates miR-515-5p. This interaction leads to a decrease in miR-515-5p expression and de-repression of SK1 expression [160]. The authors went on to report that in a small cohort of 34 tumor samples, ER+ tumors had lower miR-515-5p expression than ER- tumors. However, they do not correlate this finding with SK1 expression in their cohort [160]. In support of the findings by Pinho et. al., Takabe and colleagues found that E2 treatment resulted in increased S1P efflux from cultured MCF7 cells, and the observed increase in S1P export was dependent on the ERα receptor suggesting that active ER signaling is necessary for SK1, but not SK2, activation [161]. Taken together, active ERα signaling promotes S1P production in MCF7 cells.

In addition to Sphingosine Kinase activity, S1P receptors (S1PR1-5) seem to be modulated by ER signaling. Indeed, multiple groups have observed ERK activation by S1P/S1P receptor signaling, and correlataions between S1PR expression and ERK1/2 expression have been made [162, 163]. In a study of 304 ER+ breast tumor samples, Watson et. al. correlated S1P receptor 1 and 3 expression with ERK1/2 expression. The authors found that patients with high membrane localized S1PR1 had shorter time to recurrence of disease, and high cytoplasmic S1PR1 and 3 was associated with worse survival [158]. The authors

also noted that TRANSFAC analysis (Biobase) revealed binding sites for ERα, c-Jun, and Sp1 in the $S1P_3$ promoter region [158]. This suggests that tumors with active ER signaling (i.e. tumors with high PR and ER expression [164]) also have high S1P mediated ERK-1/2 activation.

The finding that the SK1/S1P/S1PR axis is up-regulated in ER+ tumors would suggest that targeting this axis would be beneficial in the treatment of breast carcinomas. However, targeting of the SK1/S1P/S1P receptor axis in breast cancer has been met with mixed results. A group from the Department of Chemistry at Amgen utilized the crystal structure of SK1 to generate specific inhibitors of the sphingosine kinases. The inhibitors, termed ‘compound A’ and ‘compound B,’ were potent and reproduced the phenotypes of SK1-/- mice [165]. The Amgen Oncology Research group then carried out a cell line study with compound A and compound B, as well as the inhibitor SKII, and found that their compounds reduced S1P levels, but did not impact viability of tumor cell lines at concentrations that reduced S1P levels in the tumor cells [166]. Additionally, the authors reported that ablation of SK1 or SK2 did not reduce tumor cell viability. The conclusion was that SK1 and SK2 are not high yield targets for cancer chemotherapeutics. However, targeting the S1P receptors is a very attractive target, especially in basal type tumors.

1.5.6. Ceramide Kinase

In contrast to S1P, comparatively little work has been done on delineating the role of ceramide-1-phosphate (C1P). C1P is produced by CERK mediated

phosphorylation of ceramide. In low grade breast cancer it has been noted that high CERK expression correlates with poor histologic grading of tumors and ER negativity [167]. Additionally, CERK inhibition results in M-phase arrest of MCF7 cells, and sensitized cells to protein kinase inhibitors [72]. Message level of CERK is not significantly different between tumor subtypes (Fig. 1) suggesting that post-translational regulation and subcellular localization of CERK may play a significant role in its function within the tumor cell.

1.6. Sphingolipids in Basal Type Breast Cancer

The basal like genetic signature was one of the first genetic portraits of disease to be described. This signature includes expression of mitogenic pathways, as well as high expression of keratins 5, 6, and 17 [33]. Basal Type Breast carcinomas are mostly triple negative tumors that do not express ER, PR, or HER2 receptors, but roughly 25% of basal like tumors are not triple negative. Greater than 80% of basal like tumors have mutant TP53 and loss of p53 signaling, as well as loss of RB1 and BRCA1 [37]. Myc activation, cyclin E1 amplification, and activation of the HIF1-α/ARNT pathways are prominent features of basal like tumors [37, 168]. Activation of the HIF1-α pathway suggests basal like tumors may be susceptible to angiogenesis inhibitors. Another interesting observation from TCGA is that basal like breast carcinomas share several common features with serous ovarian carcinoma, including Myc activation, cyclin E1 amplification, and inactivation of TP53 and RB1, as well as loss of BRCA1 [37]. This finding suggests that some of the processes driving

serous ovarian tumors may be active in basal type breast cancers. The lack of receptors and the aggressive nature of basal like tumors have created a significant need for identification of new therapies.

The approach to surgical treatment of triple negative breast cancers is similar to other breast carcinomas. The choice between adjuvant (treatment given after surgical excision of a primary tumor) and neoadjuvant (treatment given before surgical excision) therapy is made based on tumor size and local spread. Triple negative tumors often respond well to chemotherapy; however, there is a high recurrence rate of tumors [169]. Therefore, there is a significant need for more effective chemotherapeutics. In this regard, ceramide has been used to induce apoptosis of hormone insensitive breast cancer cell lines [170, 171], and some success has been achieved in murine models of breast cancer [172]. Ceramide causes clustering and activation of death receptors, and the apoptotic threshold of cells is modulated by the presence of ceramide at the plasma membrane [173]. Ceramide nanoliposomes can increase the concentration of ceramide at the plasma membrane of target cells [174]. Recently, ceramide nanoliposomes have been used to improve the bioavailability and efficacy of breast cancer chemotherapeutics. Nanoliposomal preparations of the tyrosine kinase inhibitor sorafenib and ceramide were shown to decrease AKT phosphorylation and Cyclin D1 expression. The authors show that ceramide nanoliposomes reduce pAkt and sensitize MDA-MB-231 cells to sorafenib-induced apoptosis [175]. Sorafenib is traditionally used to treat renal carcinoma, and has powerful anti-angiogenic and anti-mitogenic properties, making it an

interesting therapeutic for the treatment of basal type breast cancers [176]. Recent clinical trials have demonstrated a potential role for sorafenib in Her2 negative tumors as well as in tamoxifen resistant tumors [177, 178]. Ceramide nanoliposomes have also been used to improve the cellular uptake of doxorubicin in MCF7 and SKBR3 breast cancer cell lines [179]. Ceramide nanoliposomes have been used *in vivo* and may hold promise in adjuvant or neoadjuvant treatment of breast cancers [180].

The success of neoadjuvant treatment of triple negative breast tumors is assessed by the pathologic response of the tumor to chemotherapeutic agents. Achieving a preoperative pathologic complete response (pCR) is the goal of neoadjuvant therapy, but it is difficult to predict what patients will achieve pCR with a given chemotherapy regiment. Roughly 55% of patients with triple negative tumors do not respond well to multi-agent neoadjuvant therapy [181]. A series of studies has recently uncovered potential roles for UGCG, CERT, and the ceramide producing β-Glucosidase enzymes (GBA1 and GBA3) in resistance to taxanes in hormone insensitive breast tumors. The first study demonstrated that down regulation of CERT, or up-regulation of GBA1 or 3, sensitized tumor cells to taxanes [182]. As a follow up to their *in vitro* functional genomics study, the research group carried out a retrospective meta-study and found that up-regulation of UGCG and CERT, and concomitant down-regulation of GBA1 and GBA3, was highly associated with failure of 5-fluorouracil, doxorubicin, cyclophosphamide, paclitaxel (TFAC) treatment of triple negative tumors [183]. The majority of Basal type tumors have low UGCG and CERT expression (Fig.

1). Therefore, the association between high expression of these genes and poor response to treatment may make them valuable biomarkers. The results of these studies highlight the importance of enzymes that turn over the pool of ceramide in triple negative breast carcinoma cells.

Based on the work by the TCGA and others, triple negative tumors have high expression of the hypoxia inducible genes. This suggests the tumors may be susceptible to anti-vasculogenic therapies. Fingolimod (Gilenya) is a sphingoisne analog approved for treatment of multiple sclerosis that serves as a precursor for an agonist of S1P receptors that often results in internalization and shut down of the action of the receptor [184, 185]. In studies with cell lines, fingolimod has been shown to disrupt ERK1/2 and HER2 cross talk in Her2-like breast cancer cells and decrease the proliferation of Luminal type breast cancer cells [186, 187]. In studies using syngeneic mouse models of breast cancer, research has shown fingolimod decreases vascular smooth muscle motility in response to tumor-derived cytokines [188]. Since fingolimod has potent anti-vasculogenic properties, it may also serve as a potent inhibitor of basal type breast tumor growth *in vivo*. Unfortunately, observance of the anti-tumorigenic properties of fingolimod is unlikely to be made in cell culture or limited *in vitro* systems.

1.7. Sphingolipids in Her2-Like Breast Cancer

Genomic duplication of the Her2 gene results in overexpression of HER2 and HER2-associated genes. In these tumors, HER2 itself as well as FGFR4,

EGFR, and several other receptor tyrosine kinases are up regulated. Her2-like tumors have high levels of phospho-SRC and phospho-S6 [37]. Her2-like tumors are largely treated with adjuvant chemotherapy. Effective treatment relies primarily on targeted therapies such as trastuzumab (targeting HER2) in combination with a taxane or anthracycline [189, 190]. Despite the finding that EGFR signaling is up regulated in Her2-like tumors, lapatinib, an inhibitor of the Her2 and EGFR pathways, has not been clinically successful in the adjuvant treatment of Her2-like tumors [191]. On the other hand, adjuvant trastuzumab treatment has a fairly high disease free survival rate or 76% [192]. Although there is a small subset of Her2-like tumors that are ER positive, the clinical relevance of combining endocrine therapy with targeted HER2 therapies has not been rigorously evaluated. General clinical practice focuses on targeting of the HER2 receptor, and current investigations are underway to evaluate the efficacy of targeting tyrosine kinase activity in Her2 like tumors [193].

Several groups have studied the role of sphingolipids in Her2-like tumors with a focus on CERT, CERK, and sphingomyelin homeostasis. CERT seems to play a prominent role in Her2-like tumors, and has been shown to mediate paclitaxel sensitivity in these tumors. Extending their work with functional metagenomics, the Swanton group found that CERT was overexpressed in $HER2^+$ tumors, and they demonstrated that silencing of CERT in $HER2^+$ tumors sensitized them to chemotherapeutics [183, 194]. Inhibition of CERT induced autophagic flux and LAMP2 expression, and increased sensitivity to paclitaxel,

doxorubicin, cisplatin and trastuzumab. Therefore, CERT may be of both therapeutic and prognostic value in $HER2^+$ breast tumors.

The role of CERK in $HER2^+$ tumors has recently been investigated using a mouse model of breast cancer. Utilizing a doxycycline inducible *HER2/neu* mouse model of breast cancer, Payne et. al. demonstrated that CERK was required for tumor cell survival following doxycycline withdrawal. When doxycycline was withdrawn and cells were treated with shRNA to CERK, tumor cells expressed high levels of pro-apoptotic markers [195]. The authors also tested the role of CERK in BT474 (ER^+, $HER2^+$, p53 mut) and SKBR3 (ER^-, $HER2^+$, p53 mut) cells treated with the tyrosine kinase inhibitor lapatinib. As expected, the cells were dependent on CERK expression for survival. Additionally, BT20 (ER^-, $HER2^-$, p53 mut) cells treated with doxorubicin required CERK expression for growth. The authors extended their study to analyze microarray data from 2200 patient samples, and found significant correlation between CERK expression and aggressive tumors such as $HER2^+$ tumors [195]. The association between CERK and $HER2^+$ tumors progression makes CERK an attractive target for combination chemotherapy.

The role of other sphingolipids in Her2-like tumors has not been rigorously studied. However, a study investigating lipid levels in several patient samples from Her2-like tumors found elevations in the level of sphingomyelin [196]. This finding is interesting and helps validate the work by Lee et. al. because overexpression of CERT is known to increase sphingomyelin levels in cells [194, 197]. Additionally, SMPD1 is up regulated in Her2 like tumors, suggesting that

Acid Sphingomyelinase may be the source of the increased levels of sphingomyelin (Fig. 1). There are a number of interesting alterations in sphingolipid gene expression that are unique to Her2 like tumors (Fig. 1), but the functional roles of other sphingolipid metabolizing enzymes in Her2-like tumors remain to be elucidated.

1.8. Conclusions

The function of sphingolipids in breast cancer is an area of intense investigation. Sphingolipids modulate many of the growth, apoptosis, inflammatory, and perhaps even angiogenic pathways that breast carcinomas rely on. In luminal type breast cancers, conversion of ceramide to complex sphingolipids is associated with drug resistance and worse patient outcomes. The somewhat paradoxical finding by Schiffmann et. al. that luminal type tumors have up-regulated synthesis of several ceramide species highlights the different outcomes of ceramide generated in different sub cellular compartments such as the ER/Golgi versus at the plasma membrane. Ceramide is rapidly converted to other lipid species, and several groups have demonstrated the role of sphingosine kinase 1 in tumor growth. The role of acid ceramidase in luminal type tumors is complex. Acid ceramidase promotes a number of cell-cell signaling pathways, and some of the subtleties of these signaling pathways may be lost in over simplified experimental conditions.

Basal type breast tumors are highly aggressive, and have poor response to treatment. Novel therapeutics based on ceramide, as well as novel drug

delivery methods have recently shown promise in the treatment of basal type tumors. The studies showing potential roles for CERT and UGCG in basal type tumors suggest that targeting these pathways may be an effective route for treating triple negative tumors. Many current chemotherapeutics, such as doxorubicin and etoposide, cause cell death through generation of ceramide. Therefore, directly modulating ceramide metabolic pathways may increase the effectiveness of current chemotherapeutics and increase their therapeutic index. The role of sphingolipids in Her2-like tumors has not been thoroughly studied. This is despite the fact that robust murine models of Her2-like tumors are readily available. In one of the only studies on sphingolipids in Her2 driven breast cancers, Payne et. al. showed reliance on CERK in Her2-like tumors. In addition to the role of CERK, non-vessicular transport of ceramide seems to be an important process in Her2-like tumors, and inhibition of CERT results in autophagy of $HER2^{+}$ cell lines.

Sphingolipid research in other systems has demonstrated the power of multimodal bioinformatics studies focused on sphingolipid metabolic pathways [198]. Application of cross platform informatics to breast cancer will reveal new opportunities for targeted therapy focused on sphingolipid metabolic enzymes. It is obvious that more studies are needed into the specific roles of individual enzymes and pathways of sphingolipid metabolism in breast cancer and as these roles of sphingolipids become clearer, more specific rationales will emerge for targeting sphingolipid metabolism as an attractive therapeutic modality.

Chapter 2

ACID SPHINGOMYELINASE ACTIVITY IN THE GOLGI NETWORK REGULATES CCL5 THROUGH A CERK DEPENDENT MECHANISM

Abstract

Acid Sphingomyelinase (ASM) hydrolyzes sphingomyelin to produce the biologically active lipid ceramide. ASM is activated by a variety of stimuli, but the fate and mechanistic function of ASM derived ceramide in breast cancer has remained elusive. Interestingly, various ceramide generating enzymes produce distinct pools of ceramide with varied biologic functions [53]. However, the functional significance of these distinct pools of ceramide has remained unclear. In the present study, we identified a novel Golgi specific signaling pathway connecting ASM and ceramide kinase (CERK). This signaling pathway is necessary for CCL5 production and for $cPLA_2$ localization to the Golgi. Interestingly, cells lacking ASM have decreased C-1-P production following TNF-α treatment. This result suggested that ASM may be acting upstream of CERK. Consistent with this hypothesis, ablation of CERK blocks CCL5 production in response to TNF-α. Additionally, ablation of ASM is sufficient to disrupt CERK specific functions within the cell. Previous data has shown that C-1-P is necessary for cytosolic phospholipase A_2 ($cPLA_2$) localization to the Golgi network. The present study shows that $cPLA_2$ does not localize to the Golgi in cells overexpressing CERK, but ablated for ASM. Finally, localization of ASM to the Golgi network was sufficient to induce CCL5 production. Taken together, these data suggest ASM can produce ceramide in the Golgi network, the ceramide is converted to C-1-P by CERK, and that C-1-P is required for CCL5 production.

2.1. Introduction

Bioactive sphingolipids are a diverse group of signaling molecules that include ceramide, sphingosine, ceramide 1-phosphate, and sphingosine 1-phosphate, with more than 30 metabolic enzymes that generate or catabolize them [39, 167, 199-203]. Due to the large number of bioactive lipids and enzymes involved, the sphingolipid metabolic network is highly regulated and compartmentalized within the cell [204-206]. Sphingolipid metabolism can be segregated into the *de novo,* hydrolytic, and the salvage pathways.

Sphingomyelin, and other complex sphingolipids, form the substrates for the sphingolipid hydrolytic and salvage pathways. Catabolism of sphingomyelin is mediated by the activity of the sphingomyelin phosphodiesterases which generates ceramide, and subsequent metabolism of ceramide can generate sphingosine or ceramide-1-phosphate (C-1-P), the latter through the action of ceramide kinase (CERK) [207]. Ceramide has been implicated in multiple cellular functions including apoptosis, response to chemotherapeutics, and other anti-mitogenic activities. Likewise, C-1-P has many important signaling functions within the cell, including mediation of several inflammatory processes that promote tumor formation and progression [202, 208, 209]. Therefore, CERK may have a dual function in tumor promotion involving both the production of mitogenic C-1-P as well as clearance of apoptotic ceramide [210].

Recent studies have highlighted a substantial role for the tumor microenvironment in tumor progression and development of intratumoral heterogeneity [211-214]. The microenvironment is shaped and defined by pro-

inflammatory cytokines such as TNF-α, IL-1β, IL-6 and CCL5 [151, 215-218]. These cytokines can promote survival of cancer stem like cells (CSC's), resistance to chemotherapeutics, and metastasis. Specifically, TNF-α and IL-1β are produced by infiltrating macrophages and lead to the formation of a feed-forward inflammatory cycle [219-222]. In response to chronic TNF-α and IL-1β exposure, tumor cells, and tumor associated mesenchymal cells, produce high levels of IL-6 and CCL5 [223, 224]. Recent data has highlighted the significance of CCL5 in tumor progression and poor outcomes in patients [225-228]. CCL5, and its cognate receptor, CCR5, are known to be expressed in a coordinate and non-random manner in ER negative breast carcinomas [229, 230]. In addition, CCL5 was recently shown to foster a pro-tumor microenvironment, and activate STAT6 and ERK mediated survival pathways [231].

Previous work from our lab, and others, has revealed a pro-inflammatory role for the sphingolipid salvage pathway, with a particular focus on acid sphingomyelinase (ASM) [52, 53, 59, 232]. ASM is a 631 amino acid protein, encoded by the SMPD1 gene. ASM mediates the downstream signaling pathways initiated by interleukin 1β (IL-1β), tumor necrosis factor α (TNF-α), and by phorbol 12-myristate 13-acetate (PMA) [233, 234]. In particular, TNF-α induces accumulation of ceramide within the cell, and activates apoptotic as well as mitogenic pathways [43, 235].

TNF-α induces several mitogenic pathways in tumor cells and a prominent role for CERK in these pathways has been established [88, 236]. Additionally, analysis of publically available gene expression data from breast tumors has

shown that metastatic breast tumors with high expression of both ASM and CERK have very poor outcomes. Together, these data suggest ASM and CERK may play an important role in mitogenic signaling in tumor cells following stimulation by pro-inflammatory cytokines within the tumor microenvironment. Due to the findings that ASM mediates inflammatory signaling in breast cancers, that CERK promotes tumor progression, and that CCL5 has a prominent role in the tumor microenvironment, we sought to investigate a possible connection between ASM, CERK and CCL5. We hypothesized that C-1-P mediates the production of CCL5 in response to TNF-α stimulation, and, that through unique subcellular compartmentalization of ASM, CERK generates C-1-P from ceramide produced by ASM.

2.2. Experimental Procedures

2.2.1. Materials-MCF7 cells were obtained from ATCC (Manassas, VA). NPD (Cat GM16195, passage 11) and Lesch-Nyhan (Cat GM02226, passage 16) cells were obtained from Coriell Cell Repository (Camden, NJ). Trypsin-EDTA (0.05%) was from Gibco (Holtsville, NY, Cat 25300062). Blasticidin HCl was obtained from Invitrogen (Carlsbad, CA, Cat R210-01). Anti-V5 mouse monoclonal antibody was from Invitrogen (Cat 46-0705). Anti $cPLA_2$ was obtained from Santa Cruz Biotechnology (Santa Cruz, CA, Cat sc1724). Giantin was obtained from Covance (Princeton, NJ, Cat PRB-114C). Secondary HRP conjugated antibodies were obtained from Santa Cruz Biotechnology. Detection of HRP activity was perfomed using a chemiluminescence kit from ThermoFisher (Rockford, IL).

Novex fluorescently tagged secondary antibodies for confocal were obtained from ThermoFisher. Interleukin-1β and TNF-α were purchased from Peprotech (Rocky Hill, NJ). Porcine brain sphingomyelin was from Avanti Polar Lipids (Alabaster, AL, Cat 860062P).

2.2.2. Cell Culture- MCF7 cells were maintained in RPMI from Gibco (Holtsville, NY, Cat 11875-093) supplemented with 10% (v/v) heat inactivated FBS from HyClone (Port Washington, NY, Cat SH30396.03). MCF7 cells were kept in culture for no longer than 30 days. All cell lines were tested monthly for mycoplasma contamination using the MycoAlert kit from Lonza (Allendale, NJ, Cat LT07-218). Stable expression of ASM was achieved by transducing cells at an MOI of 30 with Lenti virus containing wilt type ASM, S508A ASM, S508D ASM, or LacZ. Cells were selected for 10 days with 10µg/mL blasticidin, and stable expression was confirmed by western blotting for V5 and by confocal microscopy. Cells were maintained at less than 75% confluency in standard cell culture conditions (humidified atmosphere, 95% air, 5% CO2, 37 °C). Following blasticidin selection, cells were maintained in media without blasticidin. NPD and LN cells were maintained in DMEM from Gibco (Holtsville, NY, Cat 11965-092) supplemented with 10% (v/v) heat inactivated FBS under normal cell culture conditions (humidified atmosphere, 95% air, 5% CO2, 37 °C). NPD and LN cells were maintained at less than 75% confluency. All cell treatments with TNF-α or IL-1β were carried out in serum free media, unless otherwise noted.

2.2.3. Plasmids and Transient Transfection- Wild Type ASM, and S508A ASM were cloned into pLenti6.3/TO/V5 in two steps. First, ASM was amplified from the pEF6-ASM-V5 vector [53] using a 5'-caccATGCCCCGCTACGGAGCGTCACTC-3' primer containing 24 nucleotides of the 5' translated region starting with ATG, and a 3'- GCAAAACAGTGGCCTTGGCCACAGGCTC-5' primer containing the last 27 nucleotides minus the stop codon, the amplified mouse aSMase was directionally subcloned into intermediate vector pENTR-D/TOPO (Life Tech, Cat K2400-20). Second, using Gateway LR Clonase II Enzyme Mix (Life Tech, Cat 11791-020), the intermediate pENTR-D/TOPO vector was recombined with the Destination Cloning vector pLenti6.3/TO/V5-DEST (Life Tech, Cat K531520) to produce pLenti6.3/ASM/V5-DEST. The S508D mutant of ASM was generated with QuikChange II Site Directed Mutagenesis Kit (Life Tech cat#200523) using primer 5'-GGAAACTACTCCAGGAGCGaTCACGTGGTCCTGGACCATGAGACC-3' and pLenti6.3/S508A ASM/V5-DEST as the template. The orientation of the insert was verified by restriction mapping and sequencing.

Transient transfections were carried out in 6-well trays with 1x10^5 cells per well. 24hrs after seeding cells, the media was changed and cells were transfected with 1µg of plasmid DNA per well, using X-tremeGENE DNA transfection reagent from Roche (Basel, Switzerland, Cat 06365787001) according to manufacturer's instructions.

2.2.4. Lenti Viral Production- Lentivirus particles were generated as previously described (Weinberg lab). Briefly, Lenti X cells from Clontech (Mountain View, CA, Cat 632180) were seeded in 10cm dishes in DMEM+10% FBS. After 24hrs cells were transfected with a plasmid mix containing 3µg of the relevant pLenti construct, 2.25 µg of psPAX packaging plasmid, and 750 ng of pMD2.G envelope plasmid. The transfection mix was prepared in 400µL of Opti-MEM media from ThermoFisher (Cat 31985062) containing 12µL of X-tremeGENE transfection reagent from Roche (Basel, Switzerland, Cat 06365787001). DNA complexes were added to cells, and after 36hrs of incubation, cell supernatants were collected and filtered through low protein binding, 0.45µm syringe driven filters (Fisher Cat SLHV033RS). Lentiviral particle number in the filtered supernatants was measured using the ABM Lentivirus titer kit (Richmond, BC, Cat LV900). 5x10^5 MCF7 cells were plated in each well of a 6 well dish and infected at an MOI of 30. After 24hrs of incubation, MCF7 cells were trypsinized and plated into media containing 10µg/mL blasticidin. Following 10 days of selection, resistant cells were assessed for transgene over expression by activity assays, western blot, and confocal microscopy.

2.2.5. RNA Interference- Small interfering RNA (siRNA) duplexes were obtained from ThermoScientific (Rockford, IL), and were designed against the following target sequences: aSMase, 5'-AACTCCTTTGGATGGGCCTGG-3'; CERK (prevalidated, s34929); $cPLA_2$ (prevalidated, s10592). All-Star Negative Control siRNA was obtained from Qiagen. 5x10^5 cells were plated in each well of a 6-

well tray and 20nM siRNA was transfected using Lipofectamine RNAiMAX from ThermoFisher (Cat 13778150), according to manufacturer's specifications. After 24hrs, RNAi complexes were washed out, and cells were incubated with complete media for another 24hrs. 4hrs prior to experimental manipulation, media was exchanged.

2.2.6 ELISA- Sandwich ELISA kits for Human CCL5 were obtained from R&D Systems (Minneapolis, MN, Cat DY278-05 and DY008) and used according to manufacturer specifications. Briefly, cell supernatants were harvested, and centrifuged for 5 min at 14,000 rpm in a table top microcentrifuge, and 100µL of supernatant was used per well of the ELISA assay. Cell lysates were prepared in buffer containing 50 mM TrisHCl, 0.2% TritonX-100, and protease inhibitor from Sigma (St. Louis, MO, Cat S8830-20TAB) (cell lysis buffer). Cells lysates were adjusted to a protein concentration of 0.5mg/mL, and 100µL of lysate was applied to each well of the ELISA.

2.2.7. Immunoblotting- Cells were lysed in cell lysis buffer and 25µg total protein in equal volumes was subjected to SDS-PAGE on Novex™ 4-20% Tris-Glycine Midi Protein Gels from ThermoFisher. Proteins were electrophoretically transferred onto 0.45µm nitrocellulose membrane, blocked with PBS containing 0.1% Tween 20 (PBS-T) and 5% nonfat dried milk. Membranes were incubated under constant agitation overnight at 4 °C with primary antibody (V5–1:5,000) in PBS-T containing nonfat dried milk. After overnight incubation with primary

antibody, the blots were incubated with the corresponding HRP-conjugated secondary antibody (1:5000) in PBS-T with 5% milk. After washing, enhanced chemiluminescence was used to visualize bands by autoradiography.

2.2.8. Real Time Reverse Transcriptase-Polymerase Chain Reaction (RT-PCR)- RNA purification was performed with the Purelink RNA Kit from ThermoFisher, according to manufacturer's protocol. Concentration of RNA was determined by nanodrop, and 500ng of RNA was transformed into cDNA using the Quanta cDNA Kit (Gaithersburg, MD, Cat 95047) according to the manufacturer's protocol. For RT-PCR, reactions were performed in triplicate in 96-well plates with each reaction containing 10 µl of 2 × iTAQ mastermix, 5 µl of diluted (1:12, v/v) cDNA, 1 µL of FAM tagged Taqman gene specific primer probe, 0.3 µL of VIC tagged Actin probe, and 4 µl of water. The following probes were purchased from Life Technologies: ACTB (Cat Hs01060665_g1); ASM (Cat Hs03679347_g1); CERK (Cat Hs00368483_m1); CCL5 (Cat Hs00174575_m1).

2.2.9. Sphingolipidomic Analysis- MCF7 or NPD or LN cells were seeded at 10^6 cells/plate in 10 cm plates. Following 24 h of growth in complete media, cells were treated as indicated. Following treatment, cells were scraped and pelleted in cold PBS, and lipids were extracted in 2 mL isopropanol:water:ethyl acetate (30:10:60 by vol). Cell extracts were analyzed by reverse phase high pressure liquid chromatography coupled to electrospray ionization and subsequent separation by mass spectrometry. Analysis of sphingoid bases, ceramides and

sphingomyelins was performed on a Thermo Quantum Ultra mass spectrometer, operating in a multiple reaction-monitoring positive ionization mode, as described [1]. Lipid phosphate concentrations were measured and sphingolipid levels were normalized to total lipid phosphate in each sample.

2.2.10. In Vitro Acid SMase Activity Assay- Acid Sphingomyelinase Assays were performed as previously described [2]. In brief, 200µM porcine brain sphingomyelin was mixed with [14C] labeled sphingomyelin and Triton X-100. Micelles were formed by sonication in a buffer containing 250 mM sodium acetate (pH 5.00) and 1.0 mM EDTA. Cells were lysed in buffer containing 50mM TrisHCl pH7.4, 0.2% Triton X-100, 1.0 mM EDTA, and protease inhibitor. 25µg of cell lysate in 100µL lysis buffer was added to 100µL of micelle mix and the reaction was incubated at 37ºC for 30 min. The reaction was terminated with the addition of 1.5 ml of CHCl3: MeOH (2:1, v/v) followed by 0.4 ml of water. Samples were vortexed, centrifuged (5 min at 3,000 rpm in a table top centrifuge), and 0.8 ml of the aqueous/methanolic phase was removed for scintillation counting.

2.2.11. Confocal Microscopy- 1X10^5 cells were plated in confocal dishes. The next day, cells were washed with PBS, and fixed in 3.7 % paraformaldehyde in PBS for 8 min, washed once with PBS, and permeabilized in 0.1 %Triton X-100 for 5 minutes. Samples were washed and then incubated with V5 (1:1000), Giantin (1:1000), and $cPLA_2$ primary antibodies in 2 % human serum for 24hrs at

4ºC. Samples were washed once with PBS and incubated with secondary antibodies conjugated to AlexaFluor for 1 hr at room temperature. Samples were washed 3 times with PBS and then imaged on confocal laser microscope (Leica SP8).

2.2.12. Statistical Analysis- Data are represented as mean of at least 3 independent replicates +/- standard error, unless otherwise indicated. Unpaired Student's t test, one-way ANOVA with Dunnett's post test, and two-way ANOVA with Bonferroni post test statistical analyses were performed using Prism software.

2.3. Results

2.3.1. TNF-α induces a C-1-P signaling cascade

Previously we demonstrated a role for secretory acid sphingomyelinase (S-SMase) in IL-1β and TNF-α induced CCL5 production in MCF7 breast carcinoma cells [52]. However, in these studies the functional role of the ceramide metabolites sphingosine and C-1-P (C-1-P) were unclear. In addition, inflammatory cytokines are known to induce CERK, and we have shown that TNF-α, in particular, is a potent inducer of C-1-P. Therefore, we sought to investigate the role of CERK and C-1-P in CCL5 production and clarify the interactions between acid sphingomyelinase and C-1-P.

Our previous work has implicated ASM in CCL5 production in response to TNF, and, as expected, we observed a rapid and robust time-dependent increase in the level of CCL5 following TNF treatment. CCL5 message increased 18 fold, over control, (Fig. 2A) and secreted CCL5 protein increased 120 fold, over control, (Fig. 2B) in response to TNF-α treatment. To investigate the possibility that C-1-P plays a role in the TNF-α response, we measured C-1-P levels following TNF-α stimulation, and observed a robust time dependent increase in C-1-P (Fig. 2C & D). Interestingly, sphingosine did not increase during our time course of TNF-α treatment (Fig. 2C). These data suggest TNF-α is inducing a C-1-P dependent signaling pathway in MCF7 cells.

To date, ceramide kinase (CERK) is the only identified source of C-1-P in mammalian cells [237]. As such, we sought to determine the role of CERK in production of C-1-P and CCL5. Using siRNA directed toward CERK, we were

able to knock down expression of CERK, and consequently we measured a significant decrease in both the basal and TNF-α stimulated levels of C-1-P (Fig. 3A). To rule out a possible effect on ceramide and sphingosine levels, we measured both ceramide and sphingosine in vehicle and TNF-α treated cells. TNF-α induced a significant accumulation of ceramide that was not affected by ablation of CERK (Fig. 3B). Additionally, CERK knock down did not affect sphingosine levels in these cells (Fig. 3C). From these data, we concluded that the increase in C-1-P in response to TNF-α is due to CERK activity, and that CERK knock down is not affecting levels of other bioactive lipids including ceramide and sphingosine.

2.3.2. TNF-α induced C-1-P is required for CCL5 production

Cytokines, including CCL5, are regulated at many levels including transcription, translation, and secretion [238-240]. As such, we investigated the role of CERK in CCL5 production by measuring secreted CCL5 protein by ELISA. We observed that knock down of CERK significantly reduced levels of CCL5 in the media of TNF-α treated MCF7 cells (Fig. 4A). To assess the role of CERK in CCL5 expression, we measured CCL5 mRNA in cells treated with CERK siRNA. We found that ablation of CERK caused a significant decrease in the expression of CCL5 message, commensurate with the effects on protein levels (Fig. 4B). Previous reports have shown that CCL5 highly regulated at the secretory level. CCL5 is stored in secretory vesicles and vesicular fusion and subsequent CCL5 secretion is regulated by SNARE and synaptobrevin-2 [238, 241]. To rule out a

role for CERK in vesicular fusion and secretion of CCL5, we compared secreted CCL5 to CCL5 within cells. We found that ablation of CERK reduced both secreted and cellular CCL5 (Fig. 4C & D), suggesting that deletion of CERK is not causing a secretory defect in MCF7 cells.

Sphingolipids are known to be required for cytokine production following a variety of stimuli. Previous work has shown that ASM is required for CCL5 induction by both IL-1β and TNF-α. To investigate a possible role for CERK in IL-1β dependent signaling cascades, we measured CCL5 in response to IL-1β and found that CERK is required for IL-1β induced CCL5 transcription (Fig. 4E).

2.3.3. ASM is required for C-1-P production following TNF-α stimulation

Previous data has demonstrated a role for ASM in the induction of CCL5 by IL-1β and TNF-α. Therefore, we sought to investigate a connection between ASM derived ceramide and C-1-P. We found that TNF-α treatment caused a rapid increase in ASM activity (Fig. 5A), and, correspondingly, TNF-α induces ceramide accumulation that is ASM dependent (Fig. 5B). The increases in ceramide and C-1-P, following TNF-α stimulation, are temporally related, suggesting the possibility that CERK utilizes ASM derived ceramide to produce C-1-P and induce CCL5 in response to inflammatory stimuli.

To further investigate the possible link between ASM and CERK, we used a genetic model of ASM deficiency. Nieman-Pick disease (NPD) is characterized by a significant decrease in ASM activity. Therefore, fibroblasts from NPD patients can be used as a model of ASM deficiency. Since NPD fibroblasts have

a significant defect in lysosomal function, we obtained fibroblasts from Lesch-Nyhan (LN) patients as a control. LN fibroblasts have perturbed lysosomal function, but do not have deficiencies in ASM or other sphingolipid metabolic enzymes. Both cell lines are known to respond to TNF-α treatment, and NPD fibroblasts have a significant defect in CCL5 production as compared to LN fibroblasts. Herein we found that TNF-α caused a significant increase in C-1-P in LN fibroblasts, but the ASM deficient NPD fibroblasts do not produce C-1-P in response to TNF-α (Fig. 5C). Therefore, the results suggest that C1P is produced from ASM-derived ceramide.

To further establish a role for ASM in C-1-P production, we over expressed CERK and ASM in MCF7 cells and measured C-1-P. Expectedly, we found that overexpression of CERK induced significant overproduction of C-1-P. Interestingly, overexpression of ASM also induced a modest accumulation of C-1-P. Co-expression of ASM and CERK resulted in similarly increased levels of C-1-P as with CERK over expression alone (Fig. 5D). From these data we concluded that ASM could induce C-1-P production.

Since the data suggest that CERK is utilizing ceramide produced by ASM, we tested for a possible role for C-1-P in CCL5 production. In cells overexpressing CERK and ASM we observed a significant increase in CCL5 message following overexpression of CERK (Fig. 5E). In addition, co-expression of ASM and CERK led to supra-physiologic levels of CCL5, as compared to the level seen with TNF-α treatment (Fig. 5E). These data suggest that C-1-P is able to induce CCL5 in MCF7 cells. However, some discrepancy between the level of

C-1-P and the level of CCL5 remains. A possible explanation is that C-1-P is a known inhibitor of ASM and in the context of CERK overexpression, the excess C-1-P may be inhibiting ASM and preventing any further contribution by ASM [78]. With regards to the finding that ASM is a more robust inducer of CCL5 than CERK, it is possible that ASM derived ceramide is being converted into C-1-P as well as other lipids that induce CCL5. Therefore, convergent signaling pathways may be inducing CCL5 downstream of ASM.

2.3.4. Induction of CCL5 is independent of p38/MAPK and PGE_2

Our previous work implicated p38/MAPK as a downstream target of ASM in cells stimulated with phorbol 12-myristate 13-acetate (PMA) [53]. Since TNF-α is a known inducer of PKCs and subsequent p38/MAPK activation, we investigated a role for PKCs and p38/MAPK in CCL5 production. To test this hypothesis, we pretreated cells with the classical PKC inhibitor Gö6976 (Gö) or pan-PKC inhibitor bisindoleilamide (Bis) and stimulated with TNF-α. Neither Gö nor Bis inhibited the TNF-α stimulated production of CCL5 (Fig. 6A). To test for a p38/MAPK dependent mechanism, we used the inhibitor BIRB796 (BIRB). BIRB is a potent inhibitor of p38/MAPK phosphorylation (Fig. 6B, lower panel). Interestingly, we found that inhibition p38/MAPK did not affect TNF-α stimulated CCL5 production (Fig. 6B).

2.3.5. ASM is required for CERK function

To investigate a role for ASM in C-1-P dependent pathways, we evaluated the well-studied connection between C-1-P and $cPLA_2$ localization [69, 71, 242]. The results showed that $cPLA_2$ had a faint generalized staining in logarithmically growing MCF7 cells (Fig. 7A, top panel). Since cPLA2 localization has been shown to depend on C-1-P, we overexpressed CERK and assessed $cPLA_2$ localization. The results showed that overexpression of CERK caused $cPLA_2$ to co-localize strongly with the Golgi network marker giantin (Fig. 7A, middle panel). Interestingly, in cells over expressing CERK, but ablated for ASM, $cPLA_2$ did not co-localize with Golgi markers (Fig. 7A, bottom panel). These data suggest that ASM-derived ceramide is necessary for CERK dependent signaling cascades.

Treatment with exogenous C-1-P has been shown to induce redistribution of $cPLA_2$ to the Golgi network. Since TNF-α induced C-1-P (Fig. 2 C & D), we investigated the ability of TNF-α to cause $cPLA_2$ re- localization to the Golgi. The results showed that TNF-α stimulation caused a robust redistribution of $cPLA_2$ to the Golgi network (Fig. 7B middle panel). Since we have established a role for ASM in CERK induced $cPLA_2$ localization, we asked if ASM is required for TNF-α induced Golgi localization of $cPLA_2$. Indeed, the data showed that ablation of ASM caused a significant defect in $cPLA_2$ localization to the Golgi following TNF-α stimulation (Fig. 7B, lower panel). Taken together, these results suggest that ASM is required for CERK and C-1-P dependent processes, and that ASM is acting upstream of CERK in response to TNF-α.

Previous work established a requirement for ASM in CCL5 production [52]. Since ASM can affect $cPLA_2$ localization, and presumably function, we

tested the possibility that $cPLA_2$ and PGE_2 are required for CCL5 production. To test this hypothesis, we ablated $cPLA_2$ with siRNA and measured CCL5 production following TNF-α stimulation. Interestingly, inhibition of $cPLA_2$ did not inhibit CCL5 production (Fig. 8D). In agreement with the $cPLA_2$ results, inhibition of COX2, with a the inhibitor CAY1404, did not affect CCL5 (Fig. 8E), suggesting CCL5 induction is independent of prostanoid signaling in MCF7 breast carcinoma cells. Taken together, these results suggest that although ASM and CERK form a linear pathway with respect to CCL5, $cPLA_2$ participates in a separate signaling pathway within the cell.

2.3.6. CCL5 production is a Golgi specific function of ASM

The finding that ASM regulates Golgi dependent functions of CERK, and the fact that secretion of ASM is brefeldin A sensitive, led us to hypothesize that ASM has Golgi specific function [233]. To test this hypothesis, we generated mutants of ASM with distinct patterns of subcellular localization. Previous work has shown that phosphorylation of serine 508 (S508) is required for ASM localization and function. Therefore, we mutated S508 to the non-phosphorylatable and phosphomimetic residues alanine (S508A) and aspartate (S508D), respectively. As previously reported, the non-phosphorylatable mutant, S508A, lacks secretory activity, but maintains lysosomal activity (Fig. 9B, top panels). The phosphomimetic mutant, S508D, retains minimal secretory activity, as measured in media of cells overexpressing the S508D mutant, and decreased lysosomal activity (Fig. 9B, top panels). These results led us to investigate the

subcellular localization of the S508A and D mutants. We found that wild type ASM partially co-localizes with the trans-Golgi network (TGN) marker TGN46 (Fig. 9A, top panel). Interestingly, the S508A mutant displayed diffuse cytoplasmic staining, with minimal TGN localization (Fig. 9A, middle panel). Strikingly, the S508D phosphomimetic mutant localizes almost exclusively to the TGN (Fig. 9A, bottom panel). These results led us to investigate a role for the Golgi localized S508D mutant in CCL5 production.

To test our hypothesis that ASM mediates a has Golgi specific signaling paradigm, we measured CCL5 production in MCF7 cells over expressing LacZ, wild type ASM, S508A ASM, or S508D ASM. As expected, we observed that overexpression of wild type ASM induces CCL5 as compared to the LacZ control cells. Interestingly, the secretion incompetent S508A mutant did not induce CCL5, whereas the Golgi localized S508D mutant strongly induced CCL5 (Fig. 9C). These findings suggest that the Golgi localized activity of ASM is sufficient to induce CCL5 expression.

2.4. Discussion

Past and previous data from our lab, as well as others, defined a role for ASM in the generation of ceramide following TNF-α stimulation [43, 243]. Here, we demonstrate direct evidence that ASM activity increases following TNF-α stimulation (Fig. 5A). Importantly, TNF-α induces a C-1-P dependent pathway (Fig. 2C & D) that is necessary and sufficient to induce CCL5 (Fig. 4 and 5E). Additionally, CERK acts on ceramide produced by ASM, tightly linking the

activation of ASM and formation of ceramide and C1P to CCL5 production. Moreover, the results showed that ASM is required for the translocation of $cPLA_2$, a critical CERK downstream target, to the Golgi. These data suggest that CERK is a master regulator of several inflammatory processes that can contribute to breast cancer progression.

2.4.1. TNF-α induces a CERK/C-1-P dependent signaling cascade

Although ASM has been implicated in CCL5 production, the precise identity of downstream signaling molecules remained unclear. Since sphingolipid metabolism constitutes a tightly-knit network of interconnected metabolites, the action of a specific enzyme (in this case ASM) can be directly attributed to its immediate product (ceramide), sine these metabolites are interconvertible. The results from this study demonstrate a key role for C1P and the enzyme that generates C-1-P from ceramide, CERK, in regulation of CCL5 production. Ablation of CERK leads to a significant decrease in CCL5 mRNA and CCL5 protein following TNF-α stimulation. Furthermore, TNF-α causes a rapid increase in C-1-P that correlates temporally with the increase in CCL5. In addition to being necessary for CCL5 production, over expression of CERK is sufficient to induce CCL5.

Defining a role for CERK in CCL5 production has helped elucidate the TNF-α induced CERK/C-1-P signaling cascade, and this provides novel insights into the role of C-1-P in inflammatory cytokine signaling in breast tumors. TNF-α has been shown to induce CERK activity in neuroblastoma cell lines, however

direct measurements of C-1-P were not presented [244]. The finding that TNF-α induces an accumulation of C-1-P supports the hypothesis that TNF-α is a potent inducer of CERK/C-1-P, and suggests that CERK may be an important part of the signaling cascades induced by TNF-α. In breast cancers, CERK is associated with poor outcomes, as is TNF-α [245-247]. The finding that CERK/C-1-P are activated by TNF-α may explain results demonstrating a survival advantage to tumors expressing high levels of TNF-α [248]. Therefore, targeting the CERK/C-1-P signaling axis may have profound potential in the pharmacologic treatment of non-surgical breast tumors.

Previous work has demonstrated a link between PGE2, a downstream target of C-1-P, and CCL5, suggesting that C-1-P may play a role in CCL5 production. However, this is the first report of a direct link between C-1-P and CCL5. Furthermore, the finding that cPLA2 does not participate in the signaling cascade suggests CERK may have novel downstream targets in breast cancer. CERK is known to play key roles in production of several pro-inflammatory molecules, but the exact molecular targets linking C-1-P to CCL5 production are unknown. A greater understanding of how C-1-P regulates inflammation will present new therapeutic targets for the treatment of breast tumors.

2.4.2. ASM is the major source of ceramide in TNF-α stimulated breast cancer cells

TNF-α stimulation of MCF7 cells induces both ASM activity and ceramide accumulation (Fig. 5A and B). The finding that ASM is the major source of

ceramide following TNF-α stimulation suggests that ASM is the rate-limiting source of ceramide in activated breast cancer cells. As such, ASM is tightly coupled to flux through the CERK/C-1-P signaling axis. Therefore, coordinated expression of ASM and CERK may be a novel marker of tumor progression. This data may help to explain the previously reported finding that high ceramide levels are associated with poor outcomes in breast tumors [39]. Our work supports a paradigm shift by demonstrating a strong a pro-tumor role for ASM and TNF-α through a direct link between ASM and CERK. The precise role of C-1-P in activation of inflammatory signaling seems to be independent of other ASM mediated pathways, such as modulation of p38/MAPK phosphorylation.

2.4.3. ASM initiates a Golgi specific signaling cascade involving CERK

The data supporting a connection between ASM and CERK led to an investigation of the subcellular localization of ASM and CERK. Ablation of ASM causes defects in the C-1-P stimulated localization of $cPLA_2$ to the Golgi network (Fig. 7A). Additionally, ablation of ASM decreased the TNF-α stimulated re-localization of $cPLA_2$ to the Golgi (Fig. 7B), a process likely dependent on C-1-P formation. This data suggested that ASM and CERK might be interacting in the Golgi network. Using novel serine mutants of ASM, a Golgi specific function of ASM was identified. Golgi targeted ASM is able to drive the production of CCL5. This data, together with the results presented in Figure 7, strongly support a role for ASM in the Golgi network. Since ASM can regulate Golgi specific functions of

CERK, and because CERK is largely localized to the Golgi network, we conclude that CERK is acting on ASM derived ceramide within the Golgi network.

The finding that C-1-P, but not cPLA$_2$, participates in CCL5 production suggests that C-1-P regulates CCL5 independently of previously established signaling paradigms. C-1-P has been identified as a regulator of cPLA$_2$ localization and function, but a direct role for ASM in cPLA$_2$ localization has never been established [242, 249]. The finding that ASM can regulate cPLA$_2$ localization helps clarify the role of TNF-α in cPLA$_2$ function [88, 149]. Furthermore, TNF-α stimulation is sufficient to induce cPLA$_2$ localization to the Golgi, a process that is also dependent on ASM. These data together suggest that ceramide produced by ASM is required for multiple CERK mediated signaling cascades, placing ASM upstream of CERK.

In conclusion, this work demonstrates a novel role for CERK in the regulation of CCL5. Additionally, ASM, a well-known regulator of CCL5, functions upstream of CERK to rapidly generate high levels of ceramide following TNF-α stimulation. Secondary to TNF-α stimulation, ASM can mediate several canonical CERK signaling cascades. Additionally, this work supports the existence of novel downstream targets of C-1-P. The results demonstrating a role for CERK, but not cPLA$_2$, in CCL5 production suggests the CERK/C-1-P signaling pathway has novel downstream targets.

Chapter 3

DEFINING A ROLE FOR ACID SPHINGOMYELINASE IN THE P38/INTERLEUKIN-6 PATHWAY

Abstract

Acid sphingomyelinase (ASM) is one of the key enzymes involved in regulating the metabolism of the bioactive sphingolipid ceramide in the sphingolipid salvage pathway, yet defining signaling pathways by which ASM exerts its effects has proven difficult. Previous literature has implicated sphingolipids in the regulation of cytokines such as interleukin-6 (IL-6), but the specific sphingolipid pathways and mechanisms involved in inflammatory signaling need to be further elucidated. In this work, we sought to define the role of ASM in IL-6 production because our previous work showed that a parallel pathway of ceramide metabolism, acid β-glucosidase 1, negatively regulates IL-6. First, silencing ASM with siRNA abrogated IL-6 production in response to the tumor promoter, 4-phorbol 12-myristate 13-acetate (PMA), in MCF-7 cells, in distinction to acid β-glucosidase 1 and acid ceramidase, suggesting specialization of the pathways. Moreover, treating cells with siRNA to ASM or with the indirect pharmacologic inhibitor desipramine resulted in significant inhibition of TNF-α and PMA-induced IL-6 production in MDA-MB-231 and HeLa cells. Knockdown of ASM was found to significantly inhibit PMA-dependent IL-6 induction at the mRNA level, probably ruling out mechanisms of translation or secretion of IL-6. Further, ASM knockdown or desipramine blunted p38 MAPK activation in response to TNF-α, revealing a key role for ASM in activating p38, a signaling pathway known to regulate IL-6 induction. Last, knockdown of ASM dramatically blunted invasion of HeLa and MDA-MB-231 cells through Matrigel. Taken together, these results demonstrate that ASM plays a critical role in p38 signaling and IL-6 synthesis with implications for tumor pathobiology.

3.1. Introduction

In addition to its physiological roles in inflammation and immunology, Interleukin-6 (IL-6) has been widely implicated in cancer biology [250]. IL-6 is known to stimulate proliferation, invasion, and metastasis of tumors [251-253]. Moreover, there is a strong correlation between invasiveness of cancer cell lines and the level of IL-6 production [254], suggesting that although IL-6 is capable of being produced by many cell types, tumor-derived IL-6 may be a critical determinant in a tumor's intrinsic invasive capability.

Bioactive sphingolipids have been implicated as regulators of IL-6 formation, but the specific sphingolipid pathways involved are not clearly defined. Sphingolipid metabolism is broadly divided into either *de novo* or hydrolytic/salvage pathways[50, 255]. In the salvage pathway, sphingomyelin (SM) and glucosylceramide (GC) are hydrolyzed into ceramide by acid sphingomyelinase (ASM) and acid b-glucocerebrosidase (GBA), respectively. Ceramide can be then cleaved to form sphingosine by acid ceramidase. Thus, the salvage pathway is poised to make rapid changes in downstream metabolites including ceramide and sphingosine due to the relative abundance of the complex sphingolipids such as SM and GC and also the energetically favorable process of hydrolysis. Consistent with this, activation of PKC∂ stimulates the hydrolysis of complex sphingolipids leading to the production of ceramide from either GBA or ASM leading to flux through the sphingolipid salvage pathway[234, 256, 257].

Insofar as evidence for involvement of sphingolipids in IL-6 production, early work by Laulederkind et al. demonstrated that exogenous treatment of dermal fibroblasts with bacterial sphingomyelinase (bSMase) was sufficient to induce IL-6 similar to that of IL-1b treatment[258], suggesting that a pool of ceramide at the plasma membrane could be involved in triggering signaling to IL-6. Conversely, previous work from our laboratory has demonstrated that IL-6 production and p38 activation is negatively regulated by GBA-derived ceramide in MCF-7 cells[59]. Literature related to ASM has shown that ASM is not required for p38 signaling in $ASM^{-/-}$ murine macrophages[259] whereas other work has indicated a role for ASM in cytokine production including IL-6 with the use of a SM-based ASM inhibitor[260]. While this work was in progress, Kumagai et al. showed that ASM is involved in IL-6 production in bladder cancer cells[261]; however, a signaling pathway leading to IL-6 was not identified, underscoring the need to identify signaling pathways that ASM regulates to affect IL-6 secretion.

Here, the roles of sphingolipid salvage enzymes in the regulation of IL-6 were investigated in MCF-7 cells in response to the PKC activator and tumor promoter, 4b-phorbol 12-myristate 13-acetate (PMA), and in response to TNFa, a critical regulator of IL-6 production. We found IL-6 induction to be dependent on ASM in distinction to ACD and GBA. These findings demonstrate that in MCF-7 cells, PKC/ASM-mediated induction of IL-6 mRNA is a result of increased message stability and transcription. The roles of sphingolipid salvage pathway enzymes were also assessed in p38 activation revealing a similar pattern of regulation as for IL-6. Furthermore, the role of ASM in invasion was assessed

revealing a critical role for ASM in this process in HeLa and MDA-MB-231 cells. Additionally, and in contrast to noninvasive carcinoma MCF-7 cells, invasive breast MDA-MB-231 and cervical HeLa cells displayed distinctly different IL-6 RNA dynamics with increased basal IL-6 production, also dependent on ASM. These findings raise the possibility that invasive cancer cells have increased basal IL-6 mRNA stability while also eliciting a robust transcriptional response to PMA. These results begin to define the mechanisms involved in IL-6 synthesis from invasive cell lines. Taken together, this work shows a specific function for ASM as a regulator of p38 signaling and IL-6 production, and in aggressive cancer cells, a role for ASM as a potential factor in mediating a pro-invasive phenotype to cancer cells.

3.2. Experimental Procedures

3.2.1. Materials- Active-p38 (phospho) antibody and p38∂ antibodies were from Promega (Madison, WI) and R&D Systems (Minneapolis, MN) respectively. PMA was from Calbiochem (La Jolla). TNFa was from Pepro Tech. HRP-linked secondary antibodies were from Santa Cruz Biotechnology. Actinomycin D and Myriocin were purchased form Sigma. Invasion wells were from BD Bioscences. Fumonisin B1 was from Enzo Life Sciences (Farmingdale, NY).

3.2.2. Cell Culture- MCF-7, MDA-MB-231, HeLa, control fibroblasts, and Niemann Pick fibroblasts were grown in DMEM supplemented with L-glutamine and 10% fetal bovine serum. Cells were cultured under standard conditions (37

ºC, 5% CO_2, humidified air) and kept under 90% confluence. For a 6-well plate, 50,000 cells/well were plated and then the next day transfected with 20 nM siRNA according to manufacturer's instructions using Oligofectamine (Invitrogen). After 48-72 h, media were changed 1 h prior to stimulation with either PMA (100 nM) or TNFa (20 ng/ml). For overexpression of ASM, cells were plated at 50,000 cells/well of a 6 well plate. The next day, cells were transfected with 1µg of Control Vector (pEF6-V5/6xHis) or the ASM Expression Vector (pEF6-ASM-V5/6xHis) according to manufacturer's instruction using X-tremeGENE 9 (Roche). After 24 hours, media was replaced and cells were incubated for an additional 24 hours and IL-6 expression was measured by qPCR as described.

3.2.3. Western Blotting- Cells were harvested by direct lysis in 1% SDS/ 1 mM EDTA/ 50 mM Tris HCl pH 7.4. Lysates were sonicated, and total protein was normalized by BCA method. Laemmli buffer was added (6X), and then samples were boiled for 5 min. Equal volumes were loaded onto Criterion precast gels and run at 100V. Proteins were transferred to nitrocellulose membranes, blocked with 5 % nonfat milk in PBS/0.1 % Tween 20 and were incubated overnight with primary antibodies in 5 % nonfat milk in PBS/ 0.1 % Tween 20. Membranes were washed in PBS/ 0.1% Tween 20 at least 3 times, incubated with secondary antibodies (1:5000), washed again, and then developed in ECL chemiluminescence reagent (Pierce).

3.2.4. Reverse-transcriptase Reaction and PCR- Equal amounts of RNA were isolated (Qiagen, RNeasy kit) and used in reverse-transcriptase reaction according to manufacturer's protocol (Superscript II). The final reaction was diluted to 2 mg initial RNA/ml. For qPCR analysis, 5 ml of cDNA was used per 25 ml reaction in duplicate or triplicate using SYBR Green SuperMix (BioRad). Real-time PCR was performed using an iCycler (BioRad) consisting of a program of 95 °C for 3 min followed by 40 cycles of 95 °C for 15 sec, 60 °C for 45 sec and 68 °C for 30 sec. Threshold cycle (C_t) values of target genes were normalized to actin C_t values generating mean normalized expression (MNE) using Q-gene software[262] and expressed as fold change compared to control. Primers for IL-6 (Table 1) were designed using Primer-blast (NCBI) in order to amplify specifically mature mRNA, referred to as mRNA, (reverse primer aligning to contiguous regions of exon 1 and 2), hnRNA (reverse primer completely within intron), or both (reverse primer aligning to adjacent exon, exon 2, to the forward primer in exon 1) with a common forward primer for these reverse primers (Scheme 2). IL-6 primer specificity was validated with melt curves and by DNA electrophoresis. The primer set which would amplify both species was only used for semi-quantitative PCR while the others were used for qRT-PCR. ASM, CCL5/RANTES, and β-actin primer sequences were described previously[52, 59].

3.2.5. ELISA- Cultured media were harvested and IL-6 measured by human IL-6 ELISA according to manufacturer's protocol (R&D, Quantikine). Cellular protein

was harvested and measured by BCA method. IL-6 concentrations were normalized to total cellular protein yielding pg of IL-6/mg of total protein unless otherwise indicated. In no case did normalization alter the results significantly ruling out changes in total cell number or total protein content as the determinant.

3.2.6. Confocal Microscopy- Cells were washed with cold PBS, fixed in 3.7 % paraformaldehyde, and permeabilized in 0.1 %Triton X-100 for 10 minutes. Samples were blocked in 2 % human serum for 1 hr and then incubated with vimentin primary antibody in 2 % human serum for 90 min at room temperature. Samples were washed and incubated with secondary antibodies conjugated to TRITC for 1 hr. Samples were washed again and then incubated with DRAQ5 and phalloidin and wash steps were repeated before imaging on confocal laser microscope (LSM510 Zeiss).

3.2.7. Invasion Assay- HeLa cells were treated with siRNA for 48 hrs, trypsinized, and plated in transwells coated with matrigel in serum free media with either serum free or 10% serum in the bottom chamber. The cells were allowed to grow and invade for 24 h and then stained with flourescein. Four representative images each well were acquired and the number of cells invaded through the matrigel counted. Cells were plated in triplicate.

3.2.8. ASM Activity Assay- Protein lysates from MCF-7, MDA-MB-231, or HeLa were assessed for ASM activity as described previously using radiolabeled SM[263].

3.2.9. Statistical Analysis- Statistical and kinetic analysis was performed with Prism/GraphPad using one phase exponential decay equation for calculating half life of IL-6 mRNA. Results displayed are mean ± S.E. or the range when n<3 for a given experiment. Statistical tests were performed depending on the experiment with significance set at a p value of < 0.05.

3.3. Results

3.3.1. Differential regulation of IL-6 production and p38 activation by sphingolipid salvage enzymes-

Stimulation of the breakdown of complex sphingolipids by PMA through the salvage pathway has been shown to be dependent on PKCd, a novel PKC, in MCF-7 breast cancer cells[256]. Moreover, activation of ASM, leading to ceramide accumulation, has been linked to PKCd activity[234]. Due to the interplay between PKC signaling and sphingolipids, it was of interest to define the roles of classical and novel PKCs in the context of IL-6 production. MCF-7 breast cancer cells were pretreated with either Gö6976 or bisindoleilamide (Bis) for 1 h and then stimulated with PMA after which secreted IL-6 was measured. The classical PKC inhibitor, Gö6976, had no effect on PMA-induced IL-6 protein production whereas the classical and novel PKC inhibitor, Bis, ablated the PMA

response, implicating novel PKCs in this process (Fig. 10A, **Adapted from the Dissertation of DM Perry (2012)**).

To delineate the role of distinct components of the sphingolipid salvage pathway (Scheme 1) for their specific contribution to IL-6 production, MCF-7 cells were treated with siRNA against ACD, ASM, or GBA and then stimulated with PMA for 18 h (Fig. 10B, **Adapted from the Dissertation of DM Perry (2012)**). These siRNAs were previously used and validated in our laboratory[52, 256], and were further validated either by western blot or RT-PCR (Fig. 10E-F, **Adapted from the Dissertation of DM Perry (2012)**). MCF-7 cells were chosen because they produce very low baseline levels of IL-6 but high levels in terms of fold change upon stimulation with PMA making this an ideal system to elucidate PKC-mediated mechanisms. In accordance with our previous study[59], we found that silencing GBA potentiated production of IL-6 (Fig. 10B, **Adapted from the Dissertation of DM Perry (2012)**). Conversely, downregulation of ASM significantly decreased the production of IL-6, and loss of ACD had no effect on IL-6 (Fig. 10B, **Adapted from the Dissertation of DM Perry (2012)**). The stress kinase p38 is known to play a role in regulating both transcription and message stability of IL-6[264-267]. Therefore, we tested the effect of siRNA against the sphingolipid catabolic enzymes on p38 activation. In a similar fashion, knockdown of ASM blunted PMA-induced p38 phosphorylation, whereas knockdown of GBA increased the p38 activation significantly (Fig. 10C, **Adapted from the Dissertation of DM Perry (2012)**). These results mirrored the effects of ASM, ACD, and GBA on IL-6 production, suggesting that p38 is likely a

signaling pathway that is downstream of the sphingolipid enzymes upon PKC stimulation.

To test whether downstream metabolism of sphingolipids by ACD is required for the GBA or ASM response, co-knockdown of these enzymes was tested. The results demonstrated that in the presence or absence of ACD, there was a similar fold change in IL-6 upon ASM and GBA silencing (Fig. 10D, **Adapted from the Dissertation of DM Perry (2012)**). Taken together, these results demonstrate that in MCF-7, ASM is required for the induction of IL-6, but further metabolism of the ASM product ceramide to sphingosine via ACD is not required. Furthermore, these data reveal distinct and opposing roles for GBA and ASM in regulation of IL-6 production and p38 activation in response to PMA.

3.3.2. Involvement of ASM in IL-6 mRNA induction in MCF-7 cells-

The mechanisms by which PKC and ASM regulate IL-6 RNA were next assessed in order to determine at which point of IL-6 synthesis these are involved. To achieve this goal, we utilized standard Actinomycin D timecourse and also a novel approach characterized by Zeisel et al.[268], which specifically measures mRNA or hnRNA whereby inferences can be made whether changes seen are due to changes in transcription or mRNA stability. Therefore specific primers for IL-6 mRNA and hnRNA were designed and validated (Scheme 2, **Adapted from the Dissertation of DM Perry (2012)**). Treatment of MCF-7 cells with ASM siRNA resulted in a decrease in PMA-induced IL-6 mRNA levels, likely ruling out mechanisms of translational or secretory regulation as the point of

action but implicating transcription or message stability (Fig. 11A, **Adapted from the Dissertation of DM Perry (2012)**). To assess mRNA stabilization, an Actinomycin D timecourse was performed in MCF-7 cells in the presence or absence of either PMA and ASM siRNA. PMA resulted in a doubling of IL-6 mRNA stability, and ASM silencing decreased message stability basally and with PMA (Fig. 11B, **Adapted from the Dissertation of DM Perry (2012)**). Additionally, IL-6 hnRNA was measured in a similar fashion as in Fig. 11A, which revealed no induction of IL-6 hnRNA upon treatment with PMA; however, ASM siRNA with or without PMA treatment yielded approximately a 40% decrease in IL-6 hnRNA (Fig. 11C, **Adapted from the Dissertation of DM Perry (2012)**). Taken together, these data show that ASM has effects on both transcription and stability of IL-6 mRNA. The results also show that PKC activation primarily results in increased IL-6 message stability.

Previous work has demonstrated a role for ASM in the regulation of CCL5/RANTES in response to the cytokines, TNFa and IL-1b[52]. In order to assess the possibility that PMA is also inducing RANTES through a novel mechanism, MCF-7 cells were treated with PMA and IL-6 and CCL5 mRNA was measured. PMA was found to be a specific inducer of IL-6 and not RANTES, suggesting a novel signaling function for ASM in response to PMA (Fig. 11D). Additionally, it was of interest to assess the contribution of p38 towards IL-6 expression in our system. Interestingly, there was only a modest decrease in IL-6 mRNA basally and with PMA treatment with the pan p38 inhibitor BIRB 796 in MCF-7 cells (Fig. 11E) and HeLa cells (data not shown), even though there was

robust inhibition of p38 phosphorylation (Fig. 11F), suggesting that there could be other pathways by which ASM mediates its effect on IL-6. Therefore in MCF-7 cells, ASM leads to p38 activation and eventual induction of IL-6 mediated by both changes in transcription and message stability.

3.3.3. Evaluation of IL-6 protein and RNA in normal and Niemann-Pick Fibroblasts-

Next, the role of ASM in IL-6 secretion was tested in fibroblasts, which are a significant source of IL-6 during wound healing[269] and can support tumor metastasis[270]. Moreover, the availability of fibroblasts from patients with Niemann-Pick disease (NPD), which have significantly decreased ASM activity[52], allows evaluation of the role of ASM in a genetic model. Here we found that NPD fibroblasts have profoundly defective IL-6 production basally and with TNFa when compared to healthy control fibroblasts (Fig. 12A, **Adapted from the Dissertation of DM Perry (2012)**).

Next, we investigated the IL-6 RNA dynamics basally and in response to TNFa treatment in control and NPD fibroblasts. Loss of acid sphingomyelinase activity was found to decrease levels of IL-6 mRNA basally and with TNFa (Fig. 12B) as was found at the protein level. However, no difference was found basally in hnRNA levels between control and NPD fibroblasts, but TNFa-induced IL-6 hnRNA was significantly impaired in NPD fibroblasts (Fig. 12C, **Adapted from the Dissertation of DM Perry (2012)**), suggesting that ASM is required for TNFa-mediated transcriptional activation of the IL-6 gene in fibroblasts. Taken

together, the results suggest that ASM plays a role in the basal stability of IL-6 mRNA due to the decrease of basal IL-6 mRNA (but not hnRNA) and then also in mediating TNFa-dependent transcription of IL-6 hnRNA.

3.3.4. The role of ASM in IL-6 production and p38 activation in HeLa and MDA-MB-231 cells-

The contribution of ASM to IL-6 synthesis was assessed in invasive human cervical HeLa cancer cells as well as human breast MDA-MB-231 cancer cells, since invasive cell lines make significantly more IL-6 in absolute levels than non-invasive lines, and IL-6 plays a role in their malignant properties[252, 254, 271]. First, we evaluated the role of ASM in these additional cell lines in regulating IL-6. Knockdown of ASM by siRNA in HeLa cells resulted in decreased IL-6 production in response to both PMA and TNFa (Fig. 13A, **Adapted from the Dissertation of DM Perry (2012)**). Further, treatment of MDA-231 and HeLa cells with desipramine (50mM), a lysomotropic agent that induces the degradation of ASM[272], resulted in a dramatic decrease in IL-6 production in all cases (Fig. 13B-C, **Adapted from the Dissertation of DM Perry (2012)**). Thus, these results show that ASM is involved in IL-6 production in response to TNFa and PMA in two invasive cancer cell lines. Likewise, inhibition of ASM with siRNA or desipramine abrogated p38 phosphorylation in HeLa cells (Fig. 13D-E, **Adapted from the Dissertation of DM Perry (2012)**). Next, treatment of HeLa cells with desipramine (50mM) was found to blunt PMA-induced IL-6 mRNA expression consistent with the model that ASM and p38

induce IL-6 mRNA leading ultimately to IL-6 protein secretion (Fig. 13F, **Adapted from the Dissertation of DM Perry (2012)**). The effectiveness of ASM knockdown in HeLa was demonstrated by a significant decrease in ASM mRNA and activity upon 48 h of ASM siRNA treatment (Fig. 13G-H, **Adapted from the Dissertation of DM Perry (2012)**).

3.3.5. Differential IL-6 RNA dynamics in MCF-7 compared to HeLa and MDA-MB-231 cells in response to PMA-

Synthesis of IL-6 is a dynamic process with multiple regulated steps including transcription, message stability, and translation. It is known that protein and mRNA levels of IL-6 are increased in cell lines such as MDA-MB-231 compared to MCF-7, but it is not known whether this is due to stability or transcription[254]. To investigate potential differences and mechanisms in IL-6 RNA dynamics in response to PKC signaling between MCF-7, MDA-MB-231, and HeLa cells, a time course of PMA was performed, and levels of mRNA and hnRNA were determined utilizing primers with either exonic or intronic reverse primers[268]. In MCF-7, PMA treatment resulted in a 35-fold induction of IL-6 mRNA, yet no detectable change in hnRNA was observed, suggesting that IL-6 induction is primarily due to increased message stability (Fig. 14A, **Adapted from the Dissertation of DM Perry (2012)**). To further assess the process of transcription, a luciferase-based promoter assay was utilized. Using a human IL-6 promoter assay, PMA stimulated promoter activity by 2.3-fold in MCF7 cells (data not shown). This moderate change does not explain the dramatic

induction at the mRNA and protein level in response to PMA (Fig. 10) but is difficult to reconcile with the unchanged hnRNA levels (Fig. 14A, **Adapted from the Dissertation of DM Perry (2012)**). Taken together, PKC-mediated induction of IL-6 mRNA in MCF-7 is mediated primarily by message stability and a possible minor contribution of transcription.

Next, IL-6 RNA dynamics were assessed in MDA-MB-231 and HeLa cells. PMA treatment resulted in IL-6 mRNA induction, and further, there was a 2-fold and 6-fold induction of hnRNA at 45 minutes in MDA-MB-231 and HeLa respectively, which preceded the time-dependent increase in mRNA at 90 min (Fig. 14B-C, **Adapted from the Dissertation of DM Perry (2012)**). Additionally, IL-6 promoter activity was assessed in HeLa, and the results showed a 2.8 fold increase in promoter activity in response to PMA (data not shown). Therefore, based on increased IL-6 luciferase promoter activity and increased endogenous hnRNA, PMA results in transcriptional activation of IL-6 expression in HeLa and MDA-MB-231. Conversely, we can infer that PMA also results in increased message stability since, for example in HeLa cells, a 6-fold increase in transcription is not sufficient to explain the 25-fold increase in IL-6 mRNA. Based on the RNA profiles of MDA-MB-231 and HeLa and the promoter activity assay, IL-6 RNA induction is explained by a combination of transcriptional activation and message stabilization.

3.3.6. Basal induction of the ASM/IL6 pathway in invasive cancer cells-

The most striking difference between the cell lines, in the context of IL-6, is the basal level of IL-6 mRNA despite having approximately equivalent basal hnRNA (Fig. 14D, **Adapted from the Dissertation of DM Perry (2012)**). We wondered if this difference could be due to ASM. To investigate this possibility, we hypothesized there may be differences in ASM expression between the 3 cell lines. ASM mRNA was measured by RT-PCR, and the results showed a 2-3 fold upregulation of ASM message in HeLa and MDA-MB-231 compared to MCF-7 (Fig. 14E). Furthermore, we determined the effects of silencing ASM in HeLa on basal levels of IL-6 mRNA, and the results showed that this caused a 40% reduction in basal IL-6 mRNA (Fig. 14F, **Adapted from the Dissertation of DM Perry (2012)**). Additionally, overexpression of ASM in MCF-7 lead to a 5.3-fold upregulation of basal IL-6 mRNA (Fig. 14G). In summary, upregulation of ASM in invasive cancer cells may play a role in the stabilization of IL-6 mRNA, thus explaining the previous findings that MDA-MB-231 and HeLa cells have higher levels of IL-6 mRNA than MCF7 cells.

3.3.7. Role of ASM in Cancer Cell Invasion-

Due to the abundant evidence linking IL-6 to pro-invasive biological processes, it became important to assess the role of ASM in cancer cell invasion. HeLa cells were treated with either control or ASM siRNA for 48 h and subsequently transferred to precoated matrigel invasion wells. Knockdown of ASM resulted in a dramatic decrease in serum-induced invasion through matrigel (Fig. 15A). ASM was also required for invasion in MDA-MB-231, suggesting that

ASM could be playing a fundamental role in the pathological process of invasion (data not shown). Furthermore, we assessed the roles of PKC and p38 in invasion by adding PMA or BIRB 976 to the upper chamber during invasion (Fig. 15B). PMA treatment enhanced invasion over media alone whereas BIRB 796 largely blocked PMA-induced invasion. Pretreatment of BIRB 796 with HeLa cells effectively blocks PMA-induced p38 phosphorylation showing that it is active at the used concentration (Fig. 15C). Additionally, to assess for morphologic changes, immunofluorescent microscopy was performed, which revealed significant loss of typical F-actin stress fibers with a rearrangement of cellular architecture upon ASM knockdown (Fig. 15D). This striking change was mirrored by decreased levels of phosphorylation of myosin light chain (MLC) in HeLa (data not shown). Taken together the results demonstrate a role for ASM in sustaining cytoskeletal changes toward invasion in cancer cells, which is consistent with its role in regulating p38 and IL-6.

3.4. Discussion

In this study a role for ASM was demonstrated in the regulation of p38 signaling and the pro-invasive cytokine IL-6 with potential implications for a role for ASM in cancer progression. The biochemical and signaling functions of ASM were specific in that they could be distinguished from those of GBA, the other key enzyme involved in generation of lysosomal ceramide. ASM was demonstrated to play an important role in IL-6 production at the protein and message level with effects on transcription and message stability. Further, ASM was shown to be

critically involved in the pathobiological process of invasion, a possible consequence of its regulation of IL-6.

3.4.1. Regulation of IL-6 by PKC and Sphingolipid Metabolism-

This work reveals a new role for the novel PKC family in upregulating IL-6. This relates to previous work from our laboratory which showed that the novel isoform PKCd is required for ASM activation leading to ceramide accumulation[234]. Moreover, ASM and GBA, both contribute to PKCd-dependent ceramide accumulation, which is predominantly C_{16}-ceramide[256]. However, unique biological roles for ASM- and GBA-derived ceramide had not been defined in the same context. Here we show that the novel isoforms of PKC are required for PMA-induced IL-6 production in MCF-7 (Fig. 10A). Thus, the data provide further evidence linking PKCs to sphingolipid-mediated pathways.

Our results reveal distinct roles for ASM and GBA in the regulation of IL-6, suggesting that ASM- and GBA-derived ceramides have opposing biological functions although being predominantly structurally identical (mostly C_{16}-ceramide) (Fig. 10B)[256]. These findings raise the possibility of a novel paradigm that not only the specific identity of a bioactive sphingolipid is important, but that the enzyme from which it is produced within a subcellular location may dictate its biologic function. Based on our studies, the subcellular topology was not defined, but we speculate that ASM and GBA are acting on their respective substrates at somewhat distinct points in the endolysosomal system which is involved in recycling SM and GC from the plasma membrane to

the lysosome [273, 274]. In terms of transducing a signal, the plasma membrane, or early endosomes, appear to be a more likely candidate than the lysosome, which itself is encased by the limiting membrane, where ASM and GBA are in the lumen, bound to and degrading internal membranes within the lysosome. Alternatively, or in addition, the levels of substrates of these two enzymes could play a key role in dictating the specific functions attributed to ASM versus those attributed to GBA.

3.4.2. Regulation of Cytokine Production and p38 by ASM-

Previous reports have studied cytokine regulation by ASM with varying results. This is likely due to the use of various approaches and distinct regulation of different cytokines. Previous studies have used $ASM^{-/-}$ peritoneal macrophages showing no requirement of ASM for the production of various inflammatory mediators including nitric oxide, TNFa, and IL-1b[259, 275]. Conversely, a transcriptional inhibitor of ASM, SMA-7, was shown to reduce cytokine production although the specificity of this inhibitor has not been well established [260]. Additionally, while this work was in progress, Kumagai et al. showed involvement of ASM in the synergistic production of IL-6 in response to carcinogenic electrophiles with TNFa but not TNFa alone in bladder cancer cells where these electrophiles resulted in ASM upregulation[276]. Further, recent work by Jin et al. showed ASM involvement in palmitic acid-induced IL-6 upregulation in macrophages[277], suggesting a common role for ASM in IL-6 production.

Previous work from our laboratory has demonstrated a role for ASM in the production of the chemokine, CCL5/RANTES[52]. Interestingly, this is likely a distinct pathway of regulation from that by which ASM regulates IL-6. This is supported by the requirement of ACD for induction of RANTES whereas loss of ACD trended towards an increase in IL-6 production in MCF-7, thus distinguishing these two pathways. Additionally, PMA was found to be a specific inducer of IL-6 (Fig. 11D). One explanation of these data is that IL-6 and CCL5/RANTES are distinct in their expression pattern in response to cytokine stimulation: IL-6 being rapidly induced while RANTES displays slower kinetics[278]. Consistent with this, IL-6 mRNA is basally unstable containing multiple 3' UTR AREs and is regulated substantially by increases in stability whereas RANTES mRNA is intrinsically very stable[278]. What is emerging therefore suggests coordinated regulation of these classes of cytokines by sphingolipids, such as ceramide, sphingosine, and sphingosine-1-phosphate (S1P). Ceramide, produced first metabolically, may be critical for IL-6, which is induced acutely, and then accumulation of sphingosine may trigger the transition to induction of late response genes such as RANTES.

This work provides novel evidence for a role for ASM in p38 activation in cancer cells. Previous evidence showed that ASM is not required for p38 signaling in murine macrophages by using $ASM^{-/-}$ macrophages, a different context than employed here and with inherent caveats concerning complete knockout systems for sphingolipid enzymes (i.e. they recapitulate genetic disease but may not capture the biological role of the enzyme). More likely, the

role of ASM in p38 signaling may be cell-type specific. There are some reports of exogenous ceramide activating p38 signaling, but there is no previous evidence demonstrating that a specific ceramide-producing enzyme is required for p38 activation[259, 279-281]. Moreover, if the enzyme from which ceramide is derived dictates its function, then exogenous ceramide is unlikely to recapitulate the function of specific pools of endogenous ceramides. Despite a role for ASM in p38 activation shown here, the mechanism of this effect is still elusive. ASM may be directly involved in the signaling in response to outside signals to p38 or the loss of ASM may render cells unable to activate p38 by a gain of function upon inhibition of ASM. Preliminary results show activation of p38 upon overexpression of ASM in HeLa (data not shown) arguing against the possibility that loss of ASM results in a gain of function that blocks p38 activation. Additionally, recent work by Adada et al. has shown that sphingosine kinase 1 (SK1) and S1P are involved in p38 activation in HeLa[282], which raises the possibility that ASM, ACD and SK1 may function in concert to produce S1P which could lead to activation of p38. However, this would be cell type specific since in MCF-7 cells, ACD is not required for p38 phosphorylation (Fig. 10C). In light of the body of literature showing activation of sphingomyelinase activity and ceramide accumulation in response to outside signals [234, 256, 257, 283] it is not far-fetched that ASM/ceramide participate in the acute activation of p38, and other ceramide producing enzymes contribute to resolution of p38 activity.

3.4.3. Implications for Cancer Biology-

The finding that ASM is involved in IL-6 production and invasion casts ASM in a novel role. Previous literature has implicated ASM in the accumulation of ceramide and downstream apoptosis in response to UV-light[284, 285], ionizing radiation[286] and other stimuli[287-289]. One could speculate that activation of ASM in normal cells is capable of inducing apoptosis, but once cancer cells are resistant to cell death, ASM activity could translate to increased inflammatory cytokines and invasiveness. In some ways this is analogous to the dual nature of p38 signaling in apoptosis versus oncogenic properties[290]. Additionally, due to the accumulating evidence for IL-6 as a critical player in cancer biology, targeting pathways that are involved in IL-6 synthesis or downstream effects may prove to be a powerful approach for attenuating invasion and metastasis[250, 291]. Inhibition of ASM could be a therapeutic means to block IL-6 produced in the microenvironment by tumor cells, which is required for invasion. Future work is needed evaluate the role of ASM in cancer progression or metastasis.

In summary this work provides evidence for a clear role for ASM in the regulation of p38 signaling and IL-6 production. This regulation is specific in that other sphingolipid salvage pathway enzymes did not replicate this. ASM was found to be essential for p38 activation as well, defining a role in upstream signaling to IL-6. In line with this, ASM was required for invasion of HeLa cells. Moreover, ASM may play a critical role in mediating the increased levels of IL-6 found in invasive cell lines. The contribution of ASM to both malignant

progression and IL-6 production is partially dependent on p38, however a p38 independent mechanism may still directly link ASM to invasion and IL-6 production (Fig. 15E). This implicates ASM as a novel player in several malignant cancer properties, and may indicate that ASM is an attractive target for therapeutic intervention in addition to p38. This work for the first time, demonstrates a regulatory role for ASM in a signaling pathway and a biological outcome of cytokine induction including mechanistic insights and disease implications. Further investigation is needed to understand how ASM is mediating its effects on p38 and IL-6.

Chapter 4

FUTURE DIRECTIONS AND DISCUSSION OF SPHINGOLIPID REGULATED BREAST CANCER PROGRESSION AND INDUCTION OF $CD44^{+}/CD24^{-}$ CANCER STEM LIKE CELL GROWTH THROUGH ACTIVATION OF NFATC3 SIGNALING

4.1. Introduction

The findings presented in this thesis have placed great emphasis on the role of ASM and CERK in modulation of inflammatory cytokines. As such, ASM and CERK appear to be potent regulators of the tumor microenvironment through modulation of two key cytokines: CCL5 and IL-6. Early in tumorigenesis, infiltrating macrophages secrete high levels of TNF-α and induce apoptosis in most tumor cells [292]. A subset of cells, however, is resistant to apoptosis and continues to grow. ASM and CERK have been shown to be important modulators of TNF-α stimulated signaling in a variety of tumor types [53, 68, 74, 236, 293-298]. Our recent work has clearly demonstrated that ASM and CERK are necessary for both IL-6 and CCL5 production in response to TNF-α stimulation. These findings suggests that ASM and CERK may be modulating a fundamental process underlying inflammatory signaling at large.

Beyond subcellular regulation of inflammatory signaling, ASM and CERK are key modulators of the tumor microenvironment through IL-6 and CCL5. Both IL-6 and CCL5 play prominent roles in maintenance of a pro-tumor microenvironment. With respect to CCL5, a large proportion of the CCL5 in breast tumors originates from stromal cells, however, early in tumorigenesis, tumor derived CCL5 is known to induce a tolerogenic response by the immune system [299, 300]. The result being aggregation of Th2 polarized T-cells, and a subdued tumor targeting inflammatory response [301].

IL-6 has many functions within breast tumors that are dependent on tumor type and tumor stage. In the early stages of tumorigenesis, IL-6 is mainly

secreted by tumor associated stromal cells and acts as a potent inducer of EMT in ER positive breast cancers [252, 302]. Once cells have undergone EMT, tumor derived IL-6 induces an autocrine-signaling cascade that results in very high levels of intratumoral IL-6 [303, 304]. The resulting supraphysiologic levels of IL-6 activate EMT, mitogenic, and migratory pathways in the tumor cells, leading to rapid tumor progression.

Acquisition of EMT like phenotypes is associated with rapid tumor progression. EMT is characterized by loss of cell adhesion and polarization leading to adhesion independent growth [305]. A key event in EMT progression is reduced expression of E-Cadherin secondary to random genomic mutation, epigenetic regulation, or activated repressive pathways mediated by Snail, Slug, Twist, or Zeb1 [222, 306]. Several cytokines, such as IL-6, TNF-α, and TGF-β are known to be powerful inducers of EMT in breast cancers. Specifically, TNF-α dependent activation of NF-kB induces Twist activation [307]. NF-kB activation also leads to production of several other pro-EMT cytokines such as IL-6 and TGF-β [308].

ASM and CERK are essential to the TNF-α response in breast cancer cells, and as such, regulate a wide array of pro-tumorigenic and pro-EMT signaling pathways. ASM and CERK were found to be necessary for expression of TNF-α, IL-6, CCL5, CCL2, CCL18, and TGF-β. Furthermore, CERK is required for NFAT translocation to the nucleus of TNF-α treated cells. Based on these findings, ASM and CERK define a pro-EMT signature in breast cancers and are required for tumor progression *in vivo* and *in vitro*.

4.2. Materials and Methods

4.2.1. Materials- MCF7 and MDA-MB-231 cells were obtained from ATCC (Manassas, VA). Trypsin-EDTA (0.05%) was from Gibco (Holtsville, NY, Cat 25300062). TNF-α was purchased from Peprotech (Rocky Hill, NJ).

4.2.2. Cell Culture- MCF7 cells were maintained in RPMI from Gibco (Holtsville, NY, Cat 11875-093) supplemented with 10% (v/v) heat inactivated FBS from HyClone (Port Washington, NY, Cat SH30396.03). MDA-MB-231 cells were maintained in DMEM from Gibco (Holtsville, NY, Cat 11965-092) supplemented with 10% (v/v) heat inactivated FBS under normal cell culture conditions (humidified atmosphere, 95% air, 5% CO2, 37 °C). Cells were kept in culture for no longer than 30 days. All cell lines were tested monthly for mycoplasma contamination using the MycoAlert kit from Lonza (Allendale, NJ, Cat LT07-218). Cells were maintained at less than 75% confluency in standard cell culture conditions (humidified atmosphere, 95% air, 5% CO2, 37 °C). All cell treatments with TNF-α or IL-1β were carried out in serum free media, unless otherwise noted.

4.2.3. Mammosphere assay- Mammospheres were generated as previously described [309] with the addition of 0.25% methylcellulose to the mammosphere media. Briefly, 1x10^4 MCF7 cells were plated per well of a 6 well, non-adherent tissue culture tray in DMEM/F12 media (Gibco, Cat 21041) supplemented with B27 and rEGF (20ng/mL). Cells were allowed to grow for 5 days, without

agitation, and then the resultant mammospheres were harvested by centrifugation, trypsinized, and replated in monolayer on tissue culture treated dishes. After 24hrs of growth, cells were harvested for RTPCR and ASM activity assays.

4.2.4. Real Time Reverse Transcriptase-Polymerase Chain Reaction (RTPCR) and Cytokine Arrays- RNA purification was performed with the Purelink RNA Kit from ThermoFisher, according to manufacturer's protocol. Concentration of RNA was determined by nanodrop, and 500ng of RNA was transformed into cDNA using the Quanta cDNA Kit (Gaithersburg, MD, Cat 95047) according to the manufacturer's protocol. For RT-PCR, reactions were performed in triplicate in 96-well plates with each reaction containing 10 µl of 2 × iTAQ mastermix, 5 µl of diluted (1:12, v/v) cDNA, 1 µL of FAM tagged Taqman gene specific primer probe, 0.3 µL of VIC tagged Actin probe, and 4 µl of water. The following probes were purchased from Life Technologies: ACTB (Cat Hs01060665_g1); ASM (Cat Hs03679347_g1); CERK (Cat Hs00368483_m1); CCL5 (Cat Hs00174575_m1). Cytokine arrays were obtained from ThermoFisher (Cat 4414084) and used according to manufacturer's protocol.

4.2.5. Transwell invasion assays- Invasion of cells was measured using the Corning BioCoat Tumor Invasion System (Cat 354165), according to manufacturer's protocol. Briefly, MDA-MB-231 cells were trypsinized, and resuspended in serum free media at a concentration of 5x10^4 cells/mL. 500µL of cell suspension was added to the upper well of each chamber of the transwell

plate. The lower chamber contained serum free media (control), complete media, or complete media plus TNF-α. Cells were allowed to invade for 48 hrs, and invasion of live cells was quantified by staining cells with Calcein AM and measuring fluorescence using a Spectra Max M5 mulit Plate reader.

4.2.6. Tissue microarray- Tissue Microarrays were obtained from US Biomax (Rockville, MD, Cat BR1504). Immunohistochemistry (IHC) for ASM was performed using a monoclonal antibody from Abgent (San Diego, CA, Cat AP12227b). IHC was performed as previously described [310]. Briefly, array slides were deparaffinized and rehydrated with serial ethanol dilutions. Endogenous peroxidase activity was neutralized using 0.3% Hydrogen Peroxide. Antigen retrieval was performed using sodium citrate buffer (pH 6) containing 0.05% Tween-20. After washing in PBS, sections were blocked for 10 minutes with horse serum from the VECTASTAIN ImmPress Kit (Vector Laboratories Inc.). Sections were then incubated overnight at 4°C with the ASM primary antibody (1:750), followed by 3 PBS washes. After a 30 min incubation with biotinylated secondary antibody, slides were incubated with DAB reagent per manufacturer's protocol. Slides were briefly counterstained with hematoxylin, rehydrated, and mounted for analysis by bright field microscopy.

4.2.7. Transcription Factor Arrays- MCF7 cells were treated with siRNA, and nuclei were harvested. Nuclear protein was extracted and applied to the Signosis

Transcription Factor Arrays (FA-1002) according to the manufacturer's instructions.

4.2.8. KM Plot data analysis- Outcomes analysis was performed using the KM Plot tool (http://kmplot.com/analysis/index.php?p=service&cancer=breast) [311]. The following probes were selected for analysis using the multigene classifier tool: SMPD1 (209420_s_at); CERK (218421_at); CCL5 (204655_at); CCL2 (216598_s_at); CCL18 (209924_at); and NFATc3 (207416_s_at). Patients were split into high and low expressing groups by allowing the program to auto select best cutoff based on total expression. The analysis was run on patients with metastatic disease as indicated by a positive lymph node status (n=945). To test for co-expression of selected genes, the multigene classifier was set to use the mean expression of the selected probes.

4.3. Results and Future Directions

4.3.1. Determining the role of the ASM/CERK signaling axis in cytokines associated with EMT

The ASM/CERK signaling axis promotes the production of a large number of inflammatory cytokines (Fig 16A). Of particular interest are several cytokines that are directly involved in the process of epithelial to mesenchymal transition (EMT), including TNF-α, IL-6, CCL5, CCL2, CCL18, and TGF-β [307, 312, 313]. Activation of inflammatory signaling pathways such as PI3K, p38/MAPK, STAT3, and others are well-studied activators of EMT. In the most well characterized model of EMT, epithelial cells are treated with TGF-β and the subsequent induction of Smad signaling leads to transactivation of Snail and Twist [314]. Other inducers of EMT include TNF-α, which is a potent inducer of p38/MAPK, and CCL18, which induces PI3K [307]. Additionally, IL-6, in coordination with CCL2, is known to induce EMT through activation of STAT3 [212, 312]. The role of CCL5 in EMT is largely unexplored, however, expression of CCL5 is highly expressed by post-EMT cells [315]. Together these cytokines may represent a clinical signature that defines novel therapeutic opportunities for targeting tumors that rely on the ASM/CERK signaling axis.

The loss of adhesion molecules, acquisition of mesenchymal phenotypes, and loss of cell polarity broadly characterize the process of EMT. Furthermore, the extent to which cells within an epithelial tumor have undergone EMT is closely correlated with tumor progression and poor outcomes [316]. During EMT, epithelial markers, such as E-cadherin decrease, and mesenchymal markers,

such as N-cadherin and vimentin, increase. As the cells transition from epithelial like to mesenchymal like, the cells no longer exhibit normal sheet-like growth patterns.

The data in Figure 16A suggests that ASM and CERK may be master regulators of an EMT inducing cytokine signature that defines a novel pro-metastatic pathway in breast cancer. It will be important to test the role of ASM and CERK in EMT through quantification of epithelial and mesenchymal markers in MCF7 cells induced to undergo EMT. In epithelial cancers, such as breast cancer, the process of EMT is a prerequisite for gaining metastatic potential. Breast cancer cells that have undergone EMT exhibit many CSC characteristics and are highly drug resistant and aggressive [306].

Once the contribution of ASM and CERK to EMT has been determined, additional experiments investigating the role of ASM and CERK in cancer stem like cell (CSC) growth can be carried out. Several methodologies have been developed to assay CSC formation the most common of which is the mammosphere assay. Growth of luminal breast cancer cells in a low adhesion environment produces non-adherent mammospheres, and the resultant mammospheres are enriched in $CD44^{+}/CD24^{-}$ cells [317]. CSC's exhibit phenotypes concordant with cells from advanced tumor types, however the precise correlation between CSC content within a tumor and tumor progression is not exactly known [318, 319]. By investigating the function of ASM and CERK as both regulators of CSC growth and tumor progression, the function of CSC's in tumor progression will be clarified. Preliminary data has shown CERK, CCL5,

and IL-6 are upregulated in CSC's as compared to MCF7 cells in monolayer, suggesting these genes may paly a role in CSC's (Fig. 16B). It will be of critical importance to directly test the requirement for ASM and CERK expression for efficient CSC formation.

4.3.2. Delineating the contribution of the ASM/CERK signaling pathway in tumor progression in vitro and in vivo

Using a Matrigel® tanswell invasion system, we have demonstrated that ASM and CERK play a pivotal role in the invasiveness of the post-EMT breast cancer cell line MDA-MB-231 (Fig. 17A). MDA-MB-231 cells are highly metastatic and have a mesenchymal like phenotype as well as a very high proportion of $CD44^{+}/CD24^{-}$ cells [317]. This data suggests that, in addition to being required for acquisition of EMT like phenotypes, ASM and CERK are required for tumor progression following EMT, and possibly for maintenance of EMT like phenotypes in advanced tumors. The hallmarks of EMT are loss of intracellular tight junctions and impaired α5β1 integrin activation leading to disrupted cell-to-cell adhesion. Recent literature has shown a distinct role for ASM in cell-to-cell adhesion, and inhibition of ASM may be a useful method for reducing metastasis of solid tumors [68].

In accordance with the transwell invasion results, immunostaining for ASM in breast cancer tumor microarrays has demonstrated that ASM expression is correlated with advanced tumor stage (Fig. 17B). Together these data predict that ASM is required for tumor progression, and indeed recent literature also

supports the hypothesis [294]. Additionally, analysis of publically available outcomes data has shown a strong correlation between expression of ASM and CERK and poor outcomes in metastatic disease (Fig. 17C). With these results in mind, it will be important to undertake mechanistic studies in mouse models of metastasis to delineate the role of ASM and CERK in tumor progression. To this end, genetically modified mouse breast carcinoma cells have been developed using CRISPR technology. The cells have altered lipids and decreased enzymatic activity of ASM and CERK. Utilizing these cells in tail vein injection and mammary fat pad injections will directly answer the question of weather or not ASM and CERK are required for metastasis of solid tumors. Identifying the precise role of ASM in tumor progression will be an important step toward developing therapies targeting sphingolipid metabolism.

4.3.3. Identifying the network of transcription factors regulated by CERK

Abundant data has implicated CERK in the regulation of several cytokines [320]. This suggests that CERK and C-1-P maybe regulating processes fundamental to cytokine production. To address this question, we ablated CERK, and treated cells with TNF-α. Nuclear preps from these cells were prepared and used for transcription factor binding analysis using Signosis Transcription Factor Array Plates. CERK was found to regulate a number of transcription factors (Fig. 18A and Table 3), with a very profound effect on Nuclear Factor of Activated T-cells (NFAT) family members (Fig. 18A). Considering that CERK is required for invasion, production of EMT promoting cytokines, and binding of NFAT to target

sequences, a strong argument can be made that CERK is regulating a novel pro-metastatic pathway. The prediction from this data would be that CERK is regulating cytokine production through modulation of NFAT family members, and that the resultant cytokines are inducing tumor progression.

The family of NFAT transcription factors has four members, and canonical activation of NFAT requires a transient spike in cytoplasmic Ca^{2+} and subsequent activation of calmodulin [321]. Calmodulin dependent de-phosphorylation of serine residues on NFAT results in exposure of NFAT nuclear localization signals and rapid accumulation of NFAT in the nucleus. In the nucleus, NFAT can form transcriptionally active complexes with several other transcription factors including fork-head box (FOXO) transcription factors, activator-protein 1 (AP-1), and members of the GATA transcription factor family.

Over expression of NFAT family members has been shown to induce progression in a variety of epithelial tumors including lung and colon cancer, and NFAT family members are key regulators of the balance between proliferation and EMT in breast carcinomas [322-325]. As such, it will be essential to clearly identify the relationship between NFAT and CERK mediated EMT in breast cancer. To this end, commonly available inhibitors of NFAT, such as cyclosporine and tacrolimus, as well as siRNA can be used to delineate the contribution of NFAT to mammosphere formation and production of CERK dependent cytokines including IL-6, CCL5, CCL18, and TGF-β. Furthermore, the role of NFAT in breast cancer cell invasion, as measured by Matrigel® Transwell assays, will be of particular interest. Based on the current data, it appears that NFAT is

modulating the response to TNF-α and may participate in the ASM/CERK signaling cascade.

4.3.4. Delineating the clinical significance of a pro-invasive cytokine network defined by CERK, NFAT, IL-6, CCL5, and CCL18 in primary human tumors

The ASM/CERK signaling axis is highly correlated with poor outcomes in breast cancer (Fig. 17C). Therefore, the hypothesis was put forth that tumors expressing high levels of cytokines induced by ASM and CERK are associated with poor outcomes in breast cancer. Analysis of the cytokine signature of ASM and CERK overexpressing cells revealed that of the 27 most highly expressed cytokines, IL-6, CCL5, and CCL18 are highly correlated with poor outcomes in metastatic disease (data not shown). The finding that CERK is required for NFAT function led to the hypothesis that NFAT is participating in the CERK/C-1-P dependent signaling pathway. Together this data led to the hypothesis that tumors expressing a novel signaling cascade instigated by CERK, mediated by NFAT, and resulting in IL-6, CCL5, and CCL18 production is predictive of disease advancement. Indeed, analysis of metadata has shown that the signaling cascade defined by CERK/NFATc3/IL-6/CCL5/CCL18 is highly predictive of tumor progression (Fig 19A).

The heterogeneous composition of a breast tumor complicates the investigation of tumor immunology and cytokine signaling. Since both the tumor cells and infiltrating immune cells affect cytokine production of each other, it is important to first separate the cell autonomous effects from the intrinsic effects of

secreted cytokines. For example, tumor cells produce a very high proportion of the IL-6 within breast tumors [222, 326]. Additionally, this tumor derived IL-6 initiates a feed forward, autocrine signaling pathway that promotes growth of the tumor [222]. Likewise, many of the effects of CCL5 are dependent on paracrine signaling between tumor infiltrating mesenchymal stem cells (MSC) and the tumor cells themselves. The MSC's induce tumor cells to produce high levels of CCL5, and the resulting increase in intratumoral CCL5 induces metastasis of the tumor cells [299]. The role of CCL18 in breast cancer is not well understood due to the lack of a murine homolog. Nevertheless, CCL18 is a powerful chemoattractant for a variety of breast cancer cells, and high serum levels of CCL18 are associated with very poor outcomes in breast cancer patients [313, 327-330].

Based on available data, the role of the CERK/NFATc3/IL-6/CCL5/CCL18 signaling pathway is likely to be cell intrinsic. To test this hypothesis, it will be necessary to ablate cells for CERK or NFATc3 and carry out Matrigel® Tranwell invasion assays using IL-6, CCL5, and CCL18 in combination and individually as chemoattractants. Pending these results a prediction can be made as to weather or not the function of these cytokines is cell autonomous or non-cell autonomous. To conclusively answer the question of weather or not tumor derived IL-6, CCL5, and CCL18 are promoting tumor progression, each cytokine should be genetically ablated and xenograft studies carried out with the resultant cells. Cells unable to express any or all of these cytokines would be expected to be less aggressive in a xenograft model, and the aggressiveness would be expected

to be rescued by treatment with exogenous cytokines.

ASM and CERK were shown to regulate a network of pro-tumorigenic cytokines that are known to promote EMT in epithelial cancers. Following EMT, tumor cells become highly invasive and ASM and CERK were found to be required for invasion of the mesenchymal like MDA-MB-231 cell line. In support of the *in vitro* findings, *in silico* analysis of breast cancer outcomes demonstrated that tumors expressing high levels of ASM and CERK have worse outcomes than their low expressing counter parts. Furthermore, CERK was found to regulate NFAT function, suggesting that NFAT may play a role in the ASM/CERK signaling axis. In support of a prometastatic role for NFAT, *in silico* analysis suggests that ASM and CERK define a prometastatic pathway involving NFAT, IL6, CCL5, and CCL18. Future work will focus on the role of ASM and CERK in modulating the early events of EMT and tumor progression.

References

1. Society, A.C., *Cancer Facts & Figures 2013*, 2013, American Cancer Society: Atlanta, GA.
2. Hajdu, S.I., *A note from history: landmarks in history of cancer, part 1.* Cancer, 2011. **117**(5): p. 1097-102.
3. Vargas, A., et al., *[The Edwin Smith papyrus in the history of medicine].* Rev Med Chil, 2012. **140**(10): p. 1357-62.
4. Aszmann, O.C., *The life and work of Theodore Schwann.* J Reconstr Microsurg, 2000. **16**(4): p. 291-5.
5. Triolo, V.A., *NINETEENTH CENTURY FOUNDATIONS OF CANCER RESEARCH ADVANCES IN TUMOR PATHOLOGY, NOMENCLATURE, AND THEORIES OF ONCOGENESIS.* Cancer Res, 1965. **25**: p. 75-106.
6. Hajdu, S.I. and F. Darvishian, *A note from history: landmarks in history of cancer, part 5.* Cancer, 2013. **119**(8): p. 1450-66.
7. Hajdu, S.I., *A note from history: landmarks in history of cancer, part 4.* Cancer, 2012. **118**(20): p. 4914-28.
8. Sistrunk, W.E. and W.C. Maccarty, *LIFE EXPECTANCY FOLLOWING RADICAL AMPUTATION FOR CARCINOMA OF THE BREAST: A CLINICAL AND PATHOLOGIC STUDY OF 218 CASES.* Ann Surg, 1922. **75**(1): p. 61-9.
9. Hajdu, S.I. and M. Vadmal, *A note from history: Landmarks in history of cancer, Part 6.* Cancer, 2013. **119**(23): p. 4058-82.
10. Beatson, G., *ON THE TREATMENT OF INOPERABLE CASES OF CARCINOMA OF THE MAMMA: SUGGESTIONS FOR A NEW METHOD OF TREATMENT, WITH ILLUSTRATIVE CASES.* The Lancet, 1896. **148**(3803): p. 162-165.
11. Love, R.R. and J. Philips, *Oophorectomy for Breast Cancer: History Revisited.* Journal of the National Cancer Institute, 2002. **94**(19): p. 1433-1434.
12. Rous, P., *A SARCOMA OF THE FOWL TRANSMISSIBLE BY AN AGENT SEPARABLE FROM THE TUMOR CELLS.* The Journal of Experimental Medicine, 1911. **13**(4): p. 397-411.
13. DeVita, V.T. and E. Chu, *A History of Cancer Chemotherapy.* Cancer Research, 2008. **68**(21): p. 8643-8653.
14. Umeda, M. and C. Heidelberger, *Comparative studies of fluorinated pyrimidines with various cell lines.* Cancer Res, 1968. **28**(12): p. 2529-38.
15. Oshaughnessy, J.A., et al., *Randomized, open-label, phase II trial of oral capecitabine (Xeloda) vs. a reference arm of intravenous CMF (cyclophosphamide, methotrexate and 5-fluorouracil) as first-line therapy for advanced/metastatic breast cancer.* Ann Oncol, 2001. **12**(9): p. 1247-54.
16. Kunimoto, T., M. Hori, and H. Umezawa, *Modes of action of phleomycin, bleomycin and formycin on HeLa S3 cells in synchronized culture.* J Antibiot (Tokyo), 1967. **20**(5): p. 277-81.
17. Di Marco, A., M. Gaetani, and B. Scarpinato, *Adriamycin (NSC-123,127): a new antibiotic with antitumor activity.* Cancer Chemother Rep, 1969. **53**(1): p. 33-7.
18. Moore, F.D., et al., *Carcinoma of the breast. A decade of new results with old concepts.* N Engl J Med, 1967. **277**(7): p. 343-50.

19. Jensen, E.V., *Estrogen receptors in hormone-dependent breast cancers.* Cancer Res, 1975. **35**(11 Pt. 2): p. 3362-4.
20. Block, G.E., et al., *Correlation of estrophilin content of primary mammary cancer to eventual endocrine treatment.* Ann Surg, 1978. **188**(3): p. 372-6.
21. Ward, H.W., *Anti-oestrogen therapy for breast cancer: a trial of tamoxifen at two dose levels.* Br Med J, 1973. **1**(5844): p. 13-4.
22. Slichenmyer, W.J. and D.D. Von Hoff, *Taxol: a new and effective anti-cancer drug.* Anticancer Drugs, 1991. **2**(6): p. 519-30.
23. Hanauske, A.R., et al., *Effects of Taxotere and taxol on in vitro colony formation of freshly explanted human tumor cells.* Anticancer Drugs, 1992. **3**(2): p. 121-4.
24. Seidman, A.D., et al., *Randomized phase III trial of weekly compared with every-3-weeks paclitaxel for metastatic breast cancer, with trastuzumab for all HER-2 overexpressors and random assignment to trastuzumab or not in HER-2 nonoverexpressors: final results of Cancer and Leukemia Group B protocol 9840.* J Clin Oncol, 2008. **26**(10): p. 1642-9.
25. Sparano, J.A., et al., *Weekly paclitaxel in the adjuvant treatment of breast cancer.* N Engl J Med, 2008. **358**(16): p. 1663-71.
26. Druker, B.J., et al., *Effects of a selective inhibitor of the Abl tyrosine kinase on the growth of Bcr-Abl positive cells.* Nat Med, 1996. **2**(5): p. 561-6.
27. Pegram, M., et al., *Inhibitory effects of combinations of HER-2/neu antibody and chemotherapeutic agents used for treatment of human breast cancers.* Oncogene, 1999. **18**(13): p. 2241-51.
28. Pegram, M.D., G. Konecny, and D.J. Slamon, *The molecular and cellular biology of HER2/neu gene amplification/overexpression and the clinical development of herceptin (trastuzumab) therapy for breast cancer.* Cancer Treat Res, 2000. **103**: p. 57-75.
29. Baselga, J., et al., *Mechanism of action of trastuzumab and scientific update.* Semin Oncol, 2001. **28**(5 Suppl 16): p. 4-11.
30. Hardy, N.M., D.H. Fowler, and M.R. Bishop, *Immunotherapy of metastatic breast cancer: phase I trail of reduced-intensity allogeneic hematopoietic stem cell transplantation with Th2/Tc2 T-cell exchange.* Clin Breast Cancer, 2006. **7**(1): p. 87-9.
31. Edge, S., Byrd, D.R., Compton, C.C., Fritz, A.G., Greene, F.L., Trotti, A., *AJCC Cancer Staging Manual*. 7 ed. 2010, New York, NY: Springer. 649.
32. Schott, A. *Systemic treatment of metastatic breast cancer in women: Chemotherapy*. 2014.
33. Perou, C.M., et al., *Molecular portraits of human breast tumours.* Nature, 2000. **406**(6797): p. 747-752.
34. Howlader, N., et al., *US incidence of breast cancer subtypes defined by joint hormone receptor and HER2 status.* J Natl Cancer Inst, 2014. **106**(5).
35. Sørlie, T., et al., *Gene expression patterns of breast carcinomas distinguish tumor subclasses with clinical implications.* Proceedings of the National Academy of Sciences, 2001. **98**(19): p. 10869-10874.
36. Parker, J.S., et al., *Supervised Risk Predictor of Breast Cancer Based on Intrinsic Subtypes.* Journal of Clinical Oncology, 2009. **27**(8): p. 1160-1167.

37. *Comprehensive molecular portraits of human breast tumours.* Nature, 2012. **490**(7418): p. 61-70.
38. Hartmann, D., et al., *Long chain ceramides and very long chain ceramides have opposite effects on human breast and colon cancer cell growth.* Int J Biochem Cell Biol, 2012. **44**(4): p. 620-8.
39. Schiffmann, S., et al., *Ceramide synthases and ceramide levels are increased in breast cancer tissue.* Carcinogenesis, 2009. **30**(5): p. 745-52.
40. Mesicek, J., et al., *Ceramide synthases 2, 5, and 6 confer distinct roles in radiation-induced apoptosis in HeLa cells.* Cell Signal, 2010. **22**(9): p. 1300-7.
41. Siskind, L.J., et al., *The BCL-2 protein BAK is required for long-chain ceramide generation during apoptosis.* J Biol Chem, 2010. **285**(16): p. 11818-26.
42. Novgorodov, S.A., et al., *Developmentally regulated ceramide synthase 6 increases mitochondrial Ca2+ loading capacity and promotes apoptosis.* J Biol Chem, 2011. **286**(6): p. 4644-58.
43. Hernandez-Corbacho, M.J., et al., *Tumor Necrosis Factor-alpha (TNFalpha)-induced Ceramide Generation via Ceramide Synthases Regulates Loss of Focal Adhesion Kinase (FAK) and Programmed Cell Death.* J Biol Chem, 2015. **290**(42): p. 25356-73.
44. Alves, I.D., et al., *Ligand modulation of lateral segregation of a G-protein-coupled receptor into lipid microdomains in sphingomyelin/phosphatidylcholine solid-supported bilayers.* Biochemistry, 2005. **44**(25): p. 9168-78.
45. Fantini, J. and F.J. Barrantes, *Sphingolipid/cholesterol regulation of neurotransmitter receptor conformation and function.* Biochim Biophys Acta, 2009. **1788**(11): p. 2345-61.
46. Mathias, S., K.A. Dressler, and R.N. Kolesnick, *Characterization of a ceramide-activated protein kinase: stimulation by tumor necrosis factor alpha.* Proc Natl Acad Sci U S A, 1991. **88**(22): p. 10009-13.
47. Kitatani, K., et al., *Protein kinase C-induced activation of a ceramide/protein phosphatase 1 pathway leading to dephosphorylation of p38 MAPK.* J Biol Chem, 2006. **281**(48): p. 36793-802.
48. Perry, D.M., et al., *Identification and characterization of protein phosphatase 2C activation by ceramide.* J Lipid Res, 2012. **53**(8): p. 1513-21.
49. Heinrich, M., et al., *Cathepsin D links TNF-induced acid sphingomyelinase to Bid-mediated caspase-9 and -3 activation.* Cell Death Differ, 2004. **11**(5): p. 550-63.
50. Kitatani, K., J. Idkowiak-Baldys, and Y.A. Hannun, *The sphingolipid salvage pathway in ceramide metabolism and signaling.* Cell Signal, 2008. **20**(6): p. 1010-8.
51. Chakravarthy, H., et al., *Role of acid sphingomyelinase in shifting the balance between pro-inflammatory and reparative bone marrow cells in diabetic retinopathy.* Stem Cells, 2015.
52. Jenkins, R.W., et al., *Regulation of CC ligand 5/RANTES by acid sphingomyelinase and acid ceramidase.* J Biol Chem, 2011. **286**(15): p. 13292-303.

53. Perry, D.M., et al., *Defining a Role for Acid Sphingomyelinase in the p38/Interleukin-6 Pathway.* J Biol Chem, 2014.
54. Clarke, C.J., et al., *Neutral sphingomyelinase 2 (nSMase2) is the primary neutral sphingomyelinase isoform activated by tumour necrosis factor-alpha in MCF-7 cells.* Biochem J, 2011. **435**(2): p. 381-90.
55. Sawada, M., et al., *Molecular mechanisms of TNF-alpha-induced ceramide formation in human glioma cells: P53-mediated oxidant stress-dependent and -independent pathways.* Cell Death Differ, 2004. **11**(9): p. 997-1008.
56. Pettus, B.J., et al., *The sphingosine kinase 1/sphingosine-1-phosphate pathway mediates COX-2 induction and PGE2 production in response to TNF-alpha.* FASEB J, 2003. **17**(11): p. 1411-21.
57. Davis, C.N., et al., *IL-1beta induces a MyD88-dependent and ceramide-mediated activation of Src in anterior hypothalamic neurons.* J Neurochem, 2006. **98**(5): p. 1379-89.
58. Chiba, N., et al., *Ceramide inhibits LPS-induced production of IL-5, IL-10, and IL-13 from mast cells.* J Cell Physiol, 2007. **213**(1): p. 126-36.
59. Kitatani, K., et al., *Acid beta-glucosidase 1 counteracts p38delta-dependent induction of interleukin-6: possible role for ceramide as an anti-inflammatory lipid.* J Biol Chem, 2009. **284**(19): p. 12979-88.
60. Cornell, T.T., et al., *Ceramide-dependent PP2A regulation of TNFalpha-induced IL-8 production in respiratory epithelial cells.* Am J Physiol Lung Cell Mol Physiol, 2009. **296**(5): p. L849-56.
61. Tumurkhuu, G., et al., *The inhibition of lipopolysaccharide-induced tumor necrosis factor-alpha and nitric oxide production by Clostridium perfringens alpha-toxin and its relation to alpha-toxin-induced intracellular ceramide generation.* Int J Med Microbiol, 2009. **299**(8): p. 554-62.
62. Holland, W.L., et al., *Inhibition of ceramide synthesis ameliorates glucocorticoid-, saturated-fat-, and obesity-induced insulin resistance.* Cell Metab, 2007. **5**(3): p. 167-79.
63. Haus, J.M., et al., *Plasma ceramides are elevated in obese subjects with type 2 diabetes and correlate with the severity of insulin resistance.* Diabetes, 2009. **58**(2): p. 337-43.
64. Haimovitz-Friedman, A., et al., *Lipopolysaccharide induces disseminated endothelial apoptosis requiring ceramide generation.* J Exp Med, 1997. **186**(11): p. 1831-41.
65. Goggel, R., et al., *PAF-mediated pulmonary edema: a new role for acid sphingomyelinase and ceramide.* Nat Med, 2004. **10**(2): p. 155-60.
66. Levy, M., et al., *Neutral sphingomyelinase 2 is activated by cigarette smoke to augment ceramide-induced apoptosis in lung cell death.* Am J Physiol Lung Cell Mol Physiol, 2009. **297**(1): p. L125-33.
67. Morad, S.A., et al., *Short-chain ceramides depress integrin cell surface expression and function in colorectal cancer cells.* Cancer Lett, 2016.
68. Carpinteiro, A., et al., *Regulation of hematogenous tumor metastasis by acid sphingomyelinase.* EMBO Mol Med, 2015. **7**(6): p. 714-34.
69. Ward, K.E., et al., *The molecular basis of ceramide-1-phosphate recognition by C2 domains.* J Lipid Res, 2013. **54**(3): p. 636-48.

70. Nakamura, H., et al., *Role of cytosolic phospholipase A(2)alpha in cell rounding and cytotoxicity induced by ceramide-1-phosphate via ceramide kinase.* Arch Biochem Biophys, 2011. **512**(1): p. 45-51.
71. Lamour, N.F., et al., *Ceramide 1-phosphate is required for the translocation of group IVA cytosolic phospholipase A2 and prostaglandin synthesis.* J Biol Chem, 2009. **284**(39): p. 26897-907.
72. Pastukhov, O., et al., *The ceramide kinase inhibitor NVP-231 inhibits breast and lung cancer cell proliferation by inducing M phase arrest and subsequent cell death.* Br J Pharmacol, 2014.
73. Gangoiti, P., et al., *Ceramide 1-phosphate stimulates macrophage proliferation through activation of the PI3-kinase/PKB, JNK and ERK1/2 pathways.* Cell Signal, 2008. **20**(4): p. 726-36.
74. Granado, M.H., et al., *Ceramide 1-phosphate (C1P) promotes cell migration Involvement of a specific C1P receptor.* Cell Signal, 2009. **21**(3): p. 405-12.
75. Kreydiyyeh, S.I. and Z. Dakroub, *Ceramide and its metabolites modulate time-dependently the activity of the Na(+)/K(+) ATPase in HepG2 cells.* Int J Biochem Cell Biol, 2014. **53**: p. 102-7.
76. Brogi, A., et al., *Induction of intracellular ceramide by interleukin-1 beta in oligodendrocytes.* J Cell Biochem, 1997. **66**(4): p. 532-41.
77. Mitsutake, S. and Y. Igarashi, *Calmodulin is involved in the Ca2+-dependent activation of ceramide kinase as a calcium sensor.* J Biol Chem, 2005. **280**(49): p. 40436-41.
78. Gomez-Munoz, A., et al., *Ceramide-1-phosphate blocks apoptosis through inhibition of acid sphingomyelinase in macrophages.* J Lipid Res, 2004. **45**(1): p. 99-105.
79. Boath, A., et al., *Regulation and traffic of ceramide 1-phosphate produced by ceramide kinase: comparative analysis to glucosylceramide and sphingomyelin.* J Biol Chem, 2008. **283**(13): p. 8517-26.
80. Granado, M.H., et al., *Ceramide 1-phosphate inhibits serine palmitoyltransferase and blocks apoptosis in alveolar macrophages.* Biochim Biophys Acta, 2009. **1791**(4): p. 263-72.
81. Lucki, N.C. and M.B. Sewer, *Genistein stimulates MCF-7 breast cancer cell growth by inducing acid ceramidase (ASAH1) gene expression.* J Biol Chem, 2011. **286**(22): p. 19399-409.
82. Hannun, Y.A. and R.M. Bell, *Regulation of protein kinase C by sphingosine and lysosphingolipids.* Clin Chim Acta, 1989. **185**(3): p. 333-45.
83. Hu, W., et al., *Alkaline ceramidase 3 (ACER3) hydrolyzes unsaturated long-chain ceramides, and its down-regulation inhibits both cell proliferation and apoptosis.* J Biol Chem, 2010. **285**(11): p. 7964-76.
84. Ullio, C., et al., *Sphingosine mediates TNFalpha-induced lysosomal membrane permeabilization and ensuing programmed cell death in hepatoma cells.* J Lipid Res, 2012. **53**(6): p. 1134-43.
85. Sun, Y., et al., *Orm protein phosphoregulation mediates transient sphingolipid biosynthesis response to heat stress via the Pkh-Ypk and Cdc55-PP2A pathways.* Mol Biol Cell, 2012. **23**(12): p. 2388-98.

86. Wang, K., et al., *Alkaline Ceramidase 3 Deficiency Results in Purkinje Cell Degeneration and Cerebellar Ataxia Due to Dyshomeostasis of Sphingolipids in the Brain.* PLoS Genet, 2015. **11**(10): p. e1005591.
87. Paugh, B.S., et al., *Interleukin-1 regulates the expression of sphingosine kinase 1 in glioblastoma cells.* J Biol Chem, 2009. **284**(6): p. 3408-17.
88. Billich, A., et al., *Basal and induced sphingosine kinase 1 activity in A549 carcinoma cells: function in cell survival and IL-1beta and TNF-alpha induced production of inflammatory mediators.* Cell Signal, 2005. **17**(10): p. 1203-17.
89. Doll, F., J. Pfeilschifter, and A. Huwiler, *The epidermal growth factor stimulates sphingosine kinase-1 expression and activity in the human mammary carcinoma cell line MCF7.* Biochim Biophys Acta, 2005. **1738**(1-3): p. 72-81.
90. Adada, M.M., et al., *Intracellular sphingosine kinase 2-derived sphingosine-1-phosphate mediates epidermal growth factor-induced ezrin-radixin-moesin phosphorylation and cancer cell invasion.* FASEB J, 2015. **29**(11): p. 4654-69.
91. Wang, H., et al., *Sphingosine-1-Phosphate Induces the Migration and Angiogenesis of Epcs Through the Akt Signaling Pathway via Sphingosine-1-Phosphate Receptor 3/Platelet-Derived Growth Factor Receptor-beta.* Cell Mol Biol Lett, 2015. **20**(4): p. 597-611.
92. Xia, P., et al., *Sphingosine kinase interacts with TRAF2 and dissects tumor necrosis factor-alpha signaling.* J Biol Chem, 2002. **277**(10): p. 7996-8003.
93. Takabe, K. and S. Spiegel, *Export of sphingosine-1-phosphate and cancer progression.* J Lipid Res, 2014. **55**(9): p. 1839-46.
94. Pyne, S., R. Bittman, and N.J. Pyne, *Sphingosine kinase inhibitors and cancer: seeking the golden sword of Hercules.* Cancer Res, 2011. **71**(21): p. 6576-82.
95. Hannun, Y.A. and L.M. Obeid, *The Ceramide-centric Universe of Lipid-mediated Cell Regulation: Stress Encounters of the Lipid Kind.* Journal of Biological Chemistry, 2002. **277**(29): p. 25847-25850.
96. Snyder, R.A., R.O. Brady, and P.L. Kornblith, *Ganglioside patterns of cultured human glioma cells.* Neurology, 1970. **20**(4): p. 412.
97. Keenan, T.W., et al., *Exogenous glycosphingolipids suppress growth rate of transformed and untransformed 3T3 mouse cells.* Exp Cell Res, 1975. **92**(2): p. 259-70.
98. Manuelidis, L., R.K. Yu, and E.E. Manuelidis, *Ganglioside content and pattern in human gliomas in culture. Correlation of morphological changes with altered gangliosides.* Acta Neuropathol, 1977. **38**(2): p. 129-35.
99. Bremer, E.G., J. Schlessinger, and S. Hakomori, *Ganglioside-mediated modulation of cell growth. Specific effects of GM3 on tyrosine phosphorylation of the epidermal growth factor receptor.* J Biol Chem, 1986. **261**(5): p. 2434-40.
100. Okada, Y., H. Matsuura, and S. Hakomori, *Inhibition of tumor cell growth by aggregation of a tumor-associated glycolipid antigen: a close functional association between gangliotriaosylceramide and transferrin receptor in mouse lymphoma L-5178Y.* Cancer Res, 1985. **45**(6): p. 2793-801.
101. Kim, Y.S., et al., *Expression of LeY and extended LeY blood group-related antigens in human malignant, premalignant, and nonmalignant colonic tissues.* Cancer Res, 1986. **46**(11): p. 5985-92.

102. Chen, Z., et al., *Protein kinase C-delta inactivation inhibits the proliferation and survival of cancer stem cells in culture and in vivo.* BMC Cancer, 2014. **14**: p. 90.
103. Kim, J., et al., *Sustained inhibition of PKCalpha reduces intravasation and lung seeding during mammary tumor metastasis in an in vivo mouse model.* Oncogene, 2011. **30**(3): p. 323-33.
104. Chalfant, C.E., et al., *Long chain ceramides activate protein phosphatase-1 and protein phosphatase-2A. Activation is stereospecific and regulated by phosphatidic acid.* J Biol Chem, 1999. **274**(29): p. 20313-7.
105. Hanada, K., et al., *Molecular machinery for non-vesicular trafficking of ceramide.* Nature, 2003. **426**(6968): p. 803-809.
106. Yamaji, T., et al., *Two sphingolipid transfer proteins, CERT and FAPP2: Their roles in sphingolipid metabolism.* IUBMB Life, 2008. **60**(8): p. 511-518.
107. Charruyer, A., et al., *Decreased ceramide transport protein (CERT) function alters sphingomyelin production following UVB irradiation.* J Biol Chem, 2008. **283**(24): p. 16682-92.
108. Blom, T., et al., *Tracking sphingosine metabolism and transport in sphingolipidoses: NPC1 deficiency as a test case.* Traffic, 2012. **13**(9): p. 1234-43.
109. Fyrst, H. and J.D. Saba, *An update on sphingosine-1-phosphate and other sphingolipid mediators.* Nat Chem Biol, 2010. **6**(7): p. 489-497.
110. Schnitt, S.J., *Classification and prognosis of invasive breast cancer: from morphology to molecular taxonomy.* Mod Pathol, 2010. **23**(S2): p. S60-S64.
111. Bange, J., E. Zwick, and A. Ullrich, *Molecular targets for breast cancer therapy and prevention.* Nat Med, 2001. **7**(5): p. 548-52.
112. Stemke-Hale, K., et al., *An Integrative Genomic and Proteomic Analysis of PIK3CA, PTEN, and AKT Mutations in Breast Cancer.* Cancer Research, 2008. **68**(15): p. 6084-6091.
113. Wagner, E.F. and A.R. Nebreda, *Signal integration by JNK and p38 MAPK pathways in cancer development.* Nat Rev Cancer, 2009. **9**(8): p. 537-549.
114. Tran, B. and P.L. Bedard, *Luminal-B breast cancer and novel therapeutic targets.* Breast Cancer Res, 2011. **13**(6): p. 221.
115. Wirapati, P., et al., *Meta-analysis of gene expression profiles in breast cancer: toward a unified understanding of breast cancer subtyping and prognosis signatures.* Breast Cancer Res, 2008. **10**(4): p. R65.
116. Sotiriou, C. and L. Pusztai, *Gene-expression signatures in breast cancer.* N Engl J Med, 2009. **360**(8): p. 790-800.
117. Troester, M.A., et al., *Gene expression patterns associated with p53 status in breast cancer.* BMC Cancer, 2006. **6**: p. 276.
118. Jiang, Z., et al., *Rb deletion in mouse mammary progenitors induces luminal-B or basal-like/EMT tumor subtypes depending on p53 status.* J Clin Invest, 2010. **120**(9): p. 3296-309.
119. Neve, R.M., et al., *A collection of breast cancer cell lines for the study of functionally distinct cancer subtypes.* Cancer Cell. **10**(6): p. 515-527.

120. Ruckhaberle, E., et al., *Prognostic relevance of glucosylceramide synthase (GCS) expression in breast cancer.* J Cancer Res Clin Oncol, 2009. **135**(1): p. 81-90.
121. Zhang, X., et al., *Doxorubicin influences the expression of glucosylceramide synthase in invasive ductal breast cancer.* PLoS One, 2012. **7**(11): p. e48492.
122. Bai, A., et al., *Synthesis and bioevaluation of omega-N-amino analogs of B13.* Bioorg Med Chem, 2009. **17**(5): p. 1840-8.
123. Ruckhaberle, E., et al., *Acid ceramidase 1 expression correlates with a better prognosis in ER-positive breast cancer.* Climacteric, 2009. **12**(6): p. 502-13.
124. Ruckhaberle, E., et al., *Microarray analysis of altered sphingolipid metabolism reveals prognostic significance of sphingosine kinase 1 in breast cancer.* Breast Cancer Res Treat, 2008. **112**(1): p. 41-52.
125. Liu, Y.Y., et al., *Glucosylceramide synthase, a factor in modulating drug resistance, is overexpressed in metastatic breast carcinoma.* Int J Oncol, 2011. **39**(2): p. 425-31.
126. Sun, Y.L., et al., *[Construction of glucosylceramide synthase-specific siRNA expression vector and its efficiency in reversal of drug resistance in breast carcinoma cells].* Zhonghua Yi Xue Za Zhi, 2005. **85**(8): p. 518-21.
127. Gouaze, V., et al., *Glucosylceramide synthase blockade down-regulates P-glycoprotein and resensitizes multidrug-resistant breast cancer cells to anticancer drugs.* Cancer Res, 2005. **65**(9): p. 3861-7.
128. Lavie, Y., et al., *Agents that reverse multidrug resistance, tamoxifen, verapamil, and cyclosporin A, block glycosphingolipid metabolism by inhibiting ceramide glycosylation in human cancer cells.* J Biol Chem, 1997. **272**(3): p. 1682-7.
129. Bose, R., et al., *Ceramide synthase mediates daunorubicin-induced apoptosis: an alternative mechanism for generating death signals.* Cell, 1995. **82**(3): p. 405-14.
130. Lucci, A., et al., *Multidrug resistance modulators and doxorubicin synergize to elevate ceramide levels and elicit apoptosis in drug-resistant cancer cells.* Cancer, 1999. **86**(2): p. 300-11.
131. Erez-Roman, R., R. Pienik, and A.H. Futerman, *Increased ceramide synthase 2 and 6 mRNA levels in breast cancer tissues and correlation with sphingosine kinase expression.* Biochem Biophys Res Commun, 2010. **391**(1): p. 219-23.
132. Walker, T., et al., *Sorafenib and vorinostat kill colon cancer cells by CD95-dependent and -independent mechanisms.* Mol Pharmacol, 2009. **76**(2): p. 342-55.
133. Min, J., et al., *(Dihydro)ceramide synthase 1 regulated sensitivity to cisplatin is associated with the activation of p38 mitogen-activated protein kinase and is abrogated by sphingosine kinase 1.* Mol Cancer Res, 2007. **5**(8): p. 801-12.
134. Hoeferlin, L.A., et al., *Folate stress induces apoptosis via p53-dependent de novo ceramide synthesis and up-regulation of ceramide synthase 6.* J Biol Chem, 2013. **288**(18): p. 12880-90.
135. Bareford, M.D., et al., *Sorafenib and pemetrexed toxicity in cancer cells is mediated via SRC-ERK signaling.* Cancer Biol Ther, 2012. **13**(9): p. 793-803.

136. Wooten-Blanks, L.G., et al., *Mechanisms of ceramide-mediated repression of the human telomerase reverse transcriptase promoter via deacetylation of Sp3 by histone deacetylase 1.* FASEB J, 2007. **21**(12): p. 3386-97.
137. Koybasi, S., et al., *Defects in cell growth regulation by C18:0-ceramide and longevity assurance gene 1 in human head and neck squamous cell carcinomas.* J Biol Chem, 2004. **279**(43): p. 44311-9.
138. Demircan, B., et al., *Comparative epigenomics of human and mouse mammary tumors.* Genes Chromosomes Cancer, 2009. **48**(1): p. 83-97.
139. Chalmers, I.J., et al., *Mapping the chromosome 16 cadherin gene cluster to a minimal deleted region in ductal breast cancer.* Cancer Genet Cytogenet, 2001. **126**(1): p. 39-44.
140. Vijayaraghavalu, S., et al., *Epigenetic modulation of the biophysical properties of drug-resistant cell lipids to restore drug transport and endocytic functions.* Mol Pharm, 2012. **9**(9): p. 2730-42.
141. Ito, H., et al., *Transcriptional regulation of neutral sphingomyelinase 2 gene expression of a human breast cancer cell line, MCF-7, induced by the anti-cancer drug, daunorubicin.* Biochim Biophys Acta, 2009. **1789**(11-12): p. 681-90.
142. Ellegaard, A.M., et al., *Sunitinib and SU11652 inhibit acid sphingomyelinase, destabilize lysosomes, and inhibit multidrug resistance.* Mol Cancer Ther, 2013. **12**(10): p. 2018-30.
143. Zeidan, Y.H., R.W. Jenkins, and Y.A. Hannun, *Remodeling of cellular cytoskeleton by the acid sphingomyelinase/ceramide pathway.* J Cell Biol, 2008. **181**(2): p. 335-50.
144. Canals, D., et al., *Differential effects of ceramide and sphingosine 1-phosphate on ERM phosphorylation: probing sphingolipid signaling at the outer plasma membrane.* J Biol Chem, 2010. **285**(42): p. 32476-85.
145. Bhabak, K.P., et al., *Effective inhibition of acid and neutral ceramidases by novel B-13 and LCL-464 analogues.* Bioorg Med Chem, 2013. **21**(4): p. 874-82.
146. Cain, B.S., et al., *Tumor necrosis factor-alpha and interleukin-1beta synergistically depress human myocardial function.* Crit Care Med, 1999. **27**(7): p. 1309-18.
147. Mathias, S., et al., *Activation of the sphingomyelin signaling pathway in intact EL4 cells and in a cell-free system by IL-1 beta.* Science, 1993. **259**(5094): p. 519-22.
148. Hannun, Y.A., *The sphingomyelin cycle and the second messenger function of ceramide.* J Biol Chem, 1994. **269**(5): p. 3125-8.
149. Zeidan, Y.H., et al., *Acid ceramidase but not acid sphingomyelinase is required for tumor necrosis factor-{alpha}-induced PGE2 production.* J Biol Chem, 2006. **281**(34): p. 24695-703.
150. Chen, D., et al., *Prostaglandin E(2) induces breast cancer related aromatase promoters via activation of p38 and c-Jun NH(2)-terminal kinase in adipose fibroblasts.* Cancer Res, 2007. **67**(18): p. 8914-22.
151. Soria, G. and A. Ben-Baruch, *The inflammatory chemokines CCL2 and CCL5 in breast cancer.* Cancer Lett, 2008. **267**(2): p. 271-85.

152. Pinilla, S., et al., *Tissue resident stem cells produce CCL5 under the influence of cancer cells and thereby promote breast cancer cell invasion.* Cancer Lett, 2009. **284**(1): p. 80-5.
153. Zhang, Y., et al., *Role of CCL5 in invasion, proliferation and proportion of CD44+/CD24- phenotype of MCF-7 cells and correlation of CCL5 and CCR5 expression with breast cancer progression.* Oncol Rep, 2009. **21**(4): p. 1113-21.
154. Karczewska, A., et al., *Expression of interleukin-6, interleukin-6 receptor, and glycoprotein 130 correlates with good prognoses for patients with breast carcinoma.* Cancer, 2000. **88**(9): p. 2061-71.
155. Salgado, R., et al., *Circulating interleukin-6 predicts survival in patients with metastatic breast cancer.* Int J Cancer, 2003. **103**(5): p. 642-6.
156. Dethlefsen, C., G. Hojfeldt, and P. Hojman, *The role of intratumoral and systemic IL-6 in breast cancer.* Breast Cancer Res Treat, 2013. **138**(3): p. 657-64.
157. Asgeirsson, K.S., et al., *The effects of IL-6 on cell adhesion and e-cadherin expression in breast cancer.* Cytokine, 1998. **10**(9): p. 720-8.
158. Watson, C., et al., *High expression of sphingosine 1-phosphate receptors, S1P1 and S1P3, sphingosine kinase 1, and extracellular signal-regulated kinase-1/2 is associated with development of tamoxifen resistance in estrogen receptor-positive breast cancer patients.* Am J Pathol, 2010. **177**(5): p. 2205-15.
159. Zhang, Y., et al., *Sphingosine kinase 1 and cancer: a systematic review and meta-analysis.* PLoS One, 2014. **9**(2): p. e90362.
160. Pinho, F.G., et al., *Downregulation of microRNA-515-5p by the estrogen receptor modulates sphingosine kinase 1 and breast cancer cell proliferation.* Cancer Res, 2013. **73**(19): p. 5936-48.
161. Takabe, K., et al., *Estradiol induces export of sphingosine 1-phosphate from breast cancer cells via ABCC1 and ABCG2.* J Biol Chem, 2010. **285**(14): p. 10477-86.
162. Kim, E.S., et al., *Inflammatory lipid sphingosine-1-phosphate upregulates C-reactive protein via C/EBPbeta and potentiates breast cancer progression.* Oncogene, 2014. **33**(27): p. 3583-93.
163. Rutherford, C., et al., *Regulation of cell survival by sphingosine-1-phosphate receptor S1P1 via reciprocal ERK-dependent suppression of Bim and PI-3-kinase/protein kinase C-mediated upregulation of Mcl-1.* Cell Death Dis, 2013. **4**: p. e927.
164. Hu, X., et al., *Genetic alterations and oncogenic pathways associated with breast cancer subtypes.* Mol Cancer Res, 2009. **7**(4): p. 511-22.
165. Gustin, D.J., et al., *Structure guided design of a series of sphingosine kinase (SphK) inhibitors.* Bioorg Med Chem Lett, 2013. **23**(16): p. 4608-16.
166. Rex, K., et al., *Sphingosine Kinase Activity Is Not Required for Tumor Cell Viability.* PLoS ONE, 2013. **8**(7): p. e68328.
167. Ruckhaberle, E., et al., *Gene expression of ceramide kinase, galactosyl ceramide synthase and ganglioside GD3 synthase is associated with prognosis in breast cancer.* J Cancer Res Clin Oncol, 2009. **135**(8): p. 1005-13.

168. Chandriani, S., et al., *A core MYC gene expression signature is prominent in basal-like breast cancer but only partially overlaps the core serum response.* PLoS One, 2009. **4**(8): p. e6693.
169. Liedtke, C., et al., *Response to neoadjuvant therapy and long-term survival in patients with triple-negative breast cancer.* J Clin Oncol, 2008. **26**(8): p. 1275-81.
170. Stover, T. and M. Kester, *Liposomal delivery enhances short-chain ceramide-induced apoptosis of breast cancer cells.* J Pharmacol Exp Ther, 2003. **307**(2): p. 468-75.
171. Shabbits, J.A. and L.D. Mayer, *Intracellular delivery of ceramide lipids via liposomes enhances apoptosis in vitro.* Biochim Biophys Acta, 2003. **1612**(1): p. 98-106.
172. Stover, T.C., et al., *Systemic delivery of liposomal short-chain ceramide limits solid tumor growth in murine models of breast adenocarcinoma.* Clin Cancer Res, 2005. **11**(9): p. 3465-74.
173. Miyaji, M., et al., *Role of membrane sphingomyelin and ceramide in platform formation for Fas-mediated apoptosis.* J Exp Med, 2005. **202**(2): p. 249-59.
174. Watters, R.J., et al., *Development and use of ceramide nanoliposomes in cancer.* Methods Enzymol, 2012. **508**: p. 89-108.
175. Tran, M.A., et al., *Combining nanoliposomal ceramide with sorafenib synergistically inhibits melanoma and breast cancer cell survival to decrease tumor development.* Clin Cancer Res, 2008. **14**(11): p. 3571-81.
176. Wilhelm, S.M., et al., *Preclinical overview of sorafenib, a multikinase inhibitor that targets both Raf and VEGF and PDGF receptor tyrosine kinase signaling.* Mol Cancer Ther, 2008. **7**(10): p. 3129-40.
177. Tan, Q.X., et al., *Sorafenib-based therapy in HER2-negative advanced breast cancer: Results from a retrospective pooled analysis of randomized controlled trials.* Exp Ther Med, 2014. **7**(5): p. 1420-1426.
178. Pedersen, A.M., et al., *Sorafenib and nilotinib resensitize tamoxifen resistant breast cancer cells to tamoxifen treatment via estrogen receptor alpha.* Int J Oncol, 2014.
179. Pedrosa, L.R., et al., *Improving intracellular doxorubicin delivery through nanoliposomes equipped with selective tumor cell membrane permeabilizing short-chain sphingolipids.* Pharm Res, 2013. **30**(7): p. 1883-95.
180. Zolnik, B.S., et al., *Rapid distribution of liposomal short-chain ceramide in vitro and in vivo.* Drug Metab Dispos, 2008. **36**(8): p. 1709-15.
181. Sirohi, B., et al., *Platinum-based chemotherapy in triple-negative breast cancer.* Ann Oncol, 2008. **19**(11): p. 1847-52.
182. Swanton, C., et al., *Regulators of mitotic arrest and ceramide metabolism are determinants of sensitivity to paclitaxel and other chemotherapeutic drugs.* Cancer Cell, 2007. **11**(6): p. 498-512.
183. Juul, N., et al., *Assessment of an RNA interference screen-derived mitotic and ceramide pathway metagene as a predictor of response to neoadjuvant paclitaxel for primary triple-negative breast cancer: a retrospective analysis of five clinical trials.* The Lancet Oncology, 2010. **11**(4): p. 358-365.

184. Hla, T., et al., *Sphingosine-1-phosphate signaling via the EDG-1 family of G-protein-coupled receptors.* Ann N Y Acad Sci, 2000. **905**: p. 16-24.
185. Mousseau, Y., et al., *Fingolimod inhibits PDGF-B-induced migration of vascular smooth muscle cell by down-regulating the S1PR1/S1PR3 pathway.* Biochimie, 2012. **94**(12): p. 2523-31.
186. Long, J.S., et al., *Sphingosine 1-phosphate receptor 4 uses HER2 (ERBB2) to regulate extracellular signal regulated kinase-1/2 in MDA-MB-453 breast cancer cells.* J Biol Chem, 2010. **285**(46): p. 35957-66.
187. Nagaoka, Y., et al., *Effects of phosphorylation of immunomodulatory agent FTY720 (fingolimod) on antiproliferative activity against breast and colon cancer cells.* Biol Pharm Bull, 2008. **31**(6): p. 1177-81.
188. Azuma, H., et al., *Marked prevention of tumor growth and metastasis by a novel immunosuppressive agent, FTY720, in mouse breast cancer models.* Cancer Res, 2002. **62**(5): p. 1410-9.
189. Slamon, D., et al., *Adjuvant trastuzumab in HER2-positive breast cancer.* N Engl J Med, 2011. **365**(14): p. 1273-83.
190. Joensuu, H., et al., *Adjuvant docetaxel or vinorelbine with or without trastuzumab for breast cancer.* N Engl J Med, 2006. **354**(8): p. 809-20.
191. Goss, P.E., et al., *Adjuvant lapatinib for women with early-stage HER2-positive breast cancer: a randomised, controlled, phase 3 trial.* Lancet Oncol, 2013. **14**(1): p. 88-96.
192. Goldhirsch, A., et al., *2 years versus 1 year of adjuvant trastuzumab for HER2-positive breast cancer (HERA): an open-label, randomised controlled trial.* Lancet, 2013. **382**(9897): p. 1021-8.
193. Agrawal, A., et al., *Overview of tyrosine kinase inhibitors in clinical breast cancer.* Endocr Relat Cancer, 2005. **12 Suppl 1**: p. S135-44.
194. Lee, A.J., et al., *CERT depletion predicts chemotherapy benefit and mediates cytotoxic and polyploid-specific cancer cell death through autophagy induction.* J Pathol, 2012. **226**(3): p. 482-94.
195. Payne, A.W., et al., *Ceramide Kinase Promotes Tumor Cell Survival and Mammary Tumor Recurrence.* Cancer Res, 2014.
196. Kim, I.C., et al., *Lipid profiles for HER2-positive breast cancer.* Anticancer Res, 2013. **33**(6): p. 2467-72.
197. Sano, O., et al., *Sphingomyelin-dependence of cholesterol efflux mediated by ABCG1.* J Lipid Res, 2007. **48**(11): p. 2377-84.
198. Montefusco, D.J., et al., *Distinct signaling roles of ceramide species in yeast revealed through systematic perturbation and systems biology analyses.* Sci Signal, 2013. **6**(299): p. rs14.
199. Ramirez de Molina, A., et al., *Acid ceramidase as a chemotherapeutic target to overcome resistance to the antitumoral effect of choline kinase alpha inhibition.* Curr Cancer Drug Targets, 2012. **12**(6): p. 617-24.
200. Korbelik, M., et al., *Cationic ceramides and analogues, LCL30 and LCL85, as adjuvants to photodynamic therapy of tumors.* J Photochem Photobiol B, 2013. **126C**: p. 72-77.

201. Hankins, J.L., et al., *Ceramide 1-Phosphate Mediates Endothelial Cell Invasion via the Annexin a2-p11 Heterotetrameric Protein Complex.* J Biol Chem, 2013. **288**(27): p. 19726-38.
202. Gangoiti, P., et al., *Ceramide 1-phosphate stimulates proliferation of C2C12 myoblasts.* Biochimie, 2012. **94**(3): p. 597-607.
203. Realini, N., et al., *Discovery of highly potent acid ceramidase inhibitors with in vitro tumor chemosensitizing activity.* Sci Rep, 2013. **3**: p. 1035.
204. Adada, M., C. Luberto, and D. Canals, *Inhibitors of the sphingomyelin cycle: Sphingomyelin synthases and sphingomyelinases.* Chem Phys Lipids, 2016. **197**: p. 45-59.
205. Rovina, P., et al., *Subcellular localization of ceramide kinase and ceramide kinase-like protein requires interplay of their Pleckstrin Homology domain-containing N-terminal regions together with C-terminal domains.* Biochim Biophys Acta, 2009. **1791**(10): p. 1023-30.
206. Lamour, N.F., et al., *Ceramide kinase uses ceramide provided by ceramide transport protein: localization to organelles of eicosanoid synthesis.* J Lipid Res, 2007. **48**(6): p. 1293-304.
207. Sugiura, M., et al., *Ceramide kinase, a novel lipid kinase. Molecular cloning and functional characterization.* J Biol Chem, 2002. **277**(26): p. 23294-300.
208. Pettus, B.J., C.E. Chalfant, and Y.A. Hannun, *Sphingolipids in inflammation: roles and implications.* Curr Mol Med, 2004. **4**(4): p. 405-18.
209. Pastukhov, O., et al., *The ceramide kinase inhibitor NVP-231 inhibits breast and lung cancer cell proliferation by inducing M phase arrest and subsequent cell death.* Br J Pharmacol, 2014. **171**(24): p. 5829-44.
210. Simanshu, D.K., et al., *Arabidopsis accelerated cell death 11, ACD11, is a ceramide-1-phosphate transfer protein and intermediary regulator of phytoceramide levels.* Cell Rep, 2014. **6**(2): p. 388-99.
211. Serrels, A., et al., *Nuclear FAK controls chemokine transcription, Tregs, and evasion of anti-tumor immunity.* Cell, 2015. **163**(1): p. 160-73.
212. Bonapace, L., et al., *Cessation of CCL2 inhibition accelerates breast cancer metastasis by promoting angiogenesis.* Nature, 2014. **515**(7525): p. 130-3.
213. Joyce, J.A. and D.T. Fearon, *T cell exclusion, immune privilege, and the tumor microenvironment.* Science, 2015. **348**(6230): p. 74-80.
214. Marusyk, A., et al., *Non-cell-autonomous driving of tumour growth supports sub-clonal heterogeneity.* Nature, 2014. **514**(7520): p. 54-8.
215. Grivennikov, S.I. and M. Karin, *Inflammatory cytokines in cancer: tumour necrosis factor and interleukin 6 take the stage.* Ann Rheum Dis, 2011. **70 Suppl 1**: p. i104-8.
216. Soria, G., et al., *Inflammatory mediators in breast cancer: coordinated expression of TNFalpha & IL-1beta with CCL2 & CCL5 and effects on epithelial-to-mesenchymal transition.* BMC Cancer, 2011. **11**: p. 130.
217. Ponnusamy, S., et al., *Sphingolipids and cancer: ceramide and sphingosine-1-phosphate in the regulation of cell death and drug resistance.* Future Oncol, 2010. **6**(10): p. 1603-24.

218. Dandan, L., et al., *CCL5 as a potential immunotherapeutic target in triple-negative breast cancer.* Cellular & Molecular Immunology, 2013. **10**(4): p. 303-310.
219. Wolczyk, D., et al., *TNF-alpha promotes breast cancer cell migration and enhances the concentration of membrane-associated proteases in lipid rafts.* Cell Oncol (Dordr), 2016.
220. Futakuchi, M., K. Fukamachi, and M. Suzui, *Heterogeneity of tumor cells in the bone microenvironment: Mechanisms and therapeutic targets for bone metastasis of prostate or breast cancer.* Adv Drug Deliv Rev, 2016. **99**(Pt B): p. 206-11.
221. Demirkan, B., *The Roles of Epithelial-to-Mesenchymal Transition (EMT) and Mesenchymal-to-Epithelial Transition (MET) in Breast Cancer Bone Metastasis: Potential Targets for Prevention and Treatment.* J Clin Med, 2013. **2**(4): p. 264-82.
222. Banerjee, K. and H. Resat, *Constitutive activation of STAT3 in breast cancer cells: A review.* Int J Cancer, 2016. **138**(11): p. 2570-8.
223. Juárez, P. and T.A. Guise, *TGF-β in cancer and bone: Implications for treatment of bone metastases.* Bone. **48**(1): p. 23-29.
224. Korkaya, H., S. Liu, and M.S. Wicha, *Breast cancer stem cells, cytokine networks, and the tumor microenvironment.* J Clin Invest, 2011. **121**(10): p. 3804-9.
225. Niwa, Y., et al., *Correlation of tissue and plasma RANTES levels with disease course in patients with breast or cervical cancer.* Clin Cancer Res, 2001. **7**(2): p. 285-9.
226. Luboshits, G., et al., *Elevated expression of the CC chemokine regulated on activation, normal T cell expressed and secreted (RANTES) in advanced breast carcinoma.* Cancer Res, 1999. **59**(18): p. 4681-7.
227. Bieche, I., et al., *Molecular profiling of inflammatory breast cancer: identification of a poor-prognosis gene expression signature.* Clin Cancer Res, 2004. **10**(20): p. 6789-95.
228. Velasco-Velazquez, M., et al., *CCR5 antagonist blocks metastasis of basal breast cancer cells.* Cancer Res, 2012. **72**(15): p. 3839-50.
229. Yaal-Hahoshen, N., et al., *The chemokine CCL5 as a potential prognostic factor predicting disease progression in stage II breast cancer patients.* Clin Cancer Res, 2006. **12**(15): p. 4474-80.
230. Velasco-Velázquez, M., et al., *CCR5 Antagonist Blocks Metastasis of Basal Breast Cancer Cells.* Cancer Research, 2012. **72**(15): p. 3839-3850.
231. Zhang, Q., et al., *CCL5-Mediated Th2 Immune Polarization Promotes Metastasis in Luminal Breast Cancer.* Cancer Res, 2015. **75**(20): p. 4312-21.
232. Ali, M., et al., *LPS-mediated septic shock is augmented in ceramide synthase 2 null mice due to elevated activity of TNFalpha-converting enzyme.* FEBS Lett, 2015. **589**(17): p. 2213-7.
233. Jenkins, R.W., et al., *Regulated secretion of acid sphingomyelinase: implications for selectivity of ceramide formation.* J Biol Chem, 2010. **285**(46): p. 35706-18.

234. Zeidan, Y.H. and Y.A. Hannun, *Activation of acid sphingomyelinase by protein kinase Cdelta-mediated phosphorylation.* J Biol Chem, 2007. **282**(15): p. 11549-61.
235. Sohda, M., Y. Misumi, and K. Oda, *TNFalpha triggers release of extracellular vesicles containing TNFR1 and TRADD, which can modulate TNFalpha responses of the parental cells.* Arch Biochem Biophys, 2015. **587**: p. 31-7.
236. Barth, B.M., et al., *Ceramide kinase regulates TNFalpha-stimulated NADPH oxidase activity and eicosanoid biosynthesis in neuroblastoma cells.* Cell Signal, 2012. **24**(6): p. 1126-33.
237. Mitsutake, S., et al., *The generation and behavioral analysis of ceramide kinase-null mice, indicating a function in cerebellar Purkinje cells.* Biochem Biophys Res Commun, 2007. **363**(3): p. 519-24.
238. Frank, S.P., et al., *SNAP-23 and syntaxin-3 are required for chemokine release by mature human mast cells.* Mol Immunol, 2011. **49**(1-2): p. 353-8.
239. Lim, J.K., et al., *Multiple pathways of amino terminal processing produce two truncated variants of RANTES/CCL5.* J Leukoc Biol, 2005. **78**(2): p. 442-52.
240. Hoffmann, A., et al., *The IkappaB-NF-kappaB signaling module: temporal control and selective gene activation.* Science, 2002. **298**(5596): p. 1241-5.
241. Lacy, P., et al., *Fusion protein vesicle-associated membrane protein 2 is implicated in IFN-gamma-induced piecemeal degranulation in human eosinophils from atopic individuals.* J Allergy Clin Immunol, 2001. **107**(4): p. 671-8.
242. Simanshu, D.K., et al., *Non-vesicular trafficking by a ceramide-1-phosphate transfer protein regulates eicosanoids.* Nature, 2013. **500**(7463): p. 463-7.
243. Sawai, H., H. Ogiso, and T. Okazaki, *Differential changes in sphingolipids between TNF-induced necroptosis and apoptosis in U937 cells and necroptosis-resistant sublines.* Leuk Res, 2015. **39**(9): p. 964-70.
244. Bini, F., et al., *New signalling pathway involved in the anti-proliferative action of vitamin D(3) and its analogues in human neuroblastoma cells. A role for ceramide kinase.* Neuropharmacology, 2012. **63**(4): p. 524-37.
245. Saglam, S., R. Suzme, and F. Gurdol, *Serum tumor necrosis factor-alpha and interleukin-2 concentrations in newly diagnosed ERBB2 (HER2/neu) positive breast cancer patients.* Int J Biol Markers, 2009. **24**(3): p. 142-6.
246. Omair, M.A., V. Phumethum, and S.R. Johnson, *Long-term safety and effectiveness of tumour necrosis factor inhibitors in systemic sclerosis patients with inflammatory arthritis.* Clin Exp Rheumatol, 2012. **30**(2 Suppl 71): p. S55-9.
247. Payne, A.W., et al., *Ceramide kinase promotes tumor cell survival and mammary tumor recurrence.* Cancer Res, 2014. **74**(21): p. 6352-63.
248. Qiao, Y., et al., *AP-1 Is a Key Regulator of Proinflammatory Cytokine TNFalpha-mediated Triple-negative Breast Cancer Progression.* J Biol Chem, 2016. **291**(10): p. 5068-79.
249. Lamour, N.F. and C.E. Chalfant, *Ceramide kinase and the ceramide-1-phosphate/cPLA2alpha interaction as a therapeutic target.* Curr Drug Targets, 2008. **9**(8): p. 674-82.

250. Grivennikov, S.I. and M. Karin, *Inflammatory cytokines in cancer: tumour necrosis factor and interleukin 6 take the stage.* Ann Rheum Dis. **70 Suppl 1**: p. i104-8.
251. Tawara, K., J.T. Oxford, and C.L. Jorcyk, *Clinical significance of interleukin (IL)-6 in cancer metastasis to bone: potential of anti-IL-6 therapies.* Cancer Manag Res. **3**: p. 177-89.
252. Sullivan, N.J., et al., *Interleukin-6 induces an epithelial-mesenchymal transition phenotype in human breast cancer cells.* Oncogene, 2009. **28**(33): p. 2940-7.
253. Grivennikov, S., et al., *IL-6 and Stat3 are required for survival of intestinal epithelial cells and development of colitis-associated cancer.* Cancer Cell, 2009. **15**(2): p. 103-13.
254. Faggioli, L., et al., *Nuclear factor kappa B (NF-kappa B), nuclear factor interleukin-6 (NFIL-6 or C/EBP beta) and nuclear factor interleukin-6 beta (NFIL6-beta or C/EBP delta) are not sufficient to activate the endogenous interleukin-6 gene in the human breast carcinoma cell line MCF-7. Comparative analysis with MDA-MB-231 cells, an interleukin-6-expressing human breast carcinoma cell line.* Eur J Biochem, 1996. **239**(3): p. 624-31.
255. Merrill, A.H., Jr., *Sphingolipid and glycosphingolipid metabolic pathways in the era of sphingolipidomics.* Chem Rev, 2011. **111**(10): p. 6387-422.
256. Kitatani, K., et al., *Involvement of acid beta-glucosidase 1 in the salvage pathway of ceramide formation.* J Biol Chem, 2009. **284**(19): p. 12972-8.
257. Becker, K.P., et al., *Selective inhibition of juxtanuclear translocation of protein kinase C betaII by a negative feedback mechanism involving ceramide formed from the salvage pathway.* J Biol Chem, 2005. **280**(4): p. 2606-12.
258. Laulederkind, S.J., et al., *Ceramide induces interleukin 6 gene expression in human fibroblasts.* J Exp Med, 1995. **182**(2): p. 599-604.
259. Manthey, C.L. and E.H. Schuchman, *Acid sphingomyelinase-derived ceramide is not required for inflammatory cytokine signalling in murine macrophages.* Cytokine, 1998. **10**(9): p. 654-61.
260. Sakata, A., et al., *Acid sphingomyelinase inhibition suppresses lipopolysaccharide-mediated release of inflammatory cytokines from macrophages and protects against disease pathology in dextran sulphate sodium-induced colitis in mice.* Immunology, 2007. **122**(1): p. 54-64.
261. Kumagai, T., T. Ishino, and Y. Nakagawa, *Acidic sphingomyelinase induced by electrophiles promotes proinflammatory cytokine production in human bladder carcinoma ECV-304 cells.* Arch Biochem Biophys, 2012. **519**(1): p. 8-16.
262. Muller, P.Y., et al., *Processing of gene expression data generated by quantitative real-time RT-PCR.* Biotechniques, 2002. **32**(6): p. 1372-4, 1376, 1378-9.
263. Jenkins, R.W., et al., *Regulated secretion of acid sphingomyelinase: implications for selectivity of ceramide formation.* J Biol Chem. **285**(46): p. 35706-18.
264. Carter, A.B., M.M. Monick, and G.W. Hunninghake, *Both Erk and p38 kinases are necessary for cytokine gene transcription.* Am J Respir Cell Mol Biol, 1999. **20**(4): p. 751-8.

265. Kondo, A., Y. Koshihara, and A. Togari, *Signal transduction system for interleukin-6 synthesis stimulated by lipopolysaccharide in human osteoblasts.* J Interferon Cytokine Res, 2001. **21**(11): p. 943-50.
266. Vanden Berghe, W., et al., *p38 and extracellular signal-regulated kinase mitogen-activated protein kinase pathways are required for nuclear factor-kappaB p65 transactivation mediated by tumor necrosis factor.* J Biol Chem, 1998. **273**(6): p. 3285-90.
267. Rousseau, S., et al., *Inhibition of SAPK2a/p38 prevents hnRNP A0 phosphorylation by MAPKAP-K2 and its interaction with cytokine mRNAs.* EMBO J, 2002. **21**(23): p. 6505-14.
268. Zeisel, A., et al., *Coupled pre-mRNA and mRNA dynamics unveil operational strategies underlying transcriptional responses to stimuli.* Mol Syst Biol, 2011. **7**: p. 529.
269. Gallucci, R.M., et al., *Interleukin 6 indirectly induces keratinocyte migration.* J Invest Dermatol, 2004. **122**(3): p. 764-72.
270. Studebaker, A.W., et al., *Fibroblasts isolated from common sites of breast cancer metastasis enhance cancer cell growth rates and invasiveness in an interleukin-6-dependent manner.* Cancer Res, 2008. **68**(21): p. 9087-95.
271. Oh, K., et al., *Transglutaminase 2 facilitates the distant hematogenous metastasis of breast cancer by modulating interleukin-6 in cancer cells.* Breast Cancer Res, 2011. **13**(5): p. R96.
272. Hurwitz, R., K. Ferlinz, and K. Sandhoff, *The tricyclic antidepressant desipramine causes proteolytic degradation of lysosomal sphingomyelinase in human fibroblasts.* Biol Chem Hoppe Seyler, 1994. **375**(7): p. 447-50.
273. Aureli, M., et al., *Activity of plasma membrane beta-galactosidase and beta-glucosidase.* FEBS Lett, 2009. **583**(15): p. 2469-73.
274. Schissel, S.L., et al., *The cellular trafficking and zinc dependence of secretory and lysosomal sphingomyelinase, two products of the acid sphingomyelinase gene.* J Biol Chem, 1998. **273**(29): p. 18250-9.
275. Rozenova, K.A., et al., *Studies on the role of acid sphingomyelinase and ceramide in the regulation of tumor necrosis factor alpha (TNFalpha)-converting enzyme activity and TNFalpha secretion in macrophages.* J Biol Chem, 2010. **285**(27): p. 21103-13.
276. Kumagai, T., T. Ishino, and Y. Nakagawa, *Acidic sphingomyelinase induced by electrophiles promotes proinflammatory cytokine production in human bladder carcinoma ECV-304 cells.* Arch Biochem Biophys. **519**(1): p. 8-16.
277. Jin, J., et al., *Acid Sphingomyelinase Plays a Key Role in Palmitic Acid-Amplified Inflammatory Signaling Triggered by Lipopolysaccharide at Low Concentration in Macrophages.* Am J Physiol Endocrinol Metab, 2013.
278. Hao, S. and D. Baltimore, *The stability of mRNA influences the temporal order of the induction of genes encoding inflammatory molecules.* Nat Immunol, 2009. **10**(3): p. 281-8.
279. Bauer, J., et al., *Matrix metalloproteinase-1 expression induced by IL-1beta requires acid sphingomyelinase.* FEBS Lett, 2009. **583**(5): p. 915-20.
280. Kato, Y., et al., *Acidic extracellular pH increases calcium influx-triggered phospholipase D activity along with acidic sphingomyelinase activation to*

induce matrix metalloproteinase-9 expression in mouse metastatic melanoma. FEBS J, 2007. **274**(12): p. 3171-83.
281. Liangpunsakul, S., et al., *Imipramine blocks ethanol-induced ASMase activation, ceramide generation, and PP2A activation, and ameliorates hepatic steatosis in ethanol-fed mice.* Am J Physiol Gastrointest Liver Physiol. **302**(5): p. G515-23.
282. Adada, M.M., et al., *Sphingosine kinase 1 regulates tumor necrosis factor-mediated RANTES induction through p38 mitogen-activated protein kinase but independently of nuclear factor kappaB activation.* J Biol Chem, 2013. **288**(38): p. 27667-79.
283. Modur, V., et al., *Endothelial cell inflammatory responses to tumor necrosis factor alpha. Ceramide-dependent and -independent mitogen-activated protein kinase cascades.* J Biol Chem, 1996. **271**(22): p. 13094-102.
284. Zeidan, Y.H., et al., *A novel role for protein kinase Cdelta-mediated phosphorylation of acid sphingomyelinase in UV light-induced mitochondrial injury.* FASEB J, 2008. **22**(1): p. 183-93.
285. Charruyer, A., et al., *PKCzeta protects against UV-C-induced apoptosis by inhibiting acid sphingomyelinase-dependent ceramide production.* Biochem J, 2007. **405**(1): p. 77-83.
286. Pena, L.A., Z. Fuks, and R.N. Kolesnick, *Radiation-induced apoptosis of endothelial cells in the murine central nervous system: protection by fibroblast growth factor and sphingomyelinase deficiency.* Cancer Res, 2000. **60**(2): p. 321-7.
287. Ion, G., et al., *Acid sphingomyelinase mediated release of ceramide is essential to trigger the mitochondrial pathway of apoptosis by galectin-1.* Cell Signal, 2006. **18**(11): p. 1887-96.
288. Falcone, S., et al., *Activation of acid sphingomyelinase and its inhibition by the nitric oxide/cyclic guanosine 3',5'-monophosphate pathway: key events in Escherichia coli-elicited apoptosis of dendritic cells.* J Immunol, 2004. **173**(7): p. 4452-63.
289. Zhang, Y., et al., *Acid sphingomyelinase amplifies redox signaling in Pseudomonas aeruginosa-induced macrophage apoptosis.* J Immunol, 2008. **181**(6): p. 4247-54.
290. Feng, Y., J. Wen, and C.C. Chang, *p38 Mitogen-activated protein kinase and hematologic malignancies.* Arch Pathol Lab Med, 2009. **133**(11): p. 1850-6.
291. Oh, K., et al., *Transglutaminase 2 facilitates the distant hematogenous metastasis of breast cancer by modulating interleukin-6 in cancer cells.* Breast Cancer Res. **13**(5): p. R96.
292. Ruffell, B., N.I. Affara, and L.M. Coussens, *Differential macrophage programming in the tumor microenvironment.* Trends Immunol, 2012. **33**(3): p. 119-26.
293. Kim, M.Y., et al., *Identification of sphingomyelin turnover as an effector mechanism for the action of tumor necrosis factor alpha and gamma-interferon. Specific role in cell differentiation.* J Biol Chem, 1991. **266**(1): p. 484-9.

294. Petersen, N.H., et al., *Transformation-associated changes in sphingolipid metabolism sensitize cells to lysosomal cell death induced by inhibitors of acid sphingomyelinase.* Cancer Cell, 2013. **24**(3): p. 379-93.
295. Adan-Gokbulut, A., et al., *Novel agents targeting bioactive sphingolipids for the treatment of cancer.* Curr Med Chem, 2013. **20**(1): p. 108-22.
296. Antoon, J.W., et al., *Pharmacological inhibition of sphingosine kinase isoforms alters estrogen receptor signaling in human breast cancer.* J Mol Endocrinol, 2011. **46**(3): p. 205-16.
297. Gangoiti, P., et al., *Implication of ceramide, ceramide 1-phosphate and sphingosine 1-phosphate in tumorigenesis.* Transl Oncogenomics, 2008. **3**: p. 81-98.
298. Heering, J., et al., *Loss of the ceramide transfer protein augments EGF receptor signaling in breast cancer.* Cancer Res, 2012. **72**(11): p. 2855-66.
299. Karnoub, A.E., et al., *Mesenchymal stem cells within tumour stroma promote breast cancer metastasis.* Nature, 2007. **449**(7162): p. 557-63.
300. Azenshtein, E., et al., *The CC chemokine RANTES in breast carcinoma progression: regulation of expression and potential mechanisms of promalignant activity.* Cancer Res, 2002. **62**(4): p. 1093-102.
301. Kurt, R.A., et al., *Chemokine receptor desensitization in tumor-bearing mice.* Cell Immunol, 2001. **207**(2): p. 81-8.
302. Epanchintsev, A., et al., *IL-6, IL-8, MMP-2, MMP-9 are overexpressed in Fanconi anemia cells through a NF-kappaB/TNF-alpha dependent mechanism.* Mol Carcinog, 2015. **54**(12): p. 1686-99.
303. Eichten, A., et al., *Resistance to anti-VEGF therapy mediated by autocrine IL-6/STAT3 signaling and overcome by IL-6 blockade.* Cancer Res, 2016.
304. Zheng, Y., et al., *Direct crosstalk between cancer and osteoblast lineage cells fuels metastatic growth in bone via auto-amplification of IL-6 and RANKL signaling pathways.* J Bone Miner Res, 2014. **29**(9): p. 1938-49.
305. Wu, Y., M. Sarkissyan, and J.V. Vadgama, *Epithelial-Mesenchymal Transition and Breast Cancer.* J Clin Med, 2016. **5**(2).
306. Xie, G., et al., *IL-6-induced epithelial-mesenchymal transition promotes the generation of breast cancer stem-like cells analogous to mammosphere cultures.* Int J Oncol, 2012. **40**(4): p. 1171-9.
307. Li, C.W., et al., *Epithelial-mesenchymal transition induced by TNF-alpha requires NF-kappaB-mediated transcriptional upregulation of Twist1.* Cancer Res, 2012. **72**(5): p. 1290-300.
308. Huber, M.A., et al., *NF-kappaB is essential for epithelial-mesenchymal transition and metastasis in a model of breast cancer progression.* J Clin Invest, 2004. **114**(4): p. 569-81.
309. Shaw, F.L., et al., *A detailed mammosphere assay protocol for the quantification of breast stem cell activity.* J Mammary Gland Biol Neoplasia, 2012. **17**(2): p. 111-7.
310. Snider, A.J., et al., *Distinct roles for hematopoietic and extra-hematopoietic sphingosine kinase-1 in inflammatory bowel disease.* PLoS One, 2014. **9**(12): p. e113998.

311. Gyorffy, B., et al., *An online survival analysis tool to rapidly assess the effect of 22,277 genes on breast cancer prognosis using microarray data of 1,809 patients.* Breast Cancer Res Treat, 2010. **123**(3): p. 725-31.
312. Chen, W., et al., *The CCL2/CCR2 axis enhances IL-6-induced epithelial-mesenchymal transition by cooperatively activating STAT3-Twist signaling.* Tumour Biol, 2015. **36**(2): p. 973-81.
313. Zhang, B., et al., *Nir1 promotes invasion of breast cancer cells by binding to chemokine (C-C motif) ligand 18 through the PI3K/Akt/GSK3beta/Snail signalling pathway.* Eur J Cancer, 2013. **49**(18): p. 3900-13.
314. Naber, H.P., et al., *Snail and Slug, key regulators of TGF-beta-induced EMT, are sufficient for the induction of single-cell invasion.* Biochem Biophys Res Commun, 2013. **435**(1): p. 58-63.
315. Katanov, C., et al., *Regulation of the inflammatory profile of stromal cells in human breast cancer: prominent roles for TNF-alpha and the NF-kappaB pathway.* Stem Cell Res Ther, 2015. **6**: p. 87.
316. Bae, Y.K., et al., *Epithelial-Mesenchymal Transition Phenotype Is Associated with Clinicopathological Factors That Indicate Aggressive Biological Behavior and Poor Clinical Outcomes in Invasive Breast Cancer.* J Breast Cancer, 2015. **18**(3): p. 256-63.
317. Wang, R., et al., *Comparison of mammosphere formation from breast cancer cell lines and primary breast tumors.* J Thorac Dis, 2014. **6**(6): p. 829-37.
318. Ribeiro, A.S. and J. Paredes, *P-Cadherin Linking Breast Cancer Stem Cells and Invasion: A Promising Marker to Identify an "Intermediate/Metastable" EMT State.* Front Oncol, 2014. **4**: p. 371.
319. Mani, S.A., et al., *The epithelial-mesenchymal transition generates cells with properties of stem cells.* Cell, 2008. **133**(4): p. 704-15.
320. Presa, N., et al., *Regulation of cell migration and inflammation by ceramide 1-phosphate.* Biochim Biophys Acta, 2016. **1861**(5): p. 402-9.
321. Shou, J., et al., *Nuclear factor of activated T cells in cancer development and treatment.* Cancer Lett, 2015. **361**(2): p. 174-84.
322. Tripathi, P., et al., *Activation of NFAT signaling establishes a tumorigenic microenvironment through cell autonomous and non-cell autonomous mechanisms.* Oncogene, 2014. **33**(14): p. 1840-9.
323. Baksh, S., et al., *NFATc2-mediated repression of cyclin-dependent kinase 4 expression.* Mol Cell, 2002. **10**(5): p. 1071-81.
324. Buchholz, M., et al., *Overexpression of c-myc in pancreatic cancer caused by ectopic activation of NFATc1 and the Ca2+/calcineurin signaling pathway.* EMBO J, 2006. **25**(15): p. 3714-24.
325. Neal, J.W. and N.A. Clipstone, *A constitutively active NFATc1 mutant induces a transformed phenotype in 3T3-L1 fibroblasts.* J Biol Chem, 2003. **278**(19): p. 17246-54.
326. Kim, S.Y., et al., *Role of the IL-6-JAK1-STAT3-Oct-4 pathway in the conversion of non-stem cancer cells into cancer stem-like cells.* Cell Signal, 2013. **25**(4): p. 961-9.
327. Jiang, X., et al., *Elevated autocrine chemokine ligand 18 expression promotes oral cancer cell growth and invasion via Akt activation.* Oncotarget, 2016.

328. Narita, D., et al., *Altered levels of plasma chemokines in breast cancer and their association with clinical and pathological characteristics.* Neoplasma, 2016. **63**(1): p. 141-9.
329. Gao, J., et al., *Chemokine C-C motif ligand 18 expression correlates with tumor malignancy in breast cancer.* Pathol Biol (Paris), 2015. **63**(4-5): p. 199-203.
330. Meng, F., et al., *CCL18 promotes epithelial-mesenchymal transition, invasion and migration of pancreatic cancer cells in pancreatic ductal adenocarcinoma.* Int J Oncol, 2015. **46**(3): p. 1109-20.
331. Voduc, K.D., et al., *Breast cancer subtypes and the risk of local and regional relapse.* J Clin Oncol, 2010. **28**(10): p. 1684-91.
332. Qin, J.J., et al., *NFAT as cancer target: mission possible?* Biochim Biophys Acta, 2014. **1846**(2): p. 297-311.
333. Quang, C.T., et al., *The calcineurin/NFAT pathway is activated in diagnostic breast cancer cases and is essential to survival and metastasis of mammary cancer cells.* Cell Death Dis, 2015. **6**: p. e1658.
334. Sengupta, S., S. Jana, and A. Bhattacharyya, *TGF-beta-Smad2 dependent activation of CDC 25A plays an important role in cell proliferation through NFAT activation in metastatic breast cancer cells.* Cell Signal, 2014. **26**(2): p. 240-52.
335. Malekshah, O.M., et al., *PXR and NF-kappaB correlate with the inducing effects of IL-1beta and TNF-alpha on ABCG2 expression in breast cancer cell lines.* Eur J Pharm Sci, 2012. **47**(2): p. 474-80.
336. Qiao, E.Q. and H.J. Yang, *Effect of pregnane X receptor expression on drug resistance in breast cancer.* Oncol Lett, 2014. **7**(4): p. 1191-1196.
337. Foulds, C.E., et al., *Proteomic analysis of coregulators bound to ERalpha on DNA and nucleosomes reveals coregulator dynamics.* Mol Cell, 2013. **51**(2): p. 185-99.
338. Nishi, M., et al., *Induction of cells with cancer stem cell properties from nontumorigenic human mammary epithelial cells by defined reprogramming factors.* Oncogene, 2014. **33**(5): p. 643-52.
339. Hartikainen, J.M., et al., *KEAP1 Genetic Polymorphisms Associate with Breast Cancer Risk and Survival Outcomes.* Clin Cancer Res, 2015. **21**(7): p. 1591-601.
340. Katsuoka, F. and M. Yamamoto, *Small Maf proteins (MafF, MafG, MafK): History, structure and function.* Gene, 2016.
341. Gutierrez-Hartmann, A., D.L. Duval, and A.P. Bradford, *ETS transcription factors in endocrine systems.* Trends in Endocrinology & Metabolism, 2007. **18**(4): p. 150-158.
342. Heo, S.H., et al., *ELK3 Expression Correlates With Cell Migration, Invasion, and Membrane Type 1-Matrix Metalloproteinase Expression in MDA-MB-231 Breast Cancer Cells.* Gene Expr, 2015. **16**(4): p. 197-203.
343. French, J.D., et al., *Functional variants at the 11q13 risk locus for breast cancer regulate cyclin D1 expression through long-range enhancers.* Am J Hum Genet, 2013. **92**(4): p. 489-503.
344. Matsui, A., et al., *Hepatocyte nuclear factor 1 beta induces transformation and epithelial-to-mesenchymal transition.* FEBS Lett, 2016.

345. Sokol, C.L., et al., *A mechanism for the initiation of allergen-induced T helper type 2 responses.* Nat Immunol, 2008. **9**(3): p. 310-8.
346. Haricharan, S. and Y. Li, *STAT signaling in mammary gland differentiation, cell survival and tumorigenesis.* Mol Cell Endocrinol, 2014. **382**(1): p. 560-9.
347. DeNardo, D.G. and L.M. Coussens, *Inflammation and breast cancer. Balancing immune response: crosstalk between adaptive and innate immune cells during breast cancer progression.* Breast Cancer Res, 2007. **9**(4): p. 212.
348. Brantjes, H., et al., *TCF: Lady Justice casting the final verdict on the outcome of Wnt signalling.* Biol Chem, 2002. **383**(2): p. 255-61.
349. Park, J., et al., *AF1q is a novel TCF7 co-factor which activates CD44 and promotes breast cancer metastasis.* Oncotarget, 2015. **6**(24): p. 20697-710.
350. Espinosa, I., et al., *Simultaneous carcinomas of the breast and ovary: utility of Pax-8, WT-1, and GATA3 for distinguishing independent primary tumors from metastases.* Int J Gynecol Pathol, 2015. **34**(3): p. 257-65.
351. Davidson, B., et al., *Gene expression signatures differentiate ovarian/peritoneal serous carcinoma from breast carcinoma in effusions.* J Cell Mol Med, 2011. **15**(3): p. 535-44.
352. Muratovska, A., et al., *Paired-Box genes are frequently expressed in cancer and often required for cancer cell survival.* Oncogene, 2003. **22**(39): p. 7989-97.
353. Tao, D., et al., *B-Myb regulates snail expression to promote epithelial-to-mesenchymal transition and invasion of breast cancer cell.* Med Oncol, 2015. **32**(1): p. 412.
354. Ye, X., et al., *Distinct EMT programs control normal mammary stem cells and tumour-initiating cells.* Nature, 2015. **525**(7568): p. 256-60.
355. Chen, B.J., et al., *Small molecules targeting c-Myc oncogene: promising anti-cancer therapeutics.* Int J Biol Sci, 2014. **10**(10): p. 1084-96.

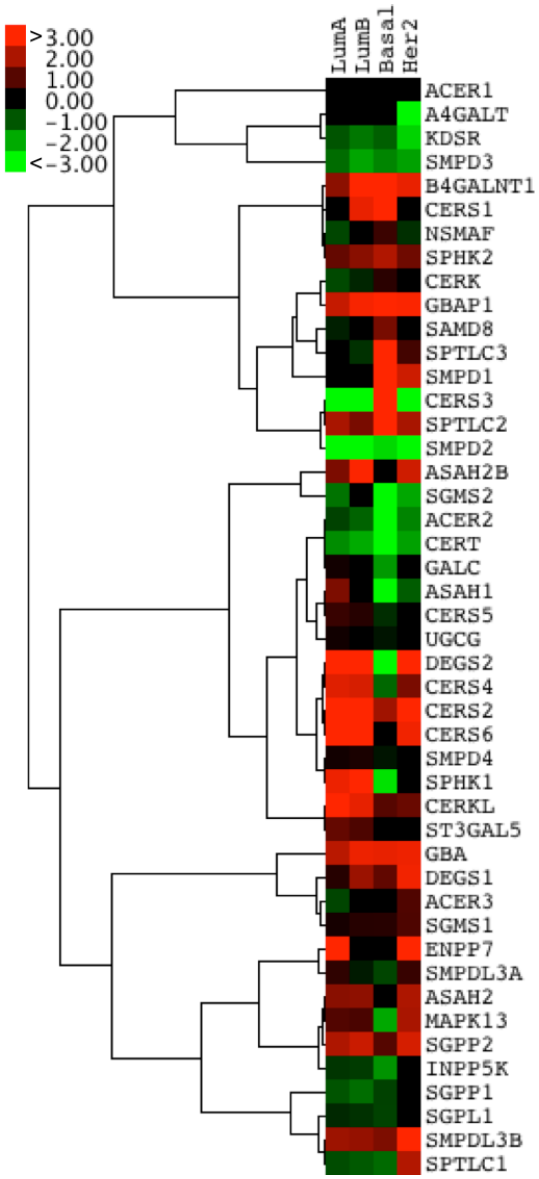

Figure 1. *Sphingolipid gene expression in molecular subtypes of breast cancer.* Publically available TCGA expression data was used to assess the expression levels of sphingolipid genes in molecular subtypes of breast cancer. Expression levels of the indicated genes were compared to expression in normal solid tissue, and the fold change was calculated. Hierarchical clustering was carried out as shown above.

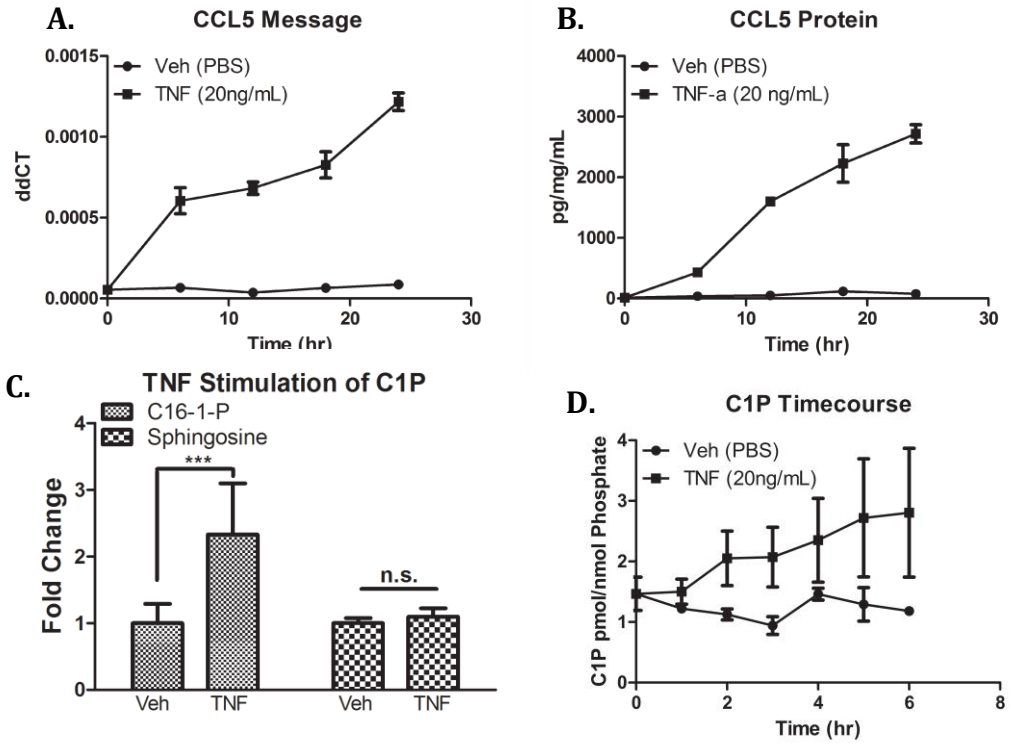

Figure 2. *Identification of a TNF-α induced C1P dependent pathway in MCF7 cells.* Logarithmically growing MCF7 Breast carcinoma cells were treated with Vehicle (PBS) or TNF-α (20ng/mL) for the indicated times. **(A)** CCL5 secretion into the media was measured by ELISA**,** and **(B)** mRNA levels of CCL5 were quantified by RTPCR**. (C)** Lipids were harvested from MCF7 cells treated with vehicle (PBS) or TNF-α (20ng/mL) for 18hrs. C1P and sphingosine were measured and normalized to total cellular lipid phosphate. **(D)** Lipids were harvested from MCF7 cells treated with vehicle (PBS) or TNF-α (20ng/mL) for the indicated time points. C1P was measured and normalized to total cellular lipid phosphate.

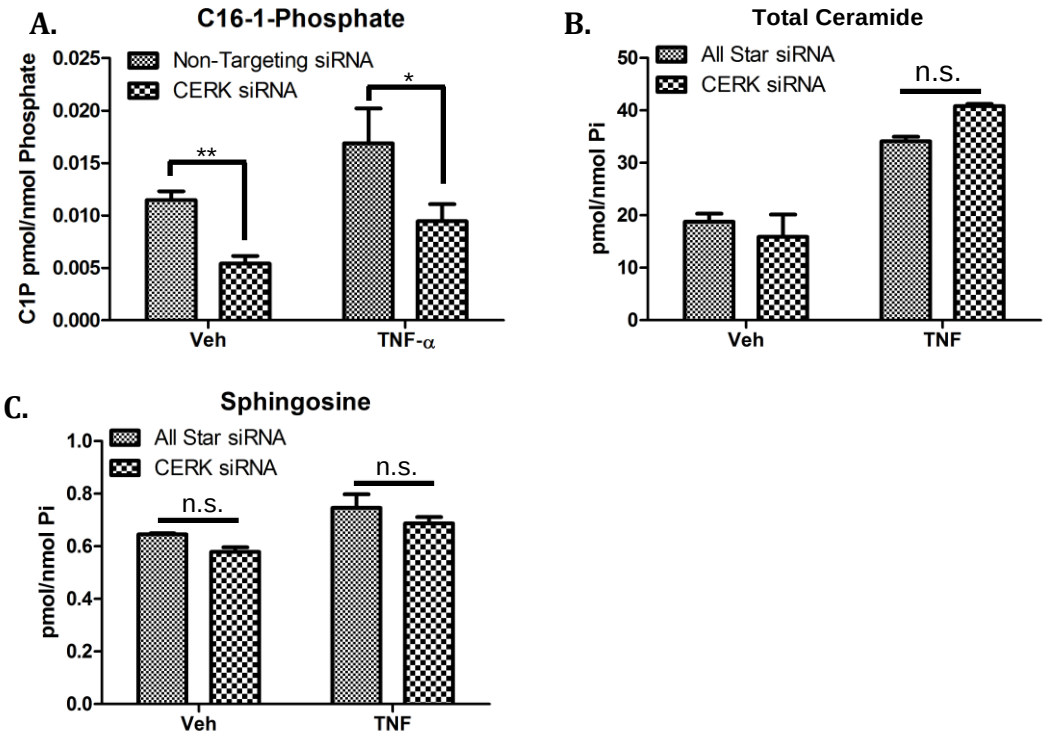

Figure 3. *Determination of a specific effect of CERK knock down on lipid levels of C1P.* MCF7 cells were treated with Non-Targeting (All Star) siRNA or CERK siRNA for 48 hrs prior to treatment with vehicle (PBS) or TNF-α for 18hrs. **(A)** C1P, **(B)** ceramide, and **(C)** sphingosine levels were analyzed and normalized to total lipid phosphate.

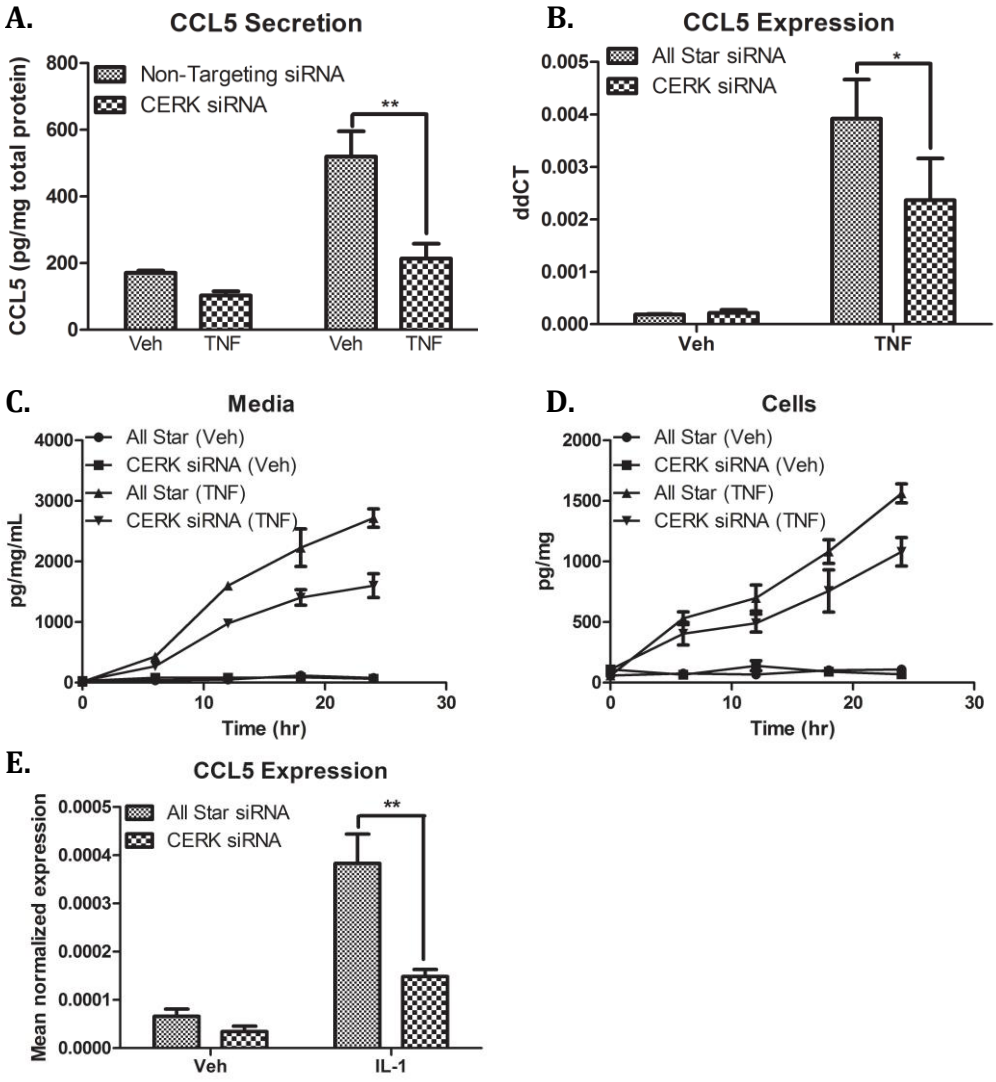

Figure 4. *CERK is required for CCL5 production in MCF7 cells.* Logarithmically growing MCF7 Breast carcinoma cells were treated with Non-Targeting (All Star) siRNA or CERK siRNA for 48 hrs prior Vehicle (PBS) or TNF-α (20ng/mL) for the indicated times. **(A)** CCL5 protein levels, and **(B)** CCL5 mRNA levels were measured. CCL5 levels were also measured in the **(C)** media and in **(D)** cells at the indicated timepoints. **(E)** MCF7 cells were transfected with the indicated siRNA, and then treated with IL-1β (20ng/mL) for 6hrs. CCL5 message level was measured.

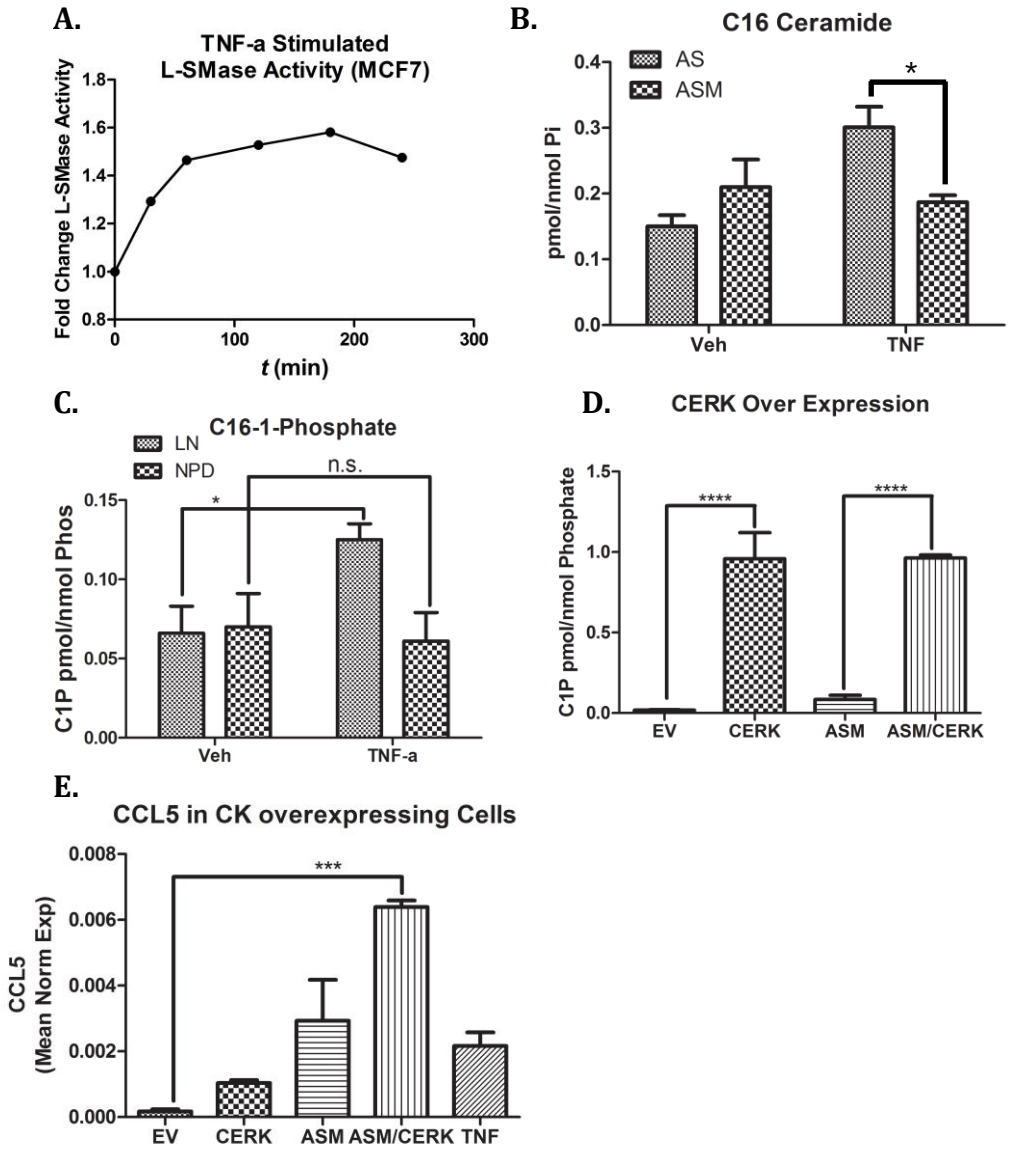

Figure 5. *Delineation of the contribution of ASM to CERK dependent C-1-P formation.* **(A)** MCF7 cells were treated with TNF-α, and ASM activity was measured at the indicated timepoints. **(B)** MCF7 cells were treated with Non-Targeting (All Star) or ASM siRNA for 48hrs, and then treated with vehicle (PBS) or TNF-α (20ng/mL) for 18hrs. Ceramide levels were measured and normalized to total lipid phosphate. **(C)** Fibroblasts from patients with Lesch Nyhan (LN) or Nieman-Pick Disease (NPD) were treated with vehicle (PBS) or TNF-α (20ng/mL) for 18 hrs. C-1-P levels were measured and normalized to total lipid phosphate. **(D)** MCF7 cells were transfected with the empty vector (EV), CERK overexpression vector (CERK), ASM overexpression vector (ASM), or ASM and CERK together. After 24hrs, C-1-P levels were measured and normalized to total lipid phosphate. **(E)** CCL5 message level was determined in MCF7 cells transfected with the indicated vectors for 24hrs.

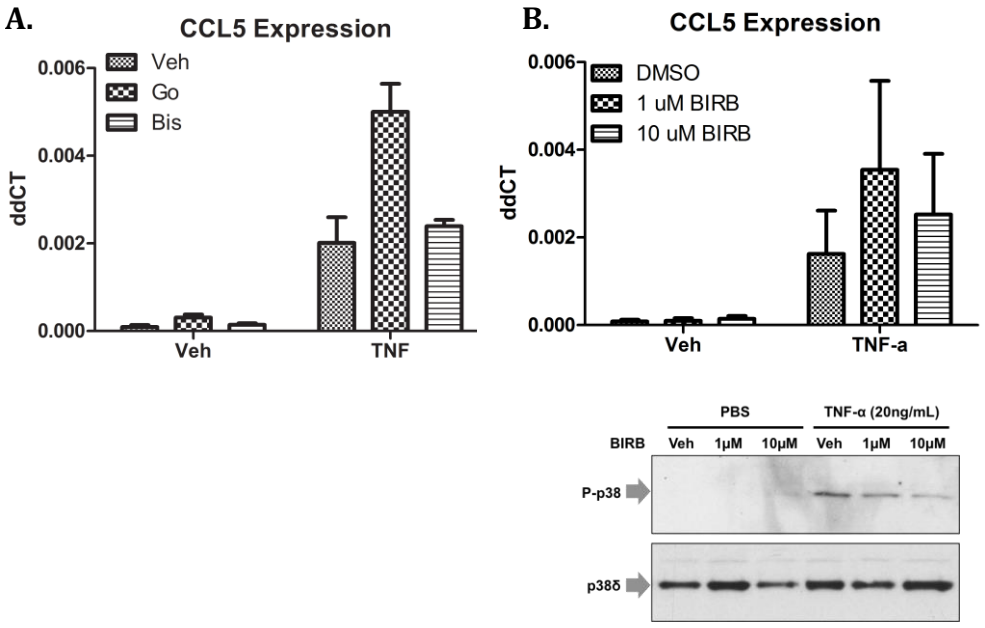

Figure 6. *Determination of the contribution of PKC and p38/MAPK to the Induction of CCL5*. **(A)** Vehicle (DMSO), or the PKC inhibitors Gö6976 (3 mM) and Bis (3mM) were added to logarithmically growing MCF-7 cells 60min prior to treatment with TNF-α (20ng/mL) for 6 hrs. CCL5 was measured by RTPCR. **(B)** Vehicle (DMSO), or the indicated concentrations of the p38 inhibitor BIRB796 were added to logarithmically growing MCF-7 cells 60min prior to treatment with TNF-α (20ng/mL) for 6 hrs. CCL5 was measured by RTPCR (top panel), and p38 phosphorylation was measured by western blot (lower panel).

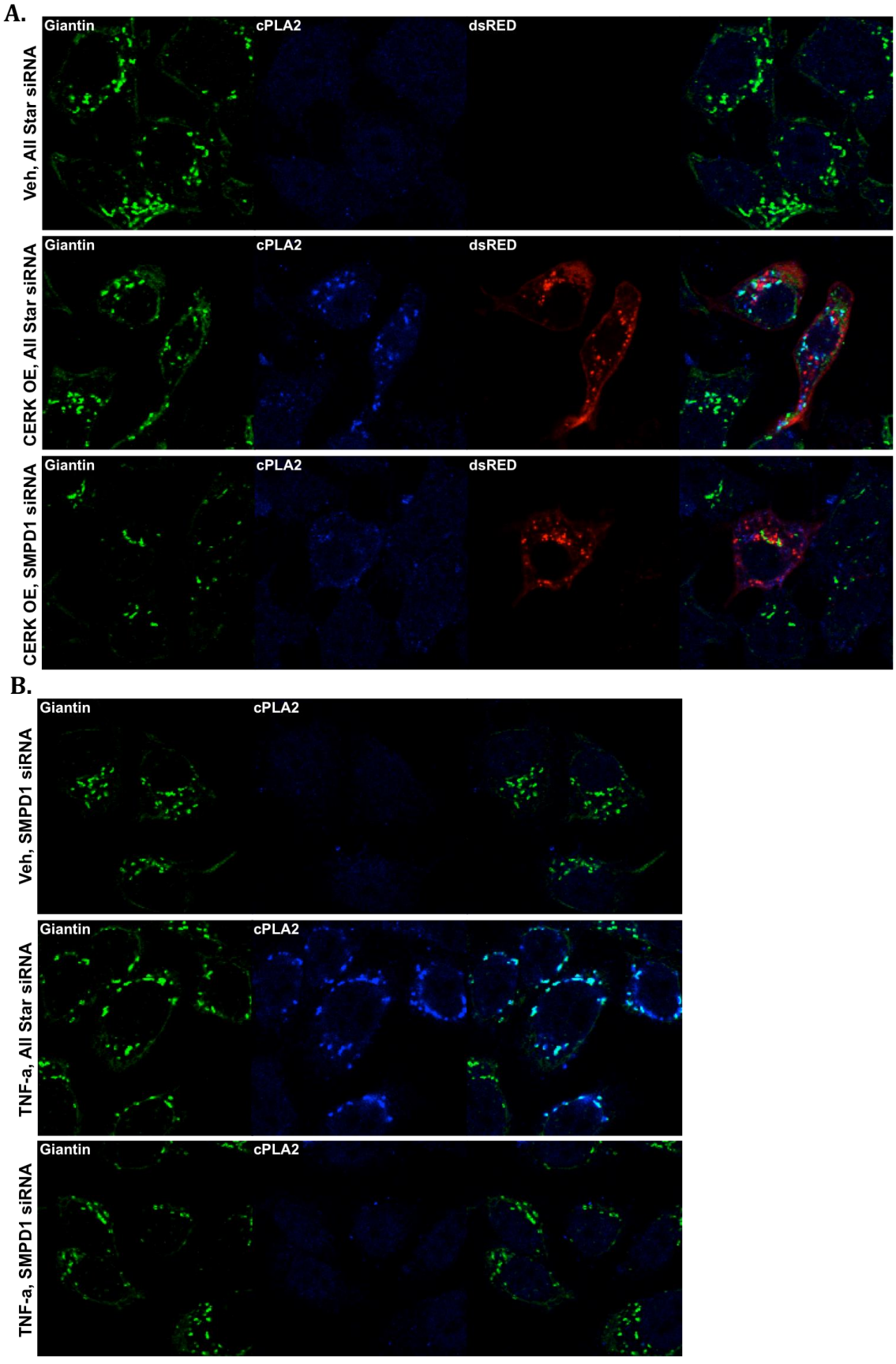
A.
Giantin
cPLA2
dsRED
Veh, All Star siRNA
CERK OE, All Star siRNA
CERK OE, SMPD1 siRNA
B.
Veh, SMPD1 siRNA
TNF-a, All Star siRNA
TNF-a, SMPD1 siRNA

Figure 7. *Identification of a role for ASM in CERK induced cPLA2 localization at the Golgi network*. **(A)** MCF7 cells were treated with Non-Targeting (All Star) or ASM siRNA and after 24hrs, transfected with EV or a CERK-dsRed overexpression vectors. Confocal microscopy was carried out using Giantin (green) and $cPLA_2$ (blue) antibodies. CERK was visualized by direct fluorescence of the dsRed tag (red). **(B)** MCF7 cells were treated with Non-Targeting (All Star) or ASM siRNA and after 48hrs, cells were treated with Vehicle (PBS) or TNF-α for 6 hours. $CPLA_2$ localization was assessed by confocal microscopy using antibodies to giantin (green) and $cPLA_2$ (blue).

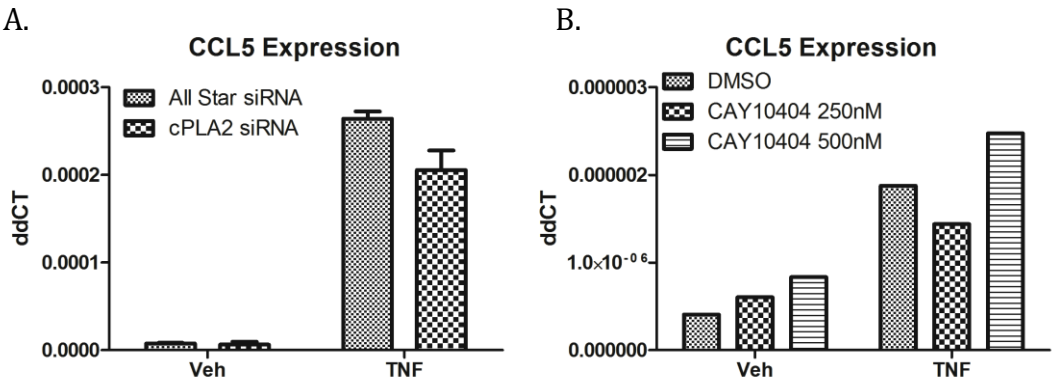

Figure 8. *Delineation of the contribution of prostaglandin signaling to CCL5 production.* **(A)** MCF7 cells were transfected with Non-Targeting (All Star) siRNA or siRNA targeting $cPLA_2$. After 48hrs of incubation, cells were treated with vehicle (PBS) or TNF-α (20ng/mL) for 18hrs, and CCL5 mRNA was measured by RTPCR. **(B)** MCF7 cells were pretreated for 60 min with vehicle (DMSO) or the COX2 inhibitor CAY1404, followed by incubation with vehicle (PBS) or TNF-α (20ng/mL) for 18 hrs. CCL5 were measured by RTPCR.

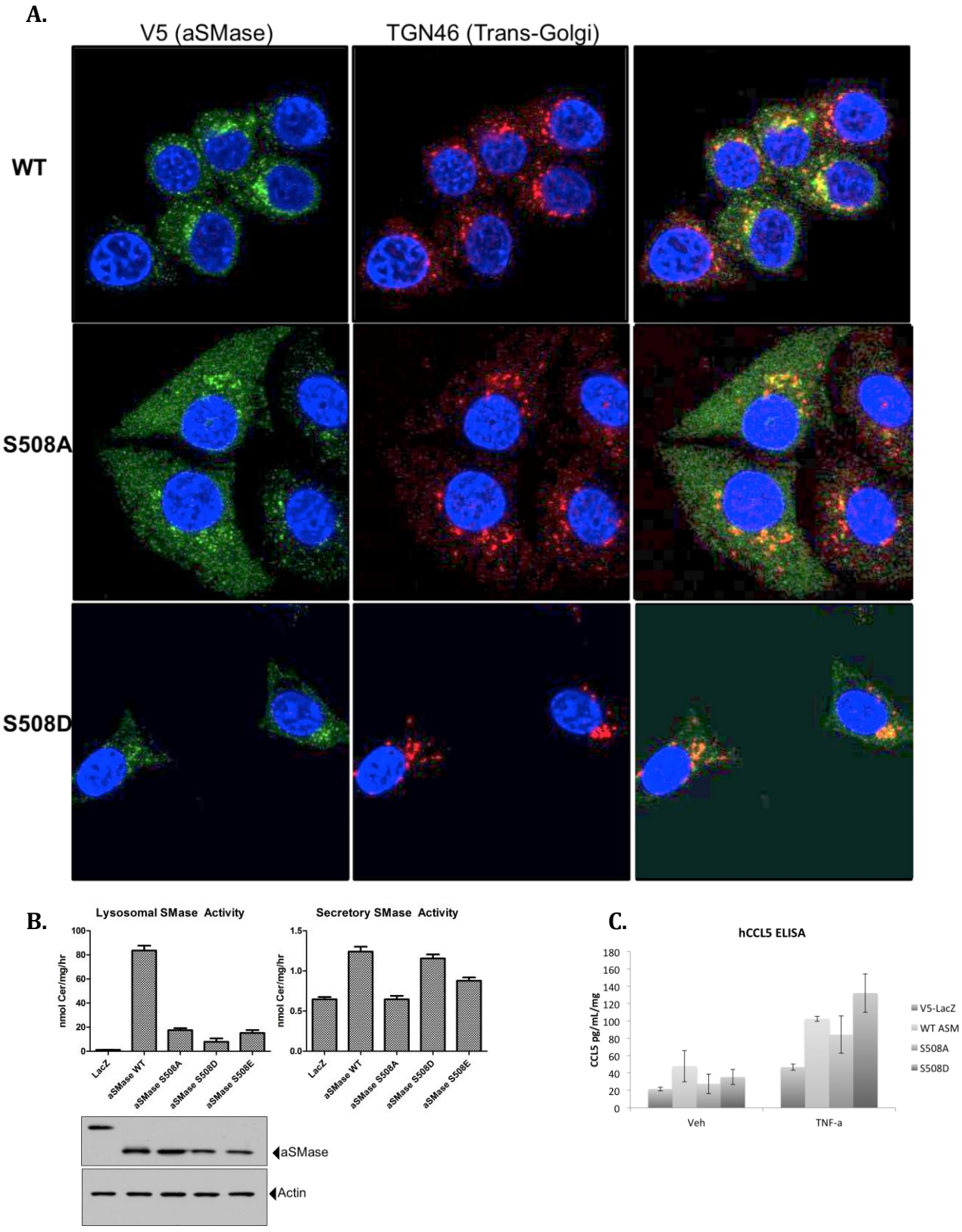
A.
V5 (aSMase)
TGN46 (Trans-Golgi)
WT
S508A
S508D
B.
Lysosomal SMase Activity
nmol Cer/mg/hr
LacZ
aSMase WT
aSMase S508A
aSMase S508D
aSMase S508E
Secretory SMase Activity
nmol Cer/mg/hr
aSMase
Actin
C.
hCCL5 ELISA
CCL5 pg/mL/mg
Veh
TNF-a
V5-LacZ
WT ASM
S508A
S508D

Figure 9. *Identification of a Golgi restricted mutant of ASM that specifically induces CCL5.* **(A)** MCF7 cells were virally transduced with mutants of ASM that were C-terminally tagged with V5, and subcellular localization was assessed by confocal microscopy. ASM was detected using an antibody to V5 (green), and the trans Golgi network was detected using an antibody to TGN46 (red). Nuclei were stained with DAPI (blue). **(B)** L-SMase (upper panel, right) and S-SMase (upper panel, left) activity was measured in cells expressing the indicated mutants of ASM. Comparable expression of each mutant was confirmend by western blot (lower panel). **(C)** MCF7 cells stably over expressing the indicated ASM mutants were treated with vehicle (PBS) or TNF-α (20ng/mL) for 18hrs, and CCL5 was measured by ELISA.

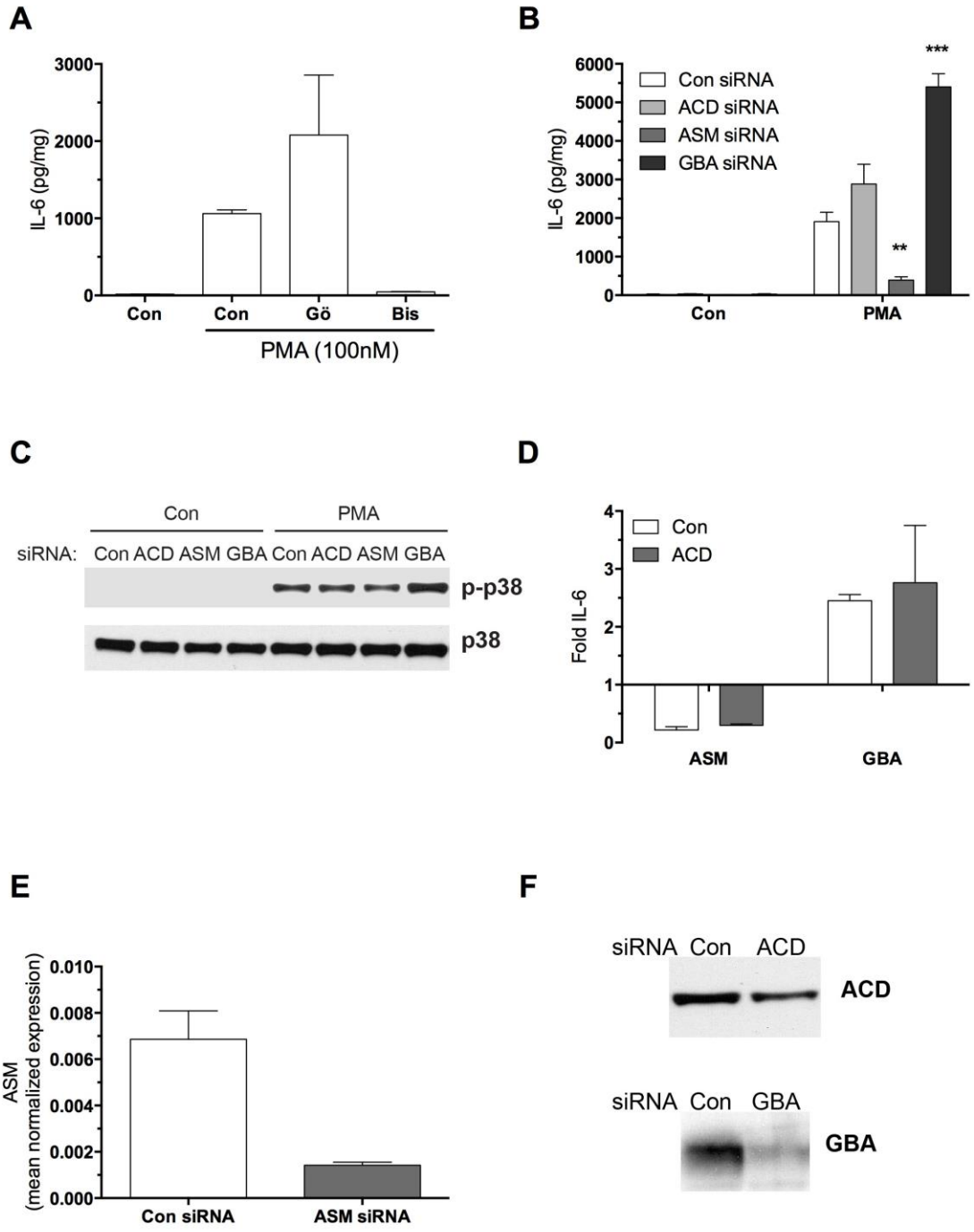

Figure 10. Adapted from the Dissertation of DM Perry (2012). *Regulation of IL-6 and p38 by Sphingolipid Salvage enzymes in MCF-7. A*, PKC inhibitors Gö6976 (3 mM) and Bis (3mM) were added to subconfluent MCF-7 cells for a 1 h pretreatment followed by PMA (100nM) treatment for 18 h. IL-6 was measured by ELISA in cultured media as described in "Experimental Procedures" (n=2). *B*,

MCF-7 cells were treated with 20 nM siRNA for the indicated enzymes for 48 h and then stimulated with PMA for 18 h; IL-6 in cultured media was measured by ELISA (2-way ANOVA, Bonferroni's post-test, ** $p<0.01$, *** $p<0.001$ compared to Con siRNA + PMA, n=3). *C,* MCF-7 cells were treated with 20 nM siRNA for 48 h and stimulated with PMA (100nM) for 30 min. Whole cell lysates were prepared and equal amounts of protein were subjected to western blotting for phospho-p38 and p38. Representative of two experiments. *D,* MCF-7 cells were cotreated with siRNA for the above enzymes for 48 h followed by PMA treatment for 18 h. Fold change was calculated to either control siRNA or ACD siRNA alone for each group (n=2). *E-F,* MCF-7 cells were treated with 20nM of various siRNAs as labeled for 48 h. Cells were harvested either for qRT-PCR (E) or immunoblotting (F) as described in "Experimental Procedures." Equal amount of protein was loaded for siRNA validation for GBA and ACD (F).

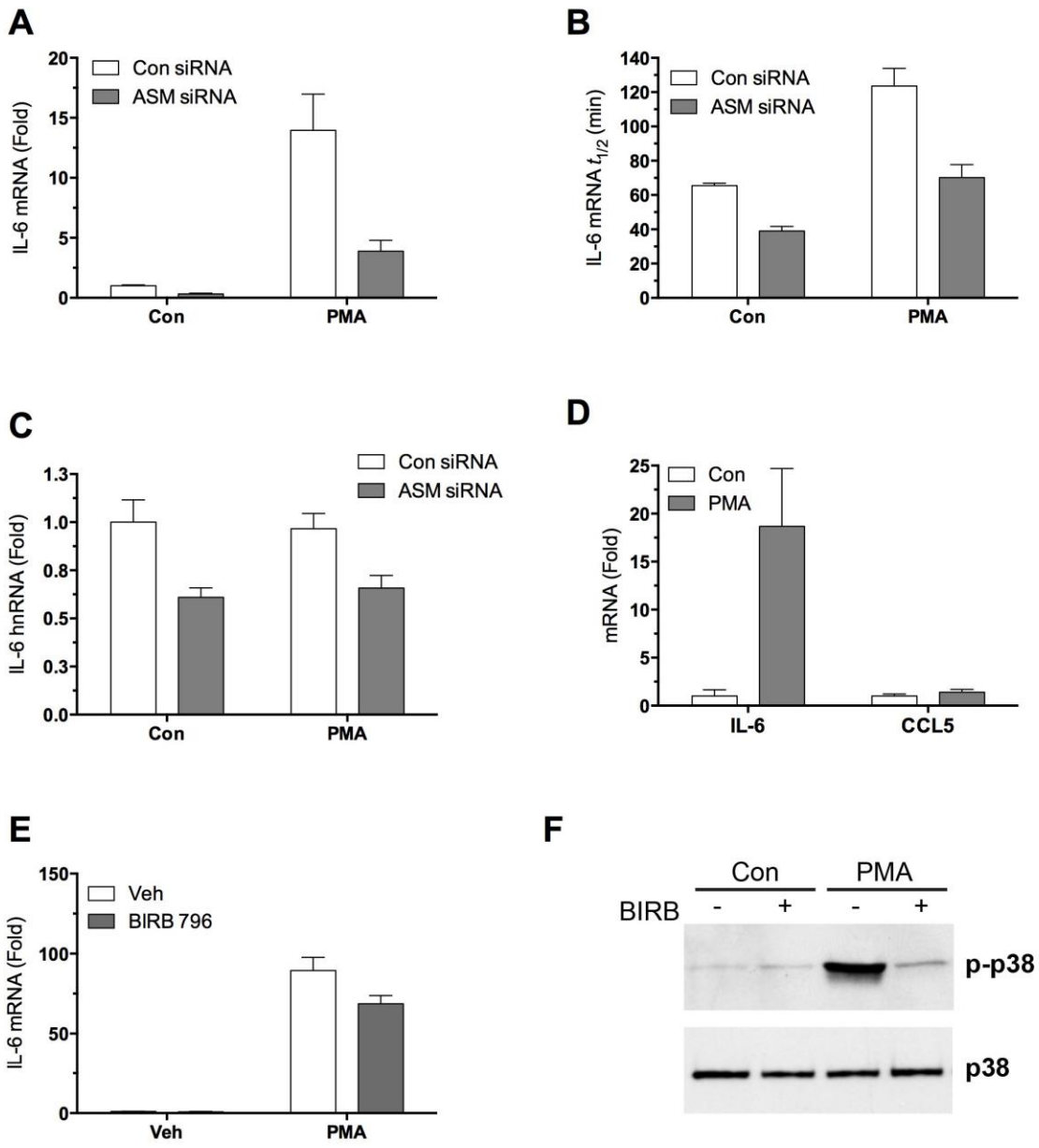

Figure 11. Adapted from the Dissertation of DM Perry (2012). *The role of ASM in the regulation of IL-6 RNA in MCF-7. A,* MCF-7 cells were treated with 20 nM siRNA for 48 h and then stimulated with PMA for 90 min. Next, cDNA was synthesized and qPCR was performed for IL-6 mRNA and normalized to actin as described in "Experimental Procedures." Fold change was calculated based on untreated, control siRNA group (n=3). *B,* MCF-7 cells were treated with siRNA as before, stimulated with PMA for 90 min, and then treated with 5 mg/ml Actinomycin D for a 3 h time course including time points of 0, 1, 2, and 3 h. RNA was harvested, cDNA prepared, and IL-6 mRNA measured by qPCR. Remaining amount of mRNA was calculated by normalizing each group to the values at t_0 of Actinomycin D. Values represent calculated $t_{1/2}$ for each sample

group (n=2). *C,* MCF-7 cells were treated with 20 nM siRNA for 48 h and then stimulated with PMA for 90 min. As in (A), cDNA was prepared but qPCR was performed utilizing primers specific for IL-6 hnRNA (n=3). *D,* MCF-7 cells were treated with either vehicle or PMA for 90 min, and cDNA was prepared and qPCR performed for IL-6 and CCL5/RANTES mRNA expressed as fold change from control group (n=5). *E,* MCF-7 cells were treated with the indicated agents for 90 min and RNA was harvested for qRT-PCR with primers specific to IL-6 (n=3). *F,* MCF-7 cells were treated with BIRB 796 and PMA for 90 min and whole cell lysates were prepared. Equal protein was loaded in each lane of a 4-12% SDS-PAGE gel and probed for total p38 or phospho-p38 as indicated.

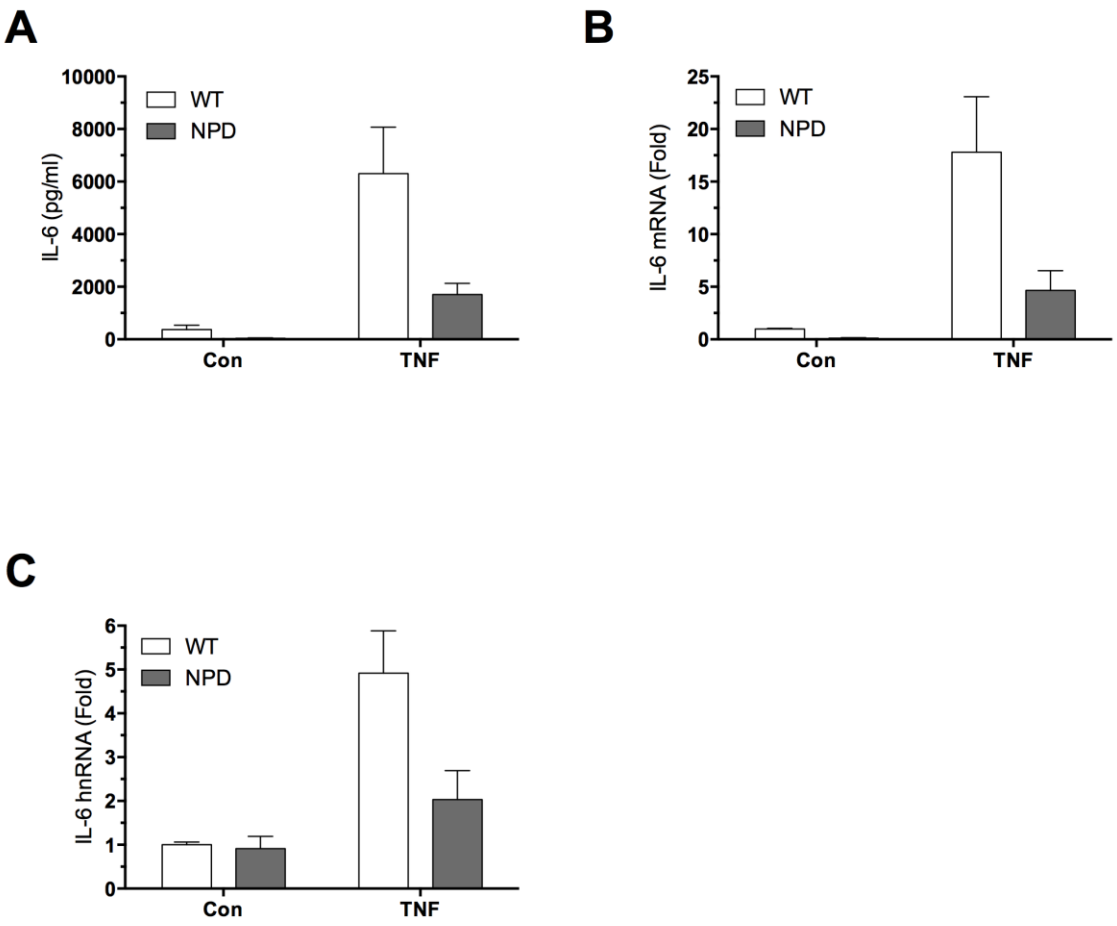

Figure 12. *Altered expression and production of IL-6 in response to TNFα in human Niemann Pick Fibroblasts*. A, Equal numbers of control or Niemann Pick Type A disease fibroblasts were plated and next day treated with TNFα for 18 h. Cultured media were assessed for IL-6 by ELISA (n=2). B-C, WT and NPD fibroblasts were treated with TNF (20 ng/mL) or untreated for 90 min. RNA and cDNA were prepared, and IL-6 mRNA (B) and hnRNA (C) were measured as described under “Experimental Procedures” (n=2).

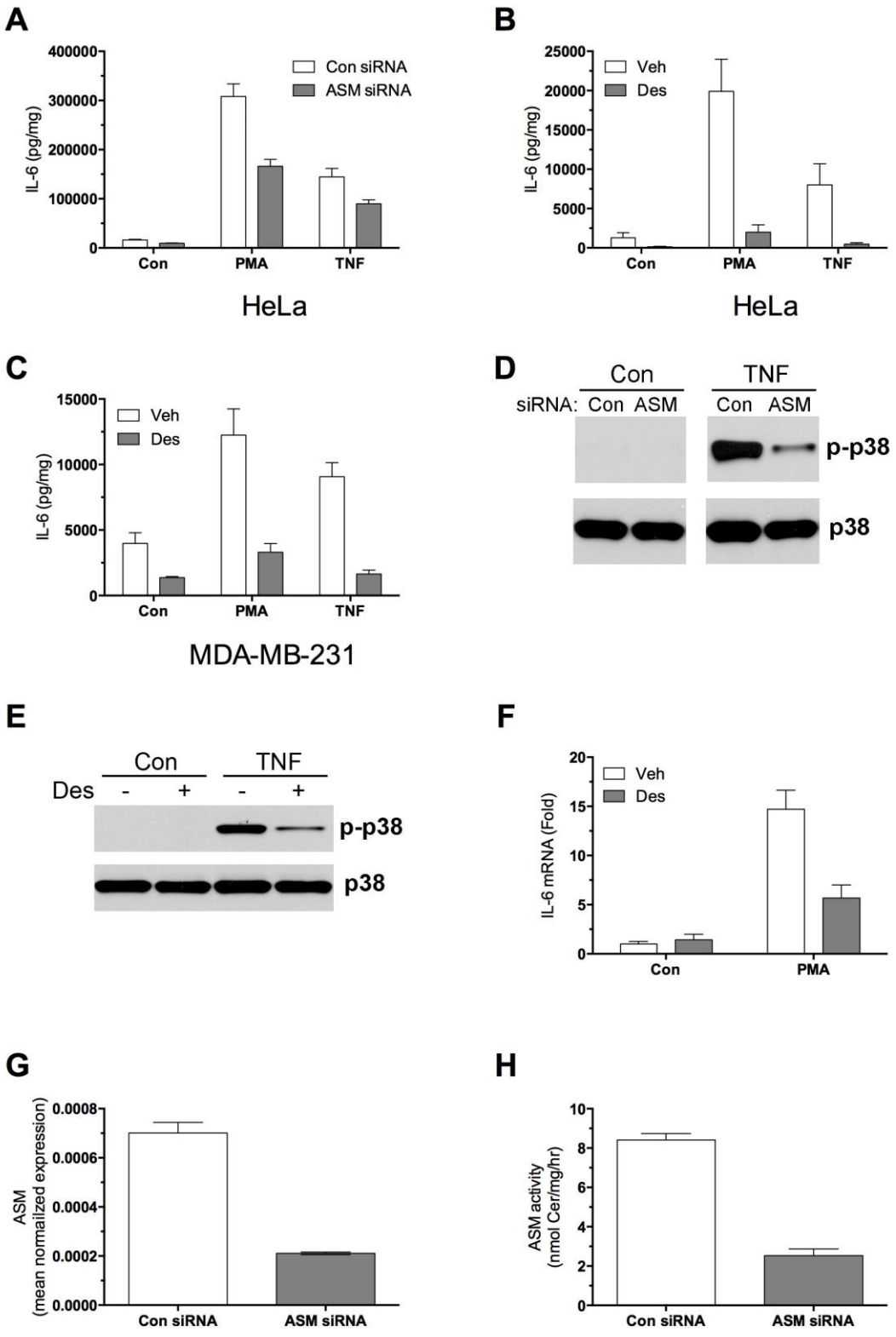

Figure 13. Adapted from the Dissertation of DM Perry (2012). *Regulation of p38/IL-6 by ASM in HeLa cells.* A, HeLa cells were treated with control or ASM siRNA for 48 h followed by 18 h PMA treatment. IL-6 in cultured media was

measured by ELISA. B-C, HeLa (B) or MDA-MB-231 (C) were treated with 50 μM desipramine or PBS control for 1h and then stimulated with PMA and TNFα for 3 h. IL-6 in cultured media was measured as above (n=2). D, HeLa cells were treated with the indicated siRNA for 72 h and then stimulated with TNFα (20ng/mL) for 15 min. Whole cell lysates were subjected to western blotting for phospho-p38 and p38. Equal amounts of protein were loaded (representative of two experiments). E, HeLa cells were pretreated with 25 μM desipramine for 1 h and treated with TNFα (20ng/ml) for 15 min. Whole cell lysates were prepared and equal amounts of protein were subjected to western blotting for phospho-p38 and p38 (representative of 3 experiments). F, HeLa cells were pretreated with PBS or desipramine (50μM) for 1 h and then stimulated with PMA for 90 min. Next, cDNA was synthesized and qPCR was performed for IL-6 mRNA and normalized to actin as described in "Experimental Procedures" (n=3) G, HeLa cells were treated with ASM siRNA for 48 h. RNA and cDNA were harvested and prepared and qPCR was performed for ASM mRNA and normalized to actin (n=3). H, HeLa cells were transfected as previously for 48 h and then lysates were harvested and acid sphingomyelinase activity was measured as described in "Experimental Procedures" (n=3).

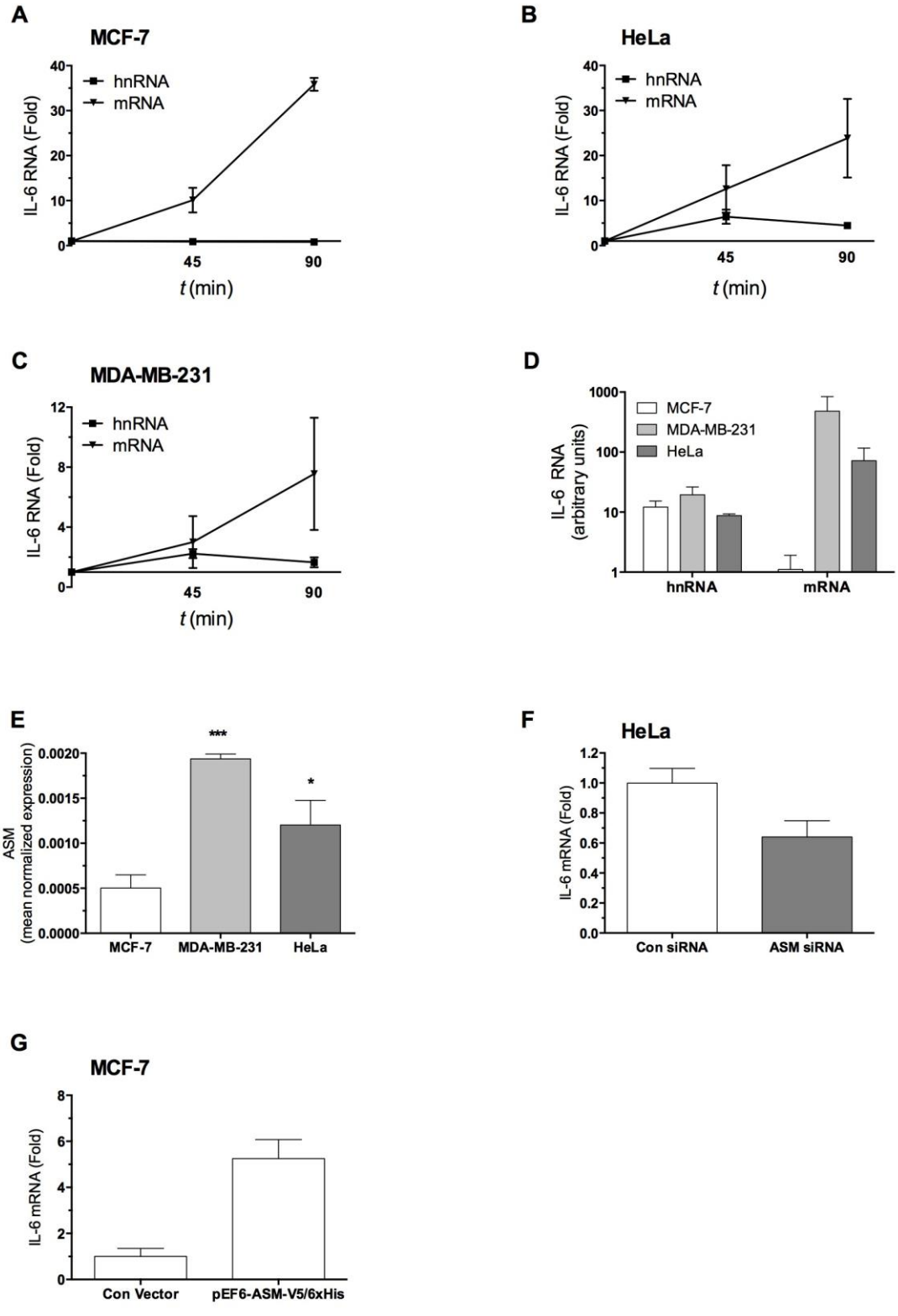
A
MCF-7
hnRNA
mRNA
IL-6 RNA (Fold)
40
30
20
10
0
45
90
t (min)
B
HeLa
hnRNA
mRNA
IL-6 RNA (Fold)
40
30
20
10
0
45
90
t (min)
C
MDA-MB-231
hnRNA
mRNA
IL-6 RNA (Fold)
12
8
4
0
45
90
t (min)
D
MCF-7
MDA-MB-231
HeLa
IL-6 RNA (arbitrary units)
1000
100
10
1
hnRNA
mRNA
E
ASM (mean normalized expression)
0.0020
0.0015
0.0010
0.0005
0.0000
***
*
MCF-7
MDA-MB-231
HeLa
F
HeLa
IL-6 mRNA (Fold)
1.2
1.0
0.8
0.6
0.4
0.2
0.0
Con siRNA
ASM siRNA
G
MCF-7
IL-6 mRNA (Fold)
8
6
4
2
0
Con Vector
pEF6-ASM-V5/6xHis

Figure 14. Adapted from the Dissertation of DM Perry (2012). *IL-6 RNA dynamics in MCF-7, MDA-MB-231, and HeLa: Upregulation of ASM and IL-6 in Invasive Cancer cells*. A-C, MCF-7 (A), MDA-MB-231 (B), and HeLa (C) cells were treated with PMA for 45 or 90 min. Total RNA was harvested and cDNA synthesized according to "Experimental Procedures." IL-6 hnRNA and mRNA were measured by qPCR using specific primers for each species as described in "Experimental Procedures." Fold change was calculated from untreated controls, and t0 was represented by the average of untreated samples at 45 and 90 min, being nearly identical (n=2). D, Basal IL-6 hnRNA and mRNA levels from the various cell lines were calculated after normalizing to actin representing relative amounts between cell lines and between hnRNA versus mRNA. E, ASM mRNA levels were measured by RT-PCR as described under "Experimental Procedures" in MCF-7, MDA-MB-231, HeLa cells under basal conditions (n=2). F, HeLa cells were transfected for 48 h with either control or ASM siRNA. RNA was harvested and RT-PCR performed for IL-6 mRNA as described above (n=2). G, MCF-7 cells were transfected for 48 h with either pEF6-EV or pEF6-ASM-V5-6xHis as described in "Experimental Procedures" after which cDNA was prepared and IL-6 mRNA was measured by RT-PCR as expressed as fold change (n=3).

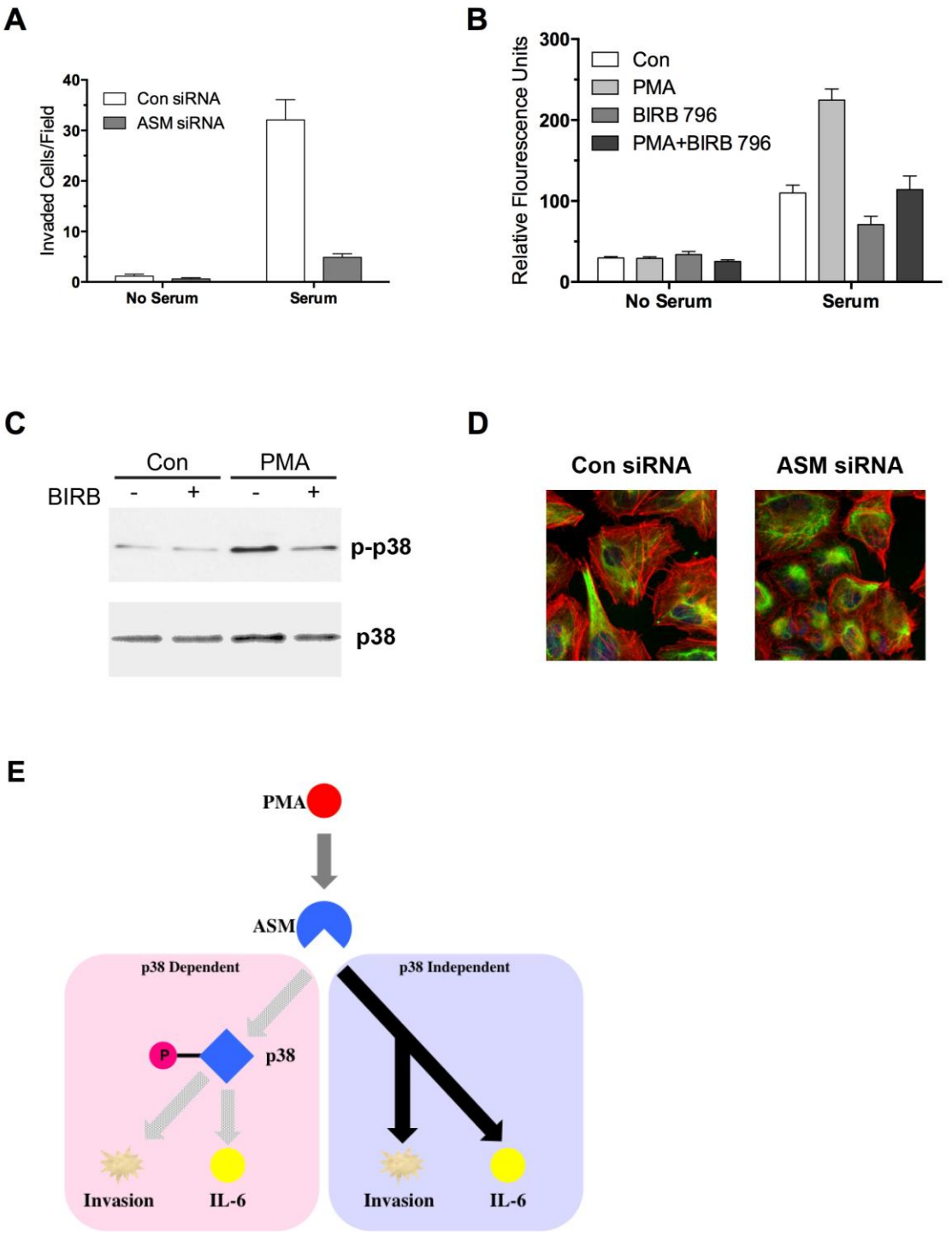

Figure 15. *Role of ASM in Invasion and Cytoskeletal Changes in HeLa cells.* A, HeLa cells were treated with control or ASM siRNA for 48 h, trypsinized, and equal cells plated in precoated matrigel wells. After 48 h of incubation with or without serum in the lower chamber, invaded cells were stained and counted in 4 fields per well (n=2). B, HeLa cells were treated with the indicated agents for 90 min, trypsinized, resuspended in serum free media and seeded at 2.5x104 cells/well in the upper well of Matrigel transwell invasion assay plate. The

indicated agents were then added to the upper wells of the transwell plate, and either serum replete or serum free media was added to the lower chamber (n=3). C, HeLa cells were treated with the indicated agents for 90 min, and total protein was harvested. Equal protein was loaded in each lane of a 4-12% SDS-PAGE gel and probed for total p38 or phospho-p38 as indicated. D, HeLa cells transfected with control or ASM siRNA for 48 h were visualized by immunofluorescence for vimentin (green), F-actin (red, phalloidin), nuclei (blue, DRAQ5). E, Scheme depicting the role of p38 and ASM in IL-6 production and malignant progression of tumor cells.

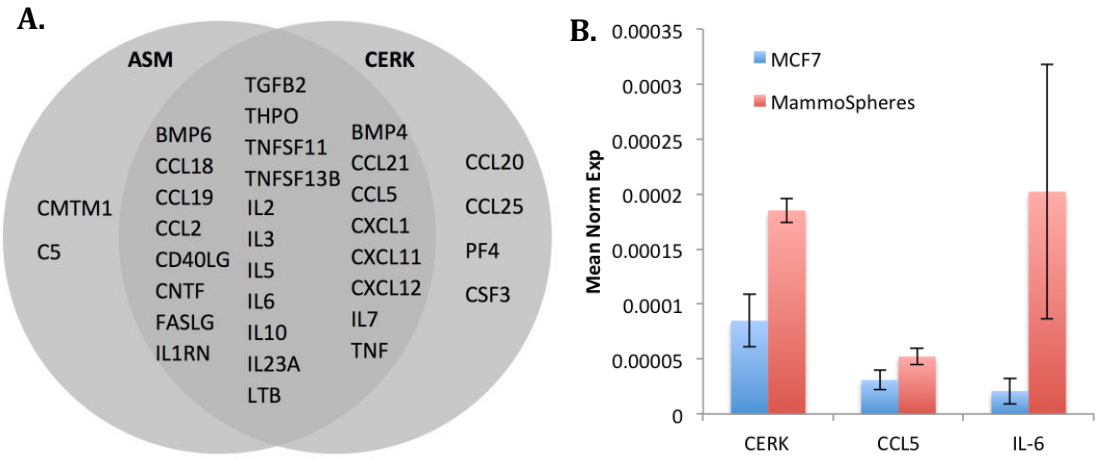

Figure 16. *Identification of a role for ASM and CERK in promoting EMT and growth of mammospheres.* **(A)** MCF7 cells were transfected with ASM or CERK overexpression constructs. After 24hrs of incubation, cDNA was prepared from the cells and cytokine expression was analyzed with TaqMan RTPCR cytokine arrays as described in Materials and Methods: Real Time Reverse Transcriptase-Polymerase Chain Reaction. **(B)** Mammospheres were grown from subconfluent MCF7 cells. The mammospheres were trypsinized and re-plated in adherent conditions and the expression levels of CERK, CCL5, and IL-6 were determined by RTPCR.

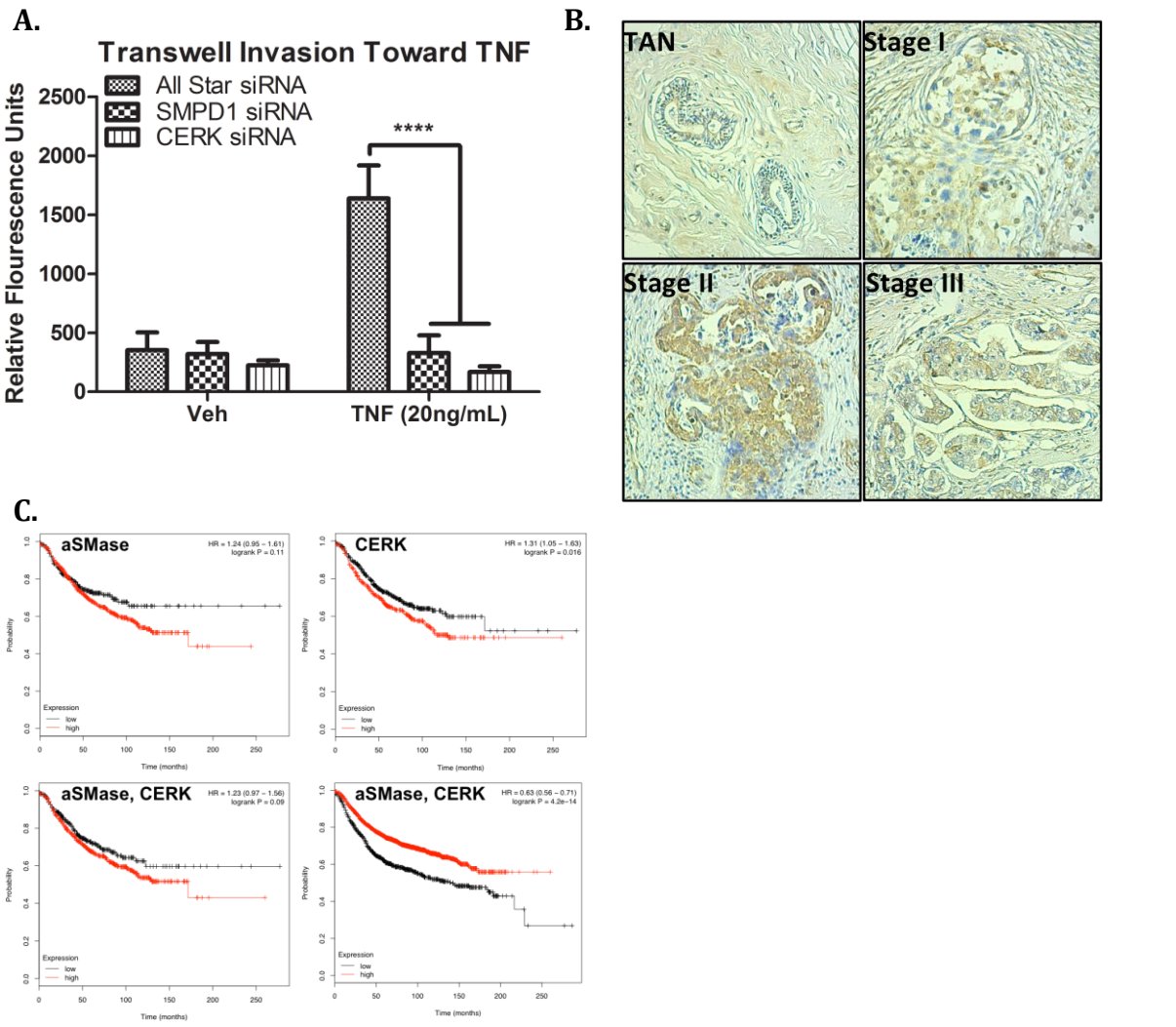

Figure 17. *Delineation of the role of ASM and CERK in breast tumor progression.* **(A)** MDA-MB-231 breast carcinoma cells were transfected with non-targeting (All Star) siRNA, or siRNA against ASM or CERK. After 48 hrs, cells were trypsinized and plated in the upper wells of Matrigel® trans-well invasion chambers. The lower well containted complete media with vehicle (PBS) or complete media with TNF-α (20ng/mL). Cells were incubated for 48hrs, and invasion was quantified by staining cells with calcein AM and measuring fluorescence. **(B)** Tissue microarray slides containing 76 cores, in duplicate, were obtained from US Biomax (BR1504). The slides were stained with a monoclonal antibody against ASM (1:750, brown), and lightly counterstained with hematoxylin to identify nuclei (purple). Cores were imaged and arranged according to tumor stage classification. Representative images of cores from Tumor Associated Normal (TAN), and Stage I, II, and III tumors are shown. **(C)** Outcomes analysis was performed on metastatic breast tumors using KM Plot software (accessed at http://kmplot.com/analysis/index.php?p=service&cancer=breast). Hazard ratios

were calculated for tumors expressing high levels of ASM (top left), CERK (top right), or ASM and CERK together (bottom left). The outcomes of non-metastatic tumors expressing high levels of ASM and CERK were also assessed (bottom right).

A.

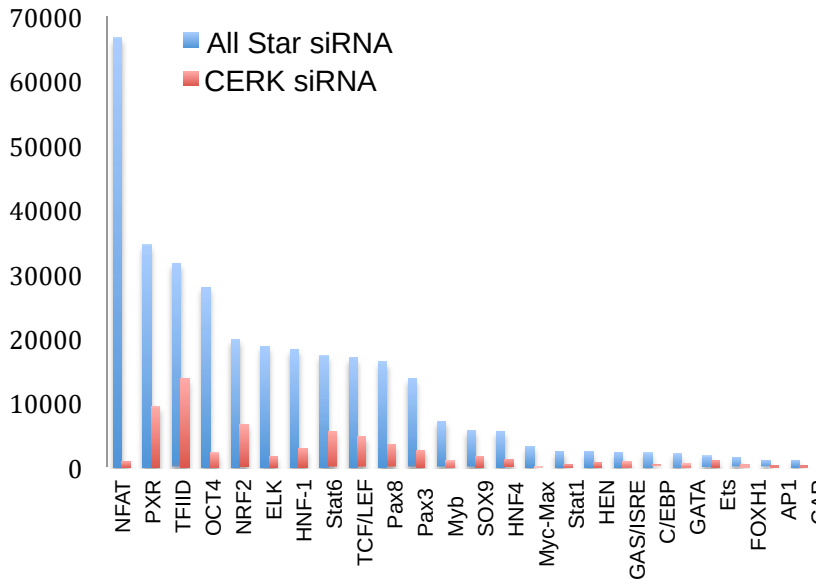

Figure 18. *Identification of transcription factors functionally dependent on CERK.* **(A)** MCF7 cells were transfected with non-targeting (All star) or CERK siRNA. After 48 hrs of incubation, cells were treated with TNF-α (20ng/mL) for 6 hrs. Nuclei were harvested and transcription factor activity was measured in the purified nuclei using Signosis Transcription Factor Arrays, as described in Material and Methods: Transcription factor arrays.

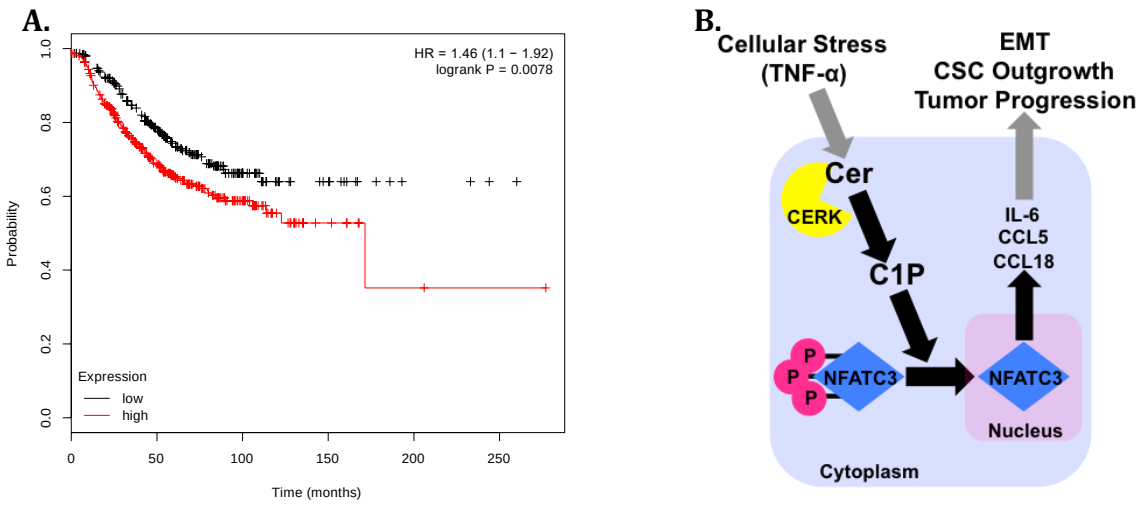

Figure 19. *High expression of CERK/NFAT/IL6/CCL5/CCL18 defines a highly aggressive subset of breast carcinomas.* **(A)** KM Plot analysis showing tumors with high expression of CERK/NFAT/IL6/CCL5/CCL18 (red line) compared to tumors with low expression of the pathway (black line). Tumors expressing high levels of CERK/NFAT/IL6/CCL5/CCL18 have very poor outcomes (HR 1.46, p=0.00078). **(B)** Graphical representation of the relationship between cellular stress, CERK, and expression of EMT promoting pathways.

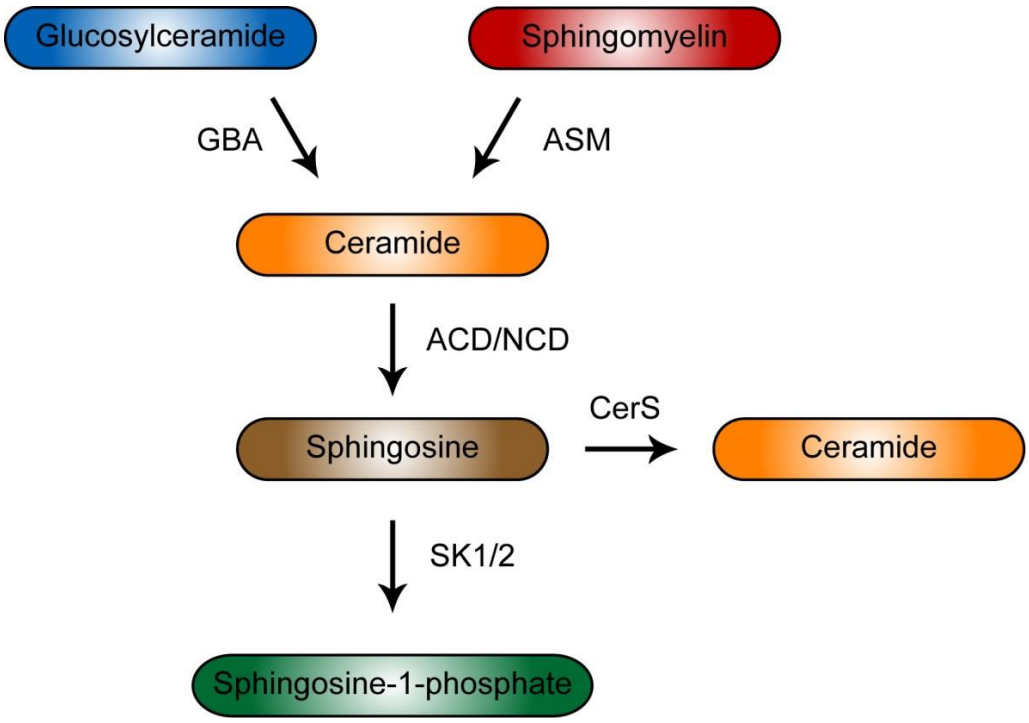

Scheme 1. Sphingolipid Metabolic Pathway

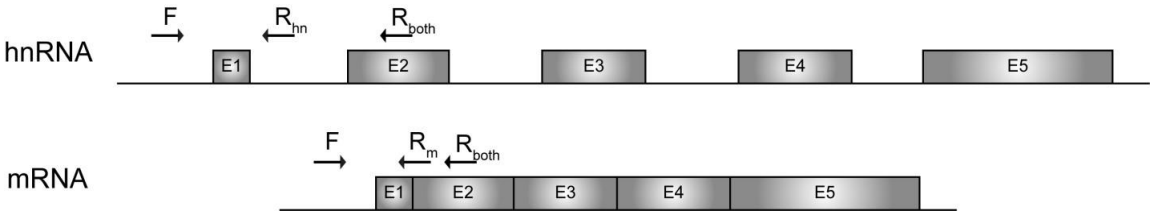

Scheme 2. IL-6 hnRNA and mRNA showing primers designed specifically for each species (Rhn or Rm) or both (Rboth) with a common forward primer (F). Approximate, relative size of exons are shown (E1-E5).

Table 1. IL-6 Primers

Primer	sequence (5' to 3')
Forward (F)	CGA GCC CAC CGG GAA CGA AA
hnRNA Reverse (R_{hn})	CCA GGG CTA AGG ATT TCC TGC ACT T
mRNA Reverse (R_m)	TGG ACC GAA GGC GCT TGT GGA
hn/mRNA Reverse (R_{both})	CAG CCC CAG GGA GAA GGC AAC T

Table 2. Molecular subtypes of breast cancer

	Luminal A	Luminal B	Basal	Her2-Like
Description	High expression of hormone receptors and ER regulated genes	High expression of hormone receptors and ER regulated genes	High expression of epithelial and cytokeratin genes	High expression of growth factor receptors
Most Common Receptor Status	ER^+ or PR^+, $Her2^-$, Low Ki67	ER^+ or PR^+, $Her2^-$ or $Her2^+$, High Ki67	ER^-, PR^-, $Her2^-$	ER^-, PR^-, $Her2^+$
General Treatment Protocol	Endocrine therapy	Endocrine therapy plus chemotherapy	Platin containing regiment	Anti-Her2 and anthracycline
Outcomes	Good (92%*)	Moderate (90%*)	Variable, but mostly poor (86%*)	Poor (79%*)
Approximate fraction of newly diagnosed cases	47%	35%	7%	7%

*10 Year Local Relapse Free Survival in patients that presented with non-metastatic disease and received breast conserving surgery.
Adapted from sources [33, 37, 110, 331].

Table 3. Transcription Factor Functions in Breast Cancer [231, 332-355].

Target Sequence	Transcription Factors	Function in breast cancer
NFAT	Nuclear Factor of Activated T-cells 1 through 5	Activated by calcineurin, GSK-3β and PKA attenuate NFAT nuclear function [292]. NFATc2 and NFAT5 induce cell motility in breast cancer [293,294].
PXR	Pregnane X Receptor	Nuclear receptor that is activated by wide array of steroids and toxic chemicals, as well as TNF-α and IL-1β [295]. Induces transcription of CYP3A4 andCYP450 enzymes and resistance to chemotherapeutics [296].
TFIID	Transcription Factor II D	Required for transcription. Binds TATA box. Important for ERα driven breast cancers [297].
OCT4	Octamer-binding Transcription Factor 4	Activated by cell survival signaling. Essential for induction of tumor stem like cell properties [298].
NRF2	Nuclear factor like 2	Activated by oxidative stress, binds antioxidant stress elements and promotes resistance to therapy in breast cancer [299,300].
ELK	ETS domain-containing protein Elk 1 through 4	Required for development of endocrine tissues [301]. ELK3 and 4 are associated with breast tumor progression [302,303].
HNF1	Hepatocyte Nuclear Factor 1 α and β	Liver and kidney specific functions. HNF-1β promotes EMT in several models [304].
Stat6	Signal Transducer and Activator of Transcription 6	Activated by RTK signaling. STAT6 plays a key role in IL-4 production and subsequent Th0 to Th2 T-cell differentiation [305]. STAT6 promotes a Th2 polarized tumor microenvironment that is permissive to tumor growth [306,307]. (CCL5 is also a very potent Th2 polarizing agent [182]).
TCF/LEF	Transcription Factor 1 trough 4, Lymphoid Enhancer binding Factor 1	Activated by wnt and recruit beta-catenin to target genes [308].Promote metastasis of breast cancer stem like cells [309].
Pax8	Paired box gene 8	Activated in developing thyroid and kidney. Potential role in gynecologic tumors, but not expressed in breast tumors [310,311].
Pax3	Paired box gene 3	Activated during facial development. May play a role in regulation of p53 [312].
Myb	Myeloblastosis proto-oncogene protein	Activated during hematopoeisis. Myb expression decreases E-Cadherin expression in breast cancer cell lines, and promotes EMT [313].
SOX9	Sex determining region Y box 9	Required for supression of development female reproductive organs, and formation of male organs. Co-expression of SOX9 and Slug is sufficient to form tumour-initiating cells [314].
HNF4	Hepatocyte Nuclear Factor 4	Activated during liver development. Function is not well annotated.
Myc-Max	Myc associated factor X	Promotes cell cycle progression and apoptosis. Small molecule inhbitors of Myc/Max dimerization slow tumor growth [315].
Stat1	Signal Transducer and Activator of Transcription 1	Activated by interferon signaling. ER- tumors with high STAT1 signaling are responsive to therapy [313].
HEN	Nescient Helix Loop Helix 1	Plays a role in development of nervous system. Unknown role in tumor biology.
GAS/ISRE	interferon stimulating responsive element/gamma-interferon-activation sites	Target sequences of STAT family of transcription factors.
C/EBP	CCAAT-enhancer-binding protein α trough ζ	Activated during neuronal differentiation. C/EBP-β enhances RTK signaling in breast cancers [314,315]
GATA	GATA Binding Protein 1 through 6	Bind GATA sequences in the promoter. Promote lobulo-alveolar development. GATA3 has best characterized role as an Erα enhancing factor in breast cancer.
Ets	Family of 29 genes (Includes ELK)	Highly diverse family. Includes ELK transcription factors.
FOXH1	Forkhead box H1	Activated by TGF-β. Negative regulator of Erα signaling in breast cancer.
AP1	Large family of txn factors	AP1 represents heterodimers between members of the c-Fos, c-Jun, ATF and JDP families of transcription factors. AP-1 Is a Key Regulator of Proinflammatory Cytokine TNFα-mediated Triple-negative Breast Cancer Progression.
CAR	Constitutive Androstane Receptor family	Related to PXR.Many overlapping functions with PXR. Deactivated by PP2A.